2018

IMPROVING HELICAL ANCHOR EFFICIENCY: AN EXPERIMENTAL STUDY

Robin Timo Zuelke
University of Rhode Island, robin_zulke@my.uri.edu

IMPROVING HELICAL ANCHOR EFFICIENCY: AN EXPERIMENTAL STUDY

BY

ROBIN TIMO PAUL ZUELKE

A THESIS SUBMITTED IN PARTIAL FULFILLMENT OF THE

REQUIREMENTS FOR THE DEGREE OF

MASTER OF SCIENCE

IN

CIVIL ENGINEERING

UNIVERSITY OF RHODE ISLAND

2018

MASTER OF SCIENCE

OF

ROBIN TIMO PAUL ZUELKE

APPROVED:

Thesis Committee:

Major Professor Aaron Bradshaw

Christopher Baxter

David Taggart

M. Reza Hashemi

Nasser H. Zawia
DEAN OF THE GRADUATE SCHOOL

UNIVERSITY OF RHODE ISLAND
2018

ABSTRACT

The growing demand of renewable energy will inspire the continued development of offshore wind farms in the future. Floating platforms are a viable alternative in water depths exceeding about 50 meters. These platforms must be anchored to the seafloor. There are a number of current research projects investigating the viability of using helical anchors (or helical piles) for floating platforms because of their high capacity to weight ratio. The objective of this study is to find ways to further improve this efficiency by reducing the forces needed to install the anchor while maximizing its resistance to pullout. To reach that goal, a series of small-scale 1g physical model tests on 1/5-scale helical piles was conducted in loose and dense sand. Modifications were made to the helical anchor that included roughening the surface of the helix plate, adding Teflon to the helix plate, as well as performing a so-called "jetting" operation to prevent plugging of the anchor shaft during installation. Anchors were installed to an embedment of about 9 times the helix diameter with constant crowd force, and then pulled out at a constant rate. The results showed that the surface modifications influenced the installation and pullout forces. Generally rough surfaces resulted in higher installation torque and increased pullout load, while smooth surfaces resulted in lower installation torque and lower pullout capacities. The jetting operation significantly reduced installation torque but also compromised the pullout capacity of the pile.

ACKNOWLEDGMENTS

First and foremost, I would like to thank all of the faculty and staff of the Civil and Ocean Engineering departments of University of Rhode Island; the dedication and support did not go unnoticed. I would like to express my genuine gratitude to my major advisor, Prof. Aaron Bradshaw for his guidance throughout this project. Your positivity and ideas gave me the motivation to complete this thesis. I am grateful for the comments and support provided by my inside committee member Prof. Christopher Baxter. Also, I am thankful for my other graduate committee members: Prof. David Taggart and Prof. M. Reza Hashemi. Thank you all for your dedication and support.

Secondly, I would like to express my gratefulness to Lars Hildebrandt, Maeve Story, Paul Sauco, Sam Lindgren, Ryan Lozinski, Fred Pease and Robin Freeland. This project would not have been possible without your know-how and your help. Also, I would like to express special thanks to Tyler Robertson and Triton Systems Inc. who provided the necessary means to complete this project.

Finally, I would like to thank those closest to me, I am extremely grateful to my parents, my sister, my grandparents and Nora. All of them have been a constant source of support in my life, and this thesis would certainly not have existed without them. Thank you for helping me become an Engineer.

TABLE OF CONTENTS

LIST OF TABLES

LIST OF FIGURES

CHAPTER 1 - INTRODUCTION

Helical piles are a type of deep foundation that can be installed quickly and easily. They cause minimal vibration and can be loaded immediately after installation. After their invention in the early 19th century, they have been used for different applications such as power transmission lines, residential construction, reinforcement of structures and retaining floating platforms at sea. According to the U.S. Department of energy and U.S. Department of the Interior, the renewable energy sector is growing continuously, and offshore wind energy production is going to increase.

Currently most wind turbines are installed on shore or near shore in shallow water depths. Up to a certain depth, monopiles and jacket structures can be used. But decreasing space and higher energy output pushes platforms further offshore and thus in deeper waters. At a water depth of more than about 50 meters, fixed-bottom structures are not viable anymore and floating platforms have to be used. Therefore, offshore platforms carrying wind turbines will have to be maintained at a fixed position in the sea. Especially for offshore applications, it is very important to have a high overall anchor efficiency. Since offshore installations are more expensive and more complicated than onshore, one should consider the benefits of improved efficiency. This thesis investigates ways to increase the efficiency of a helical pile. Therefore, a series of small-scale physical model experiments are conducted as described later in this thesis.

1.1 Statement of the Problem and Objectives

Helical anchors (or helical piles) may be a viable alternative for anchoring future floating offshore wind platforms. Improving the geotechnical efficiency of helical anchors could reduce costs, particularly for offshore applications. The objective of this study is to further enhance pile efficiency, by finding ways to decrease installation forces while maximizing pullout capacity. This was achieved through a small-scale physical modeling study. Anchors with different blade modifications were installed and installation forces as well as pullout loads were measured. The modifications that were made to the helical anchor included roughening the surface of the helix plate, adding Teflon to the helix plate, as well as performing a so-called “jetting” operation to prevent plugging of the anchor shaft during installation.

CHAPTER 2 –LITERATURE REVIEW

In the early 19th century the first helical anchor was developed by Alexander Mitchell. Back then he called it a screw pile and it was mainly used to tie mooring lines to the ground. After it was patented in 1833, the first major application was a foundation for a lighthouse on very unstable ground. At this time, it took about 20 persons and nine days to install nine anchors with bare hands. Further applications in the 19th century were mainly piers and bridges throughout the British empire. The first application in the United States was a lighthouse depending on the source either in Black Rock Harbor, Connecticut (1843) or Brandywine Shoal, Delaware (1850) (Perko 2009).

Throughout time the helical anchor has been further developed. Nowadays many different types of anchors exist: Single helix anchors, which have only one blade; multi-helix anchors with more than one blade; anchors with square and round shafts and deep and shallow anchors [see Figure. 1]. Further development led to more applications. Today, helical anchors are used in many different fields for example: foundation anchors for transmission towers, piers, wetlands and retaining the position of floating platforms in the sea.

Some advantages, or reasons why they are used frequently is the easy installation - a simple auger device or small excavator usually suffices. Also, helical anchors and piles can be loaded immediately after installation, since no concrete has to

harden. Another advantage is that they can be installed at a batter angle and thus withstand lateral forces more effectively.

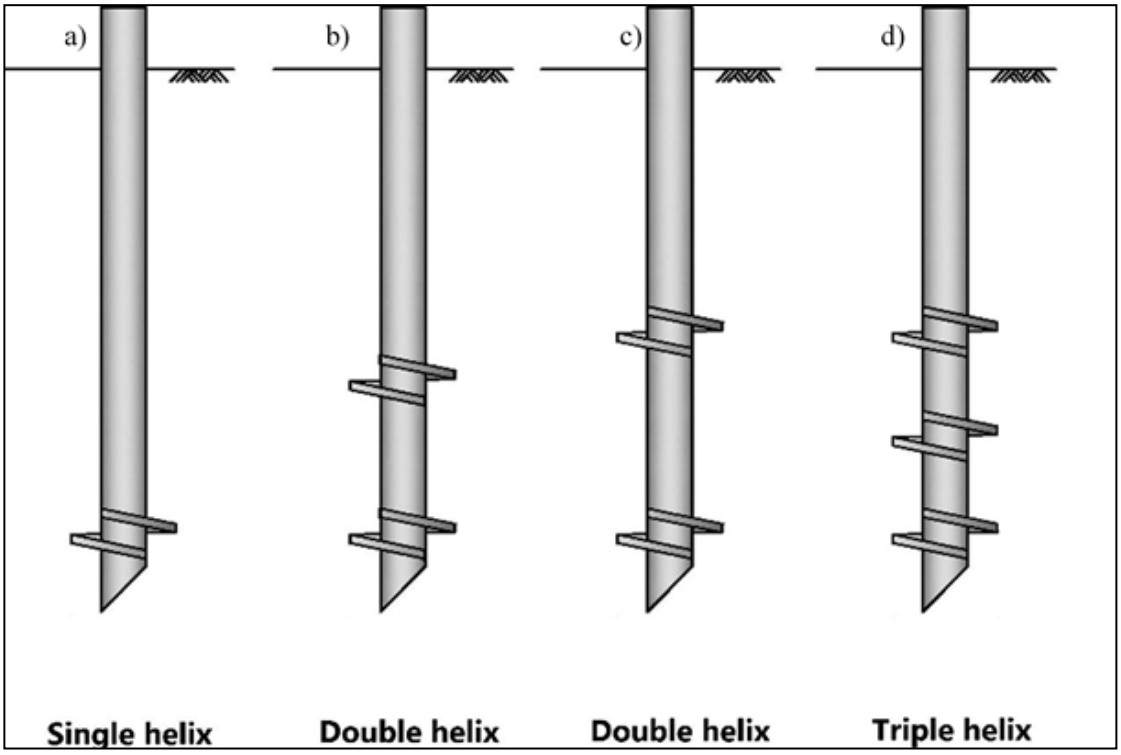

Figure 1 – Examples for single and multiple helix anchors [Wang 2017]

Moreover, these piles are cost effective, can be used in remote areas or narrow spaces, they can be removed easily, installation torque is a reliable indicator for their capacity and installation causes minimal vibrations, noise and disturbance.

Along with the development of further applications, research has brought up a deeper understanding of forces acting on these piles. The main installation forces are torque, a twisting force that causes rotation of the pile, and crowd, a downward force that causes advancement of the pile into the soil. Many of the previous studies on helical anchors or piles have focused primarily on predicting the uplift capacity either

from basic soil properties, or from the measured installation torque, analogous to the way that pile-driving energy is used to estimate the capacity of driven piles.

2.1 Installation Forces

One of the earliest studies on the forces needed to install helical anchors was done by Ghaly and Hanna (1991). In their experiments, they used five different anchor geometries in loose, medium, or dense sand. Anchors were installed by applying the torque and crowd force to the anchors through a power auger. The differences among the anchors were mainly the pitch height and number of blades, while the blade and rod diameter remained constant [see Figure 2]. The properties of the sand used in the study are shown in Table 1. The experimental setup also consisted of various stress transducers distributed in the sand box to keep track of lateral and vertical stresses.

Table 1 – Sand properties used for experiments by Ghaly and Hanna

Property	Value
Dense Sand	
Unit weight [kN/m^3]	19.03
Angle of shearing resistance [°]	42
Relative density [%]	83
Medium Sand	
Unit weight [kN/m3]	18.74
Angle of shearing resistance [°]	36
Relative density [%]	52
Loose Sand	
Unit weight [kN/m3]	17.75
Angle of shearing resistance [°]	31
Relative density [%]	20

Each anchor was installed and pulled out individually. Findings showed that installation force generally increased with relative sand density and installation depth.

Also, the ratio of pitch (p) to blade diameter (B) was an important factor for installation forces. Increasing p/B resulted in higher installation forces.

Ghaly and Hanna (1991) also developed a model that predicted the required installation torque of specific anchor properties. The main influences on torque were "the frictional resistance exerted on the anchor's shaft and the locally compacted column of sand overlying the screw blade and the bearing resistance exerted on the screw blades."

Ghaly and Hanna also developed a model to predict the uplift capacity and a torque Factor F_t defined below:

$$Nq_u = \left[\frac{Q_U}{\gamma AH}\right] \qquad (1)$$

$$F_t = \left[\frac{T}{\gamma AHp}\right] \qquad (2)$$

where γ = unit weight of sand, A = surface area of the anchor, H = installation depth and p = pitch of the anchor blades, Q_u = the uplift capacity and T = total installation torque [Equations 1 and 2]. Finally, the model was tested in previously mentioned experiments and was consistent with measured results.

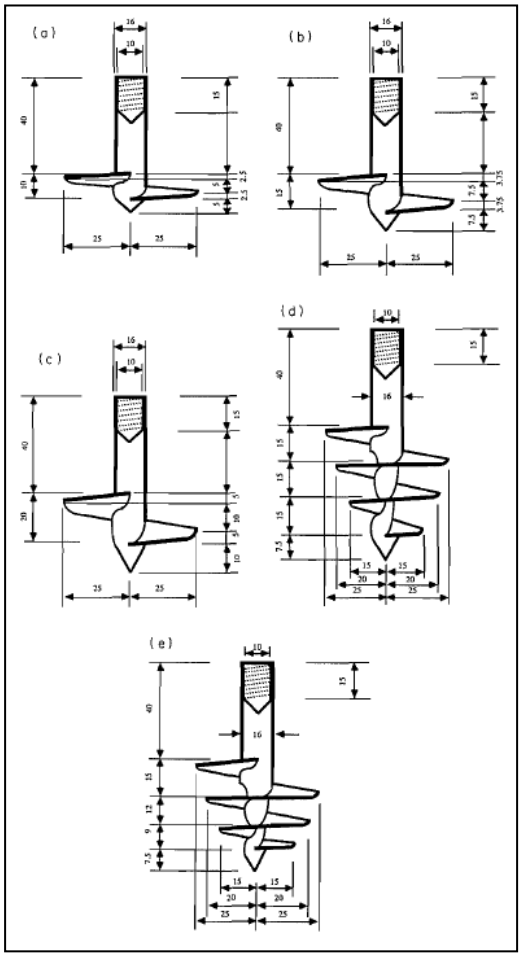

Figure 2 – Anchor models used by Ghaly and Hanna

In order to predict uplift capacity from installation force, they developed the following relationship [see Figure 3]:

$$\left[\frac{Q_u}{\gamma AH}\right] = 2\left[\frac{T}{\gamma AHp}\right]^{1.1} \quad (3)$$

where Q_u = uplift capacity, γ = unit weight of soil, A = pile surface area, H = installation depth, T = total installation torque and p = blade pitch.

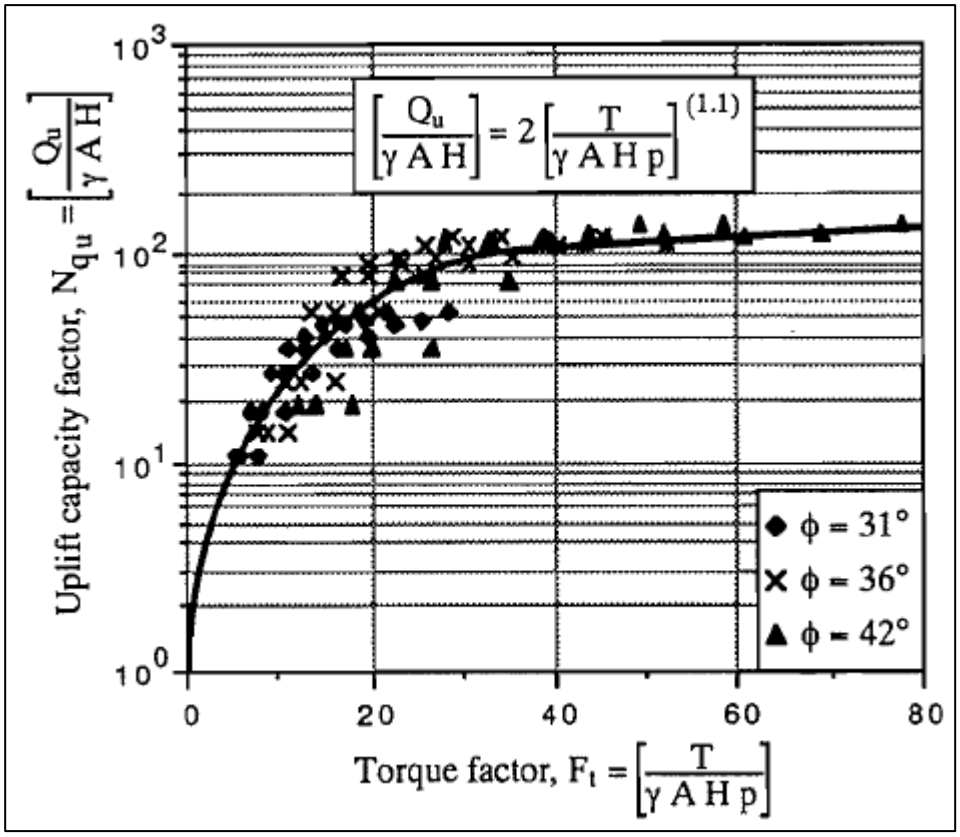

Figure 3 – Relationship between uplift capacity factor and torque factor [Ghaly and Hanna 1991]

Ghaly (1995), subsequently focused on the effect of seepage pressures during the installation and the pullout of anchors.

Table 2 Sand Properties used for experiments by Ghaly

Property	Value
Dry unit weight [kN/m3]	16.7
Submerged unit weight [kN/m3]	11.0
Angle of shearing resistance [°]	40
Coefficient of permeability [m/sec]	$3{,}4x10^{-4}$
Relative density [%]	80
Specific gravity [Gs]	2.67
Effective size [mm]	0.11
Coefficient of uniformity [Cu]	2.09
Coefficient of curvature [Cc]	1.42

The setup was similar to the earlier experiments of Ghaly and Hanna. Sand was placed in the tank in layers of 150 mm and compacted after each layer. To simulate seepage conditions, perforated pipes were also placed in the box surrounded by a 100-mm fine gravel layer. The helical screw had similar dimensions as the ones previously used by Ghaly and Hanna: 50 mm blade diameter, 15 mm pitch and a 12 mm rod. The mechanical properties of the sand are shown in Table 2. Besides that, a piezometer tube was placed in the tank to measure the flow through the sand.

Test results showed that the installation torque was highest in dry sand, lower in submerged sand and even lower in sand subjected to seepage. The installation torque was lower with higher flow velocity. The same goes for the uplift capacity: Highest in dry sand, lower in submerged sand and further decreasing with rising flow

velocity - so it was concluded that installation force and pullout capacity are affected by water and especially by seepage. Also, installation torque increased with depth, confirming previous experiments conducted by Ghaly and Hanna. Furthermore, these results confirm the work by Ghaly and Hanna that "the resistance of the sand to the penetrating helix is a function of many factors, two of which are unit weight and angle of shearing resistance" [Ghaly and Hanna 1991]

Since unit weight decreases significantly in submerged conditions [Terzaghi and Peck 1996] installation torque decreases as well. However, seepage also lowers the resistance, since upward flow further decreases the effective confining pressures in the soil. Consequently, Ghaly adapted the relationship between torque and pullout capacity to his new findings for submerged sands in hydrostatic and seepage conditions:

$$\left[\frac{Q_u}{\gamma' AH}\right] = 0.52\left[\frac{T}{\gamma' AHp}\right]^{1.2} \quad (4)$$

where Q_u = uplift capacity, γ' = saturated unit weight of soil, A = pile surface area, H = installation depth, T = installation torque and p = blade pitch. Finally, Ghaly concluded that submerged or sand in upward seepage conditions eases installation, the relationship between installation torque and pullout capacity is confirmed, and the dimensionless relationship between uplift capacity and installation torque was updated [Equation 4].

2.2 Pullout Capacity and Failure Modes

Ghaly et al. (1991) proposed three different types of failure for helical anchors in soil: shallow failure, deep failure and transit failure as shown in Figures 4 & 5. They also establish a relationship between installation depth over blade diameter and the dilation angle over soil friction angle to determine whether deep, transit or shallow failure occurs, and this is shown in Figure 4.

The proposed failure surfaces are inclined at an angle of θ to the vertical plane at the blade edge. In case of the shallow anchor, this plane reaches the surface. It was stated that θ is 2/3 of Φ for shallow anchors. For deep installed anchors, the failure plane does not reach the sand surface. They merely form the shape of a closed bulb, which was observed during their experiments [Ghaly et al. 1991] The height of the bulb (h_0) was estimated at 4B, 5B and 6B for loose, medium and dense sand respectively. Ghaly et al. propose that the dilation angle equals the maximum dilation angle of shallow failure – 2/3 Φ. In the transit zone, the failure surfaces of deep and shallow anchors kind of overlay and form a vase shape. In this case, θ can be measured from the sand surface deflection (r) and installation depth (H).

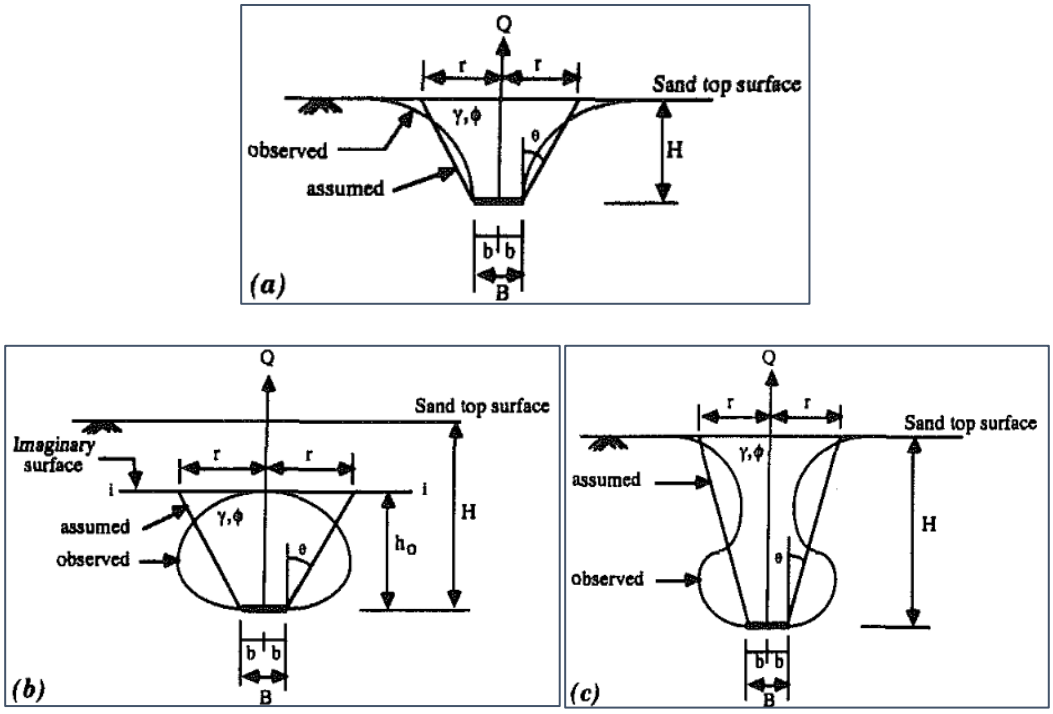

Figure 4 – failure surfaces observed by Ghaly and Hanna (a) shallow anchor, (b) deep anchor and (c) transitional anchor [Ghaly and Hanna 1991]

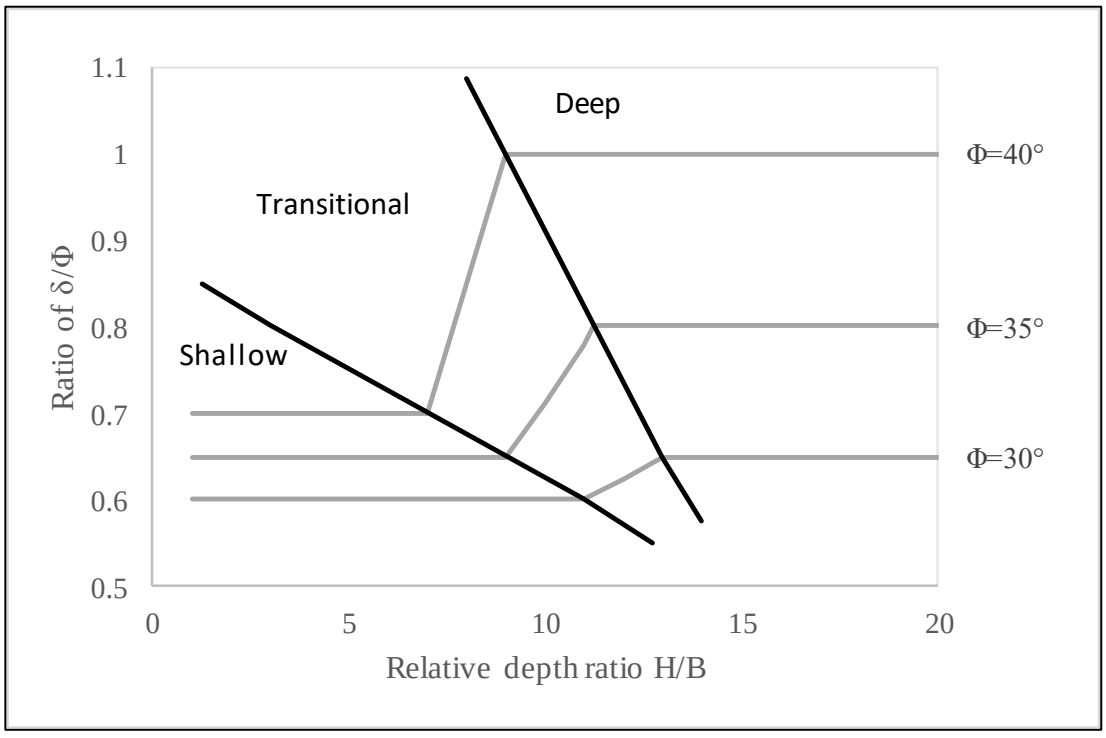

Figure 5 – Relationship of δ/Φ and H/D [Ghaly and Hanna 1991]

A variety of studies have been done on the pullout capacity of helical anchors. Clemence et al. [1994] compared the accuracy of five different methods. Full-scale load tests were conducted on nine anchors and the results were compared with different analytical and empirical methods.

In the experiments, three types of anchors were installed - three single helix, three double helix and three triple helix anchors. The site used was Eaton Dam deposit with uniform soil conditions throughout installation depth. Each anchor was installed to a depth of 6.1 meters and torque was monitored during the installation. To avoid interference between the anchors a minimum center-to-center distance of 4.5 meters was kept. Testing was performed 24 hours after installation using a steel A-frame and a hydraulic cylinder attached to a hydraulic pump.

Pullout loads were applied at a rate of 22.24 KN per minute and deflection was monitored every 15 seconds. If the deflection was still going on after one minute the load was maintained another 15 seconds until deformation stabilized. Failure was defined as the load at which continuous upward movement occurred.

After the experiments, the test results were compared with the five different methods. Each method relies on either one or two different approaches for predicting uplift capacity. The three approaches are: individual plate bearing method, cylindrical shear method and the correlation of installation torque and uplift capacity (torque factor). In general, all methods give poor predictions for uplift capacity. The A.B.

Chance methods uses the plate bearing approach, gives the most precise results and is at the same time the easiest to apply. Also, the A.B. Chance torque method under predicted the results. A torque factor of $10ft^{-1}$ was used. However, if the torque factor was increased to $20ft^{-1}$, predictions would have been within 5% of the actual test results. This shows again that the torque factor approach is a reliable way to determine uplift capacity.

Table 3 - Summary of analytical methods predicting uplift capacity in lbs. [Clemence et al. 1994]

	Method					
Anchor Size	Field measurement	Matsch and Clemence	F.H. Kuhlawy	Kuhlawy Udwari, Rodgers and Singh	A.B. Chance Method	A.B. Chance torque method
Single Helix	44,000	60,600	31,190	50,240	34,560	24,220
Double Helix	60,000	66,470	34,080	54,220	63,930	32,330
Triple Helix	80,000	68,340	36,500	55,950	88,120	38,670

Experiments conducted by Clemence et al., Ghaly, and Ghaly and Hanna (1994, 1991, 1995) brought great progress to the understanding of helical piles and anchors. Their developed equations predict uplift capacity fairly well and the established torque factor is a useful number to compare anchor capacities. However, all their experiments were conducted on a small scale. This can result in overprediction of capacity for full-scale anchors and piles. To get more precise results and equations, centrifuge tests are conducted. The centrifuge simulates deeper soil conditions by raising the acceleration from 1g to much higher values, (up to 50g) and thus produces identical self-weight stresses in the model and the prototype.

2.3 Torque Factor

One way to quantify efficiency is through the torque factor, defined as the ratio of the ultimate pullout capacity to the installation torque. Tsuha and Aoki (2007) examined the relationship between installation torque and uplift capacity. Their research focus lies on experiments with centrifuges on 12 different types of piles. They also present a different approach for the relationship between the uplift capacity and installation torque - the power screw design procedure by Faires (1943). Theory states that Q_u is function of shaft resistance T_s and helix resistance T_h. They defined by the following equation:

$$Q_u = \left(\frac{2T_s}{d}\right) + \left(\frac{2T_h}{d_c tan(\theta+\delta_r)}\right) \quad (5)$$

where Q_u = uplift capacity, d_c = diameter of a circle corresponding to the helix surface area, θ = helix angle and δ_r = residual interface friction angle.

Respectively, the final installation torque (T) can be computed with a function of shaft resistance (Q_s) and uplift helix bearing capacity (Q_h). Values of δ_r were found by conducting direct interface shear tests in the centrifuge and in the field. To prove the second part of the equation 5, centrifuge tests were executed:

Two containers with sand of different densities are used to conduct experiments with 12 piles each. Piles were installed and pulled under the influence of 22g.

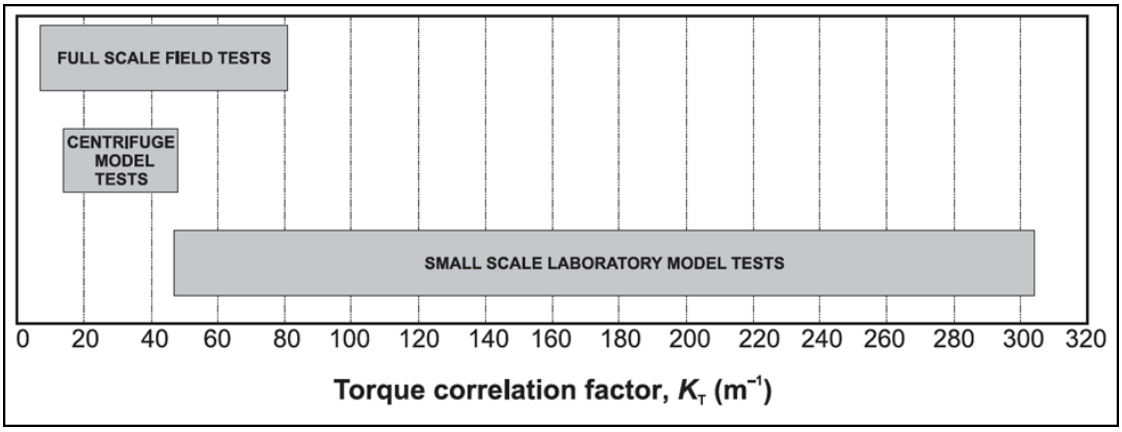

Figure 6 - Comparison of measured torque factors - differently scaled tests [Tsuha and Aoki 2010]

The experiments did show that the estimated relation as seen in equation 5 is reliable with a value Q_h (measured)/Q_h (predicted) of 98%. However, this research paper does not mention effects of saturated sand and seepage as Ghaly (1995) did before. Another finding of Tsuha and Aoki was that the torque correlation factor $K_T=Q_u/T$ decreases significantly with increasing pile dimensions. Compared to previous results of the literature they came up with a comparison of small-scale, centrifuge and full-scale tests [see Figure 6].

Aside from that, Davidson et al (2018) recently published a paper on screw piles for offshore wind farm applications. The objective of the study was to increase anchor efficiency by changing the shape of the helical pile itself. The modifications included using a smaller diameter shaft at the location of the helix plates and a larger diameter above. Centrifuge tests on model piles showed a decrease in installation torque and an increase capacity.

2.3.2 Geotechnical Efficiency

The geotechnical efficiency of marine anchors is often defined by the capacity to weight ratio. For example, Aubeny (2017) compared the efficiencies of Caisson anchors and plate anchors. He indicated that plate anchors have a 5 times higher capacity to weight ratio then the Caisson anchor. This is because for vertical loading the plate anchor gets its resistance from bearing capacity, whereas the caisson gets its resistance from friction on the sides of the anchor.

Another driver of cost is the transport volume (Aubeny 2017). Since plate anchors are much easier to store and transport, they exceed caisson piles in this efficiency rating again. Instead of a large transportation and installation vessel, which would be necessary for caisson anchors, plate anchors can be installed by a smaller one and thus reduce costs.

2.4 Scale Effects in 1g Physical Models

The research in this thesis will utilize small-scale physical models that are known to have scale effects (Aoki and Tsuha 2007). Bradshaw et al. (2016) proposed an approach to scale the results of physical model tests on small anchor models in sand to larger scale anchors (prototypes). The key is to present the results in dimensionless form and scale the constitutive behavior of the sand.

In order to scale the constitutive behavior of sand, they took Boltons (1986) concept of a relative dilatancy index. Since dilation in a soil with constant void ratio increases with decreasing confining pressures, model soils behave more dilative. Therefore, the relative density of the model soil must be lower than the relative density of the prototype soil to behave the same way. So, whenever soil is prepared to the same dilatancy index, whether in model scale or full scale, test results should yield the same breakout factor. To get the same dilatancy index, relative soil density must be scaled using the following equations (6)(7):

$$e_m = e_{max} - \left[\frac{Q-\left(\ln(p'_{fp})\right)}{Q-\left(\ln(p'_{fm})\right)}\right](e_{max} - e_m) \quad (6)$$

$$D_{rp} = \frac{e_{min}-e_p}{e_{max}-e_{min}} \quad (7)$$

where e_m, e_p, e_{max}, e_{min} = void ratio of model soil, prototype soil, maximum void ratio and minimum void ratio respectively, Q = Boltons Parameter (constant), p'_{fp} = effective confining pressure in prototype soil, p'_{fm} = effective confining pressure in model soil and D_{rp} = relative sand density for the prototype soil.

CHAPTER 3 - METHODOLOGY

This chapter presents a description of the small-scale physical model tests that are performed as part of this study. First, scaling and boundary conditions in the physical model are discussed, followed by the experimental setup and procedures.

3.1 Scaling and Boundary Conditions

The physical model testing described later on will be performed on 1/5-scale models of a helical pile. Yet, soil values cannot simply be scaled down 1/5 of the prototype soil. As explained before, the small-scale sample would behave more dilative when prepared in the same relative density as the prototype soil at constant void ratio. Therefore, the model soil must be prepared looser to represent the constitutive behavior of the prototype soil. The goal is to cover a realistic range of full-scale (prototype) relative densities from medium dense (D_{rp} of ~65%) to very dense (D_{rp} of ~100%).

The tests were performed using Westerly Beach sand having an e_{min} and e_{max} of 0.44 and 0.84, respectively (Bradshaw et al. 2016). As presented earlier by Equations 6 and 7, the corresponding values of relative density of the model soils would need to be 28% for a prototype density of 65%, and 65% for a prototype relative density of 100%.

It is also important to ensure that the walls and bottom of the test tank will have minimal influence on the test results. As a first approximation the anticipated failure surface during pullout should not intersect with the tank walls. Embedment ratios of less than 5 have a shallow failure where the failure extends to the ground surface as shown in Figure 3a. Meyerhof and Adams (1968) state that embedment ratios (H/D) > 5 suggest deep failure mode which has more of a localized flow failure (Figure 4). Mitch and Clemence (1985) suggest a H/D ratio of larger than 4 for the deep failure mode. The embedment ratio of the anchor used in the current study is 9. Hence the expected failure shape is anticipated to be a deep failure.

Equations by Das et al. (2013) suggest that the radial zone of influence for a deep failure mode would be roughly 48 cm for dense sand and 42 cm for loose sand [see Figure 3b]. Thus, the tank and anchor diameter were selected to meet this criterion. Also, the tank will be buried in the ground and would provide similar lateral stiffness conditions as in the free field.

3.2 Experimental Setup

The 1g physical model testing facility at URI Bay Campus consists of two 250-gallon plastic tanks buried about 1.2 m into the ground. Westerly Beach sand was used for all experiments and the properties of the sand properties are given in Table 4.

Figure 7 – Photographs of the test site setup with driver and anchor attached.

A hydraulic driver system was used to install anchors into the sand as shown in Figure 6. The driver system was designed and fabricated by Triton Systems, Inc. The installation system is suspended from a gantry crane and lowered using a block and tackle system. For lower loads (i.e. < 3000 N) the anchors were pulled out using the gantry crane using an electric winch. For higher loads, load frame with a pneumatic jack was used as shown in Figure 19.

During installation and pullout using the gantry crane, the following sensors were used:

- A 20,000 lb. Load Cell manufactured by Transducer Techniques [Figure 8a]
- A 5,000 lb.-in Torque sensor manufactured by Transducer Techniques [Figure 8b]
- A 50” string potentiometer manufactured by TE Connectivity [Figure 9b].

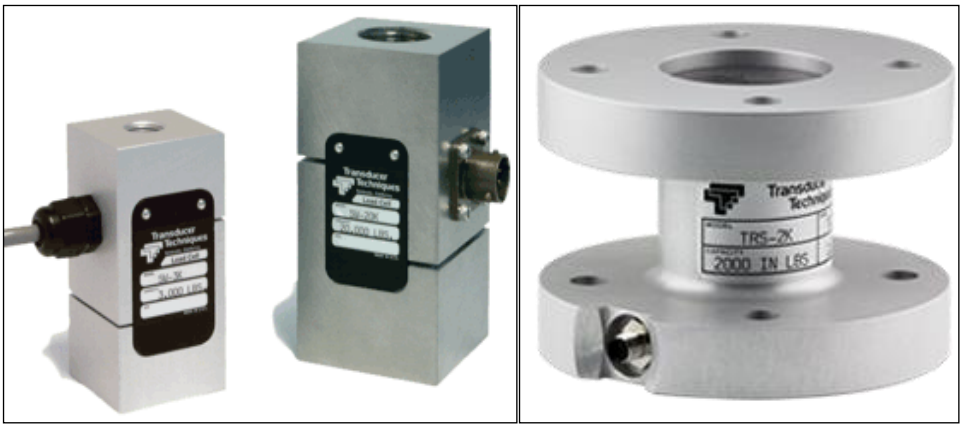

Figure 8 – (a) 20,000 lbs. load cell and (b) 5,000 lb-in torque transducer both manufactured by transducer techniques [Transducer Techniques 2018]

For pullout with the pneumatic load frame system the following sensors were used:

- A 10,000 lb. Through-hole load cell manufactured by Omega [Figure 9a]
- A 50” string potentiometer manufactured by TE Connectivity [Figure 9b]

are used.

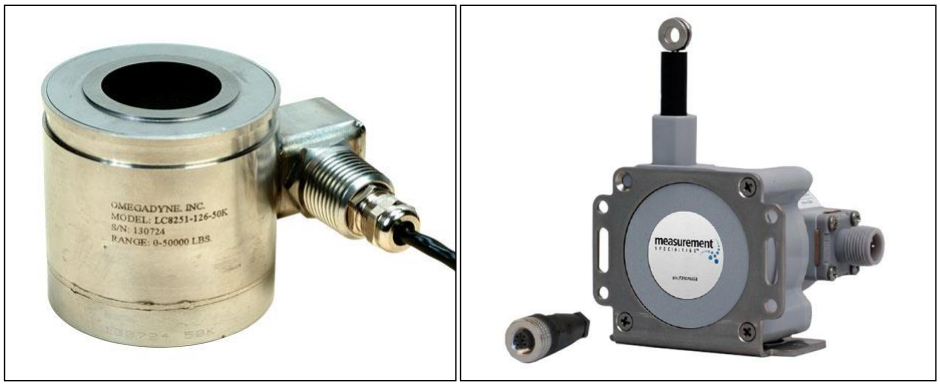

Figure 9 –(a) 10,000 lbs. through-hole load cell manufactured by Omega and (b) 50" string pot manufactured by TE Connectivity [TE Connectivity 2018] [Omega [2018]

All the devices were connected to an IO-Tech Personal DAQ56, which is then connected to the computer via USB. Electrical power for the computer and sensors was provided by a portable Honda generator. Data were acquired at a rate of 3.096Hz. Data points were recorded in real time to an Excel spreadsheet. This way, every data series had the same time stamps and could be compared easily.

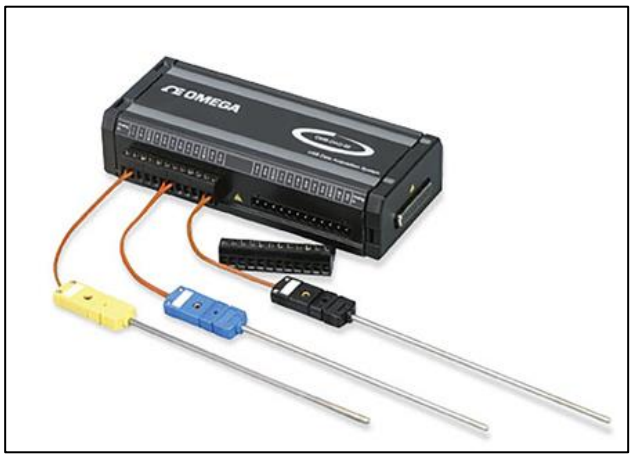

Figure 10 – Personal DAQ56 manufactured by Omega [Omega 2018]

3.3 Sensor Calibration

Since the Personal DAQ 56 can only provide data in the form of voltage, calibration had to be done for some of the devices. However, the 20,000 lbs. load cell came with an “OPT-TEDS Plug & Play Option”, a device which calibrates he load cell automatically when plugged in the associated load cell display. But the voltage data received by the Personal DAQ56 still had to be converted to load in Newtons. Therefore, weights were put on the load cell and voltage was recorded for 20 seconds to get a reasonable average output. The load in Newton was compared to voltage and the average was taken as factor of conversion. As shown in Figure 10 the calibration constant was 445.6N/V.

The 10,000-lb through-hole load cell was calibrated similar to the block load cell. Weights were put on a steel bar attached with a screw nut. Measurements for various increments were taken and compared to the output voltage. The resulting factor is 1,821,605N/V. This value is also comparable to the given values in the manual for the load cell.

For the SP2-50 string pot, voltage ranges between 0V for 0m displacement and 10.1 V for 1.27m (50 inch) maximum displacement. These values have been provided by the user manual, but they have also been confirmed. Calibration was performed by pulling out the string at various measured distances and recording the voltage for 10 seconds. The resulting calibration factor was 0.1265m/V.

Calibration of the torque transducer required a more complex setup. Since the torque transducer is permanently fixed to the driver, the driver was put in a leveled position. Then, a steel bar was put through the pinhole, poisoned centered and fixed in

that position. Voltage was recorded for 10 seconds and later taken as the zero reading. After that, a 4 kg weight was put on the steel bar in increments of 10 cm distance on either side of the bar. Voltage was recorded again for 10 seconds and averaged. For each increment a value for Nm/V was computed and averaged over all increments. The conversion factor for the torque transducer was 29,375 Nm/V.

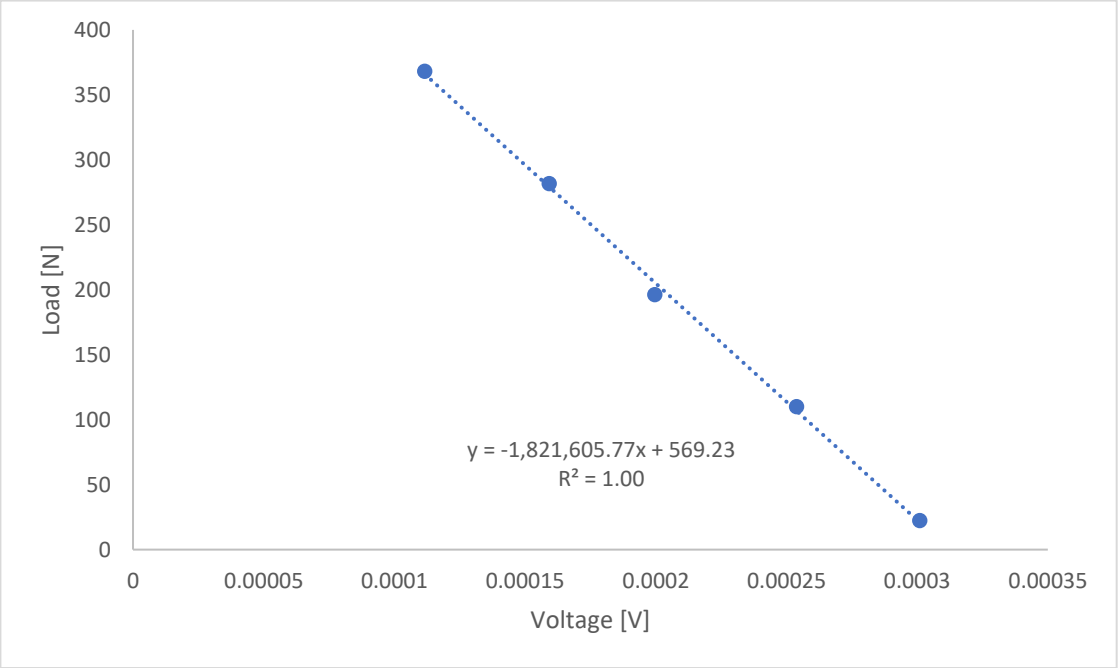

Figure 11 – Calibration data for 10,000 lbs. load cell

3.4 Sample Preparation

Pluviation of dry sand was performed using all-purpose bucket with a hose containing a plate with holes and sieves as shown in Figure 11a. The density of the deposited sand could be controlled by changing the diameter of the holes in the plate and/or drop height of the sand.

In order to get a sample of loose sand with about 28% relative density, the bucket was filled up with sand and the hose was placed 15 cm above the base of the tank. For this density, the hose only has two steel meshes as sieves. The sand was pluviated at a rate of about 1 cm per minute in the tank.

The dense sample was pluviated with the same device. To get a relative sand density of about 65%, a plastic plate with eleven 8mm diameter holes was placed in the middle of the hose. Pluviation was much slower with a rate of only 0.25cm per minute. The sand grains have more time to align and leave fewer voids, thus creating a denser sample. The sand properties can be found in Table 4.

To monitor the soil unit weight and assure constancy, three plastic containers of a known volume were put in the tank and pluviated every 30 cm [see Figure 12b]. The containers were then weighed, and the unit weight and relative density were calculated. Once the sand was pluviated to a height of about 135cm, pluviation was complete. The data for the different test containers can be found in Table 4. After pluviation, a single anchor was installed and subsequently pulled out.

Table 4 - Average Sand Properties for loose and dense sand experiments

Sand Type	Relative Density [%]	Unit Weight [kN/m^3]	Peak Friction Angle [°]	Average grain size [mm]
Loose Sand	28	15.00	37.5	0.3
Dense Sand	65	16.50	42.7	0.3

Figure 12 – Photographs of (a) pluviator device and sand tank (b) sand containers before pluviation

3.5 Initial Test Setup

The initial setup was adjusted by exchanging the pluviator device for the 20k load cell, which is zeroed with only its own weight. Below the load cell, the driver was attached using a shackle and a swivel. Also, the driver system comes with two horizontal bars, which were used to balance the driver and to put additional crowd force on the anchor for the dense sand experiments. The torque transducer was built into the driver system and the string pot was also attached to a fixed point on the driver. The anchor was attached to the driver using a single through-bolt and installed at a constant rate that depended on the anchor that was tested as described below.

Figure 13 – Photograph of the driver system in installation setup without (a) and with anchor (b)

3.6 Anchors used for Experiments

3.6.1 Plain Anchor

The model anchor that was used in all experiments was manufactured by Triton Systems, Inc. using low carbon Structural Steel. It is approximately a 1/5 scale version of the *C107-0861 24" X 8" pipe A.B. Chance Anchor*. The overall length is 152.4 cm. The shaft has an outer diameter of 4.57 cm and inner diameter of 4.27 cm. On the bottom part of the shaft, a 12.7 cm diameter blade is attached to the pile. Also, the leading edge of the pile is sharpened in a 45-degree angle. The thickness of the helix plate was 3.8 mm. At the bottom of the pile, a removable steel plug was mounted inside of the pile shaft to force a "plugged" condition as needed [see Figure 14]. This so called plain or baseline anchor was used for experiments to have a reference for comparing the performance of the anchors having various modifications as described in the next sections.

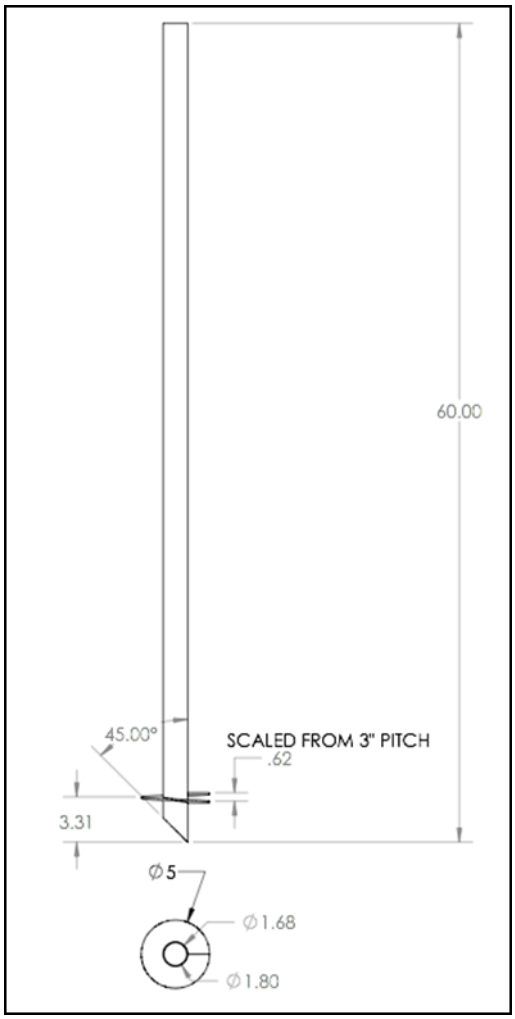

Figure 14 – Drawing of the anchor used in all experiments.

Figure 15 – Photograph of the baseline anchor.

3.6.2 Anchor with Rough Plate Surfaces

One modification that was made to the anchor was to roughen the anchor plate surfaces. The top and bottom of the blade were coated in a two-component epoxy adhesive. A sheet of sandpaper was attached to the blade. The sandpaper made the plate thicker, with a dimension of 4.7 mm. Also, installation and pullout were conducted in the same way as the baseline anchor [Figure 16].

Figure 16 – Photograph of the anchor with sand paper attached to the helix plates.

3.6.3 Anchor with Smooth Plate Surfaces

Another modification was to make the helix anchor plates smooth. Thus, all impurities and previous changes are removed, and a sheet of Teflon was attached to the pile blade using the 3M 300 LSE adhesive. Again, the anchor shaft remained unmodified. For the smoothened anchor, the plate thickness was 5.1 mm. Installation speed was still at 12 rpm [see Figure 17].

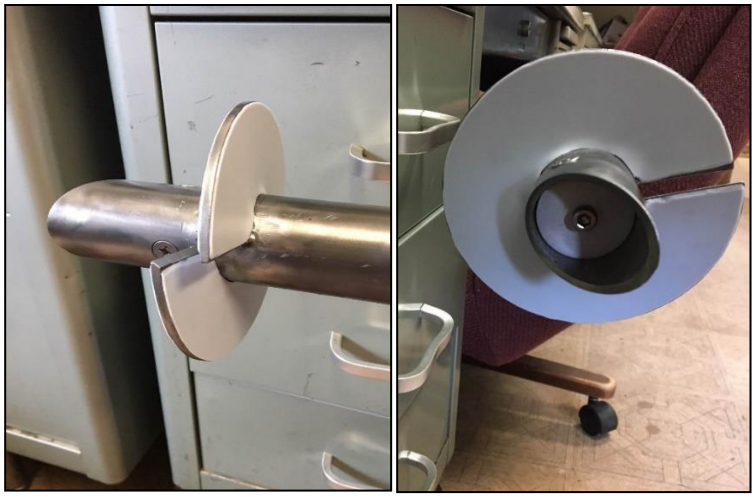

Figure 17 – Photograph of the anchor with Teflon sheet attached

3.6.4 Anchor with Internal Shaft “Jetting”

The third change of the anchor was to avoid shaft plugging by removing soil from inside the shaft during installation. It is presumed that in the full-scale anchor, the soil could be removed from inside the shaft using water jets, for example. A vacuum was used to remove the soil in the model. Flexible silicone tubes were fixed inside the anchor shaft with a piece of Styrofoam. The tubes were led out of the shaft at the anchor top. These tubes were attached to a vacuum. An extended hose was wrapped around the pile during installation. Through these tubes, sand from the inside of the shaft was vacuumed out to avoid formation of a sand plug in the shaft. This technique will be called “jetting” and it does not bring any changes to the anchors dimensions. For the “jetting” method, installation speed is decreased to 8 rpm. This is because the tubes attached to the anchor can only vacuum out sand at a rate of 0.3 kg/minute. Which equals roughly 14.5 cm of pile advancement into the sand and

thus a theoretical volume of 184cm^3 of displaced sand. Vacuuming speed could not be increased, since the hoses were too small and would clog up otherwise. The Styrofoam plug was used to maintain the position of the tubes and guarantee constant sand removal from the inside of the shaft. Also, the "jetting" process was not initiated until the pile has plunged and revolved 3 times. This is because otherwise a crater would form under the pile [see Figure 18].

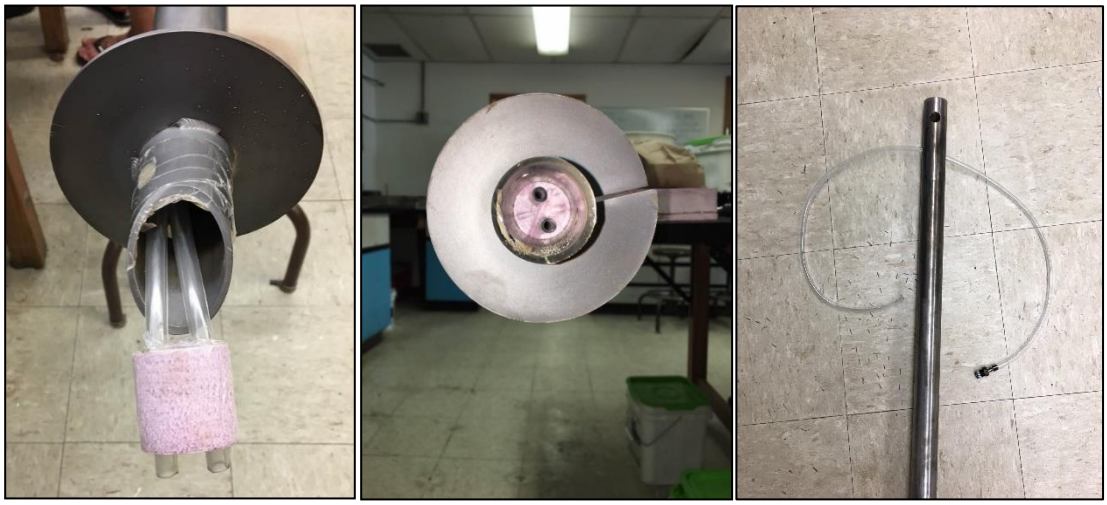

Figure 18 – Photograph of the anchor with vacuuming / jetting equipment attached.

3.7 Anchor Load Testing

At the start of each test all measurement devices were connected to the data acquisition system. A “zero” reading for Torque was noted with the anchor attached and freely hanging. The zero reading of the string pot was taken as the helix touched the sand surface but did not yet statically plunge under the self-weight of the driver. At this point the pulley system was released and the anchor could move freely, thus statically plunging. The anchors were installed with a constant downward vertical crowd force, which is exerted by dead weight. The plunge depth was noted, and the installation process was started by activating the hydraulic pump. Installation occurred at a rate of 8 to 12 rpm. The total installation depth was approximately 115 cm and measured from the lowest part of the helix to the original sand surface of the sand. During installation, the position of the driver was constantly monitored and corrected to ensure that the anchor remained vertical. Also, it was very important that the pulley system was not blocked and could move freely, so that constant crowd force can be assured. During installation the data cable for the torque transducer was wrapped around the pile top / driver.

Once the installation process was complete, the string pot was disconnected from the driver and the driver was carefully removed from the pile. This was particularly important the for loose samples that were more prone to disturbance.

Figure 19 – Photograph of the driver and a fully installed anchor in loose sand

The anchor was then load tested using the gantry and electric winch for loose tests or a hydraulic jack for the dense tests. For the loose sand, the 20k load cell was attached to the pulley system and connected to the pile shaft with a rope. The string pot was attached to the pile to measure displacement. The anchor was pulled out at a rate of about 0.025m/s. Vertical force and displacement were monitored throughout the entire pullout process and then plotted on the same scale for comparability.

The anchors in the dense sand were load tested using a load frame and pneumatic jack as shown in Figure 20. A steel beam consisting of two steel I-beam sections was supported by several bricks on each side of the tank. A steel rod was attached to the pile and leads through the gap between the two I-beams. The steel rod was placed through the hydraulic jack and a through-bolt load cell. A nut tied the rod down to the load cell. Besides that, the string pot was attached to the system to monitor displacement. Pullout was performed at a much slower rate of about 10cm / minute. Also, pullout was carried out in many increments, since the steel bar had to be raised for each pullout step. After a few loading increments, the gantry crane was used

to remove the anchor. Again, vertical force and displacement were measured and plotted to compare each pullout process in dense sand.

Figure 20 – Photograph of a pullout performed by pneumatic jack system

CHAPTER 4 – RESULTS AND DISCUSSION

This chapter presents the results of the experimental program including an analysis and discussion of test results. The data from all load tests are also presented in the appendix.

4.1 Results

4.1.1 Preliminary Tests

Three preliminary tests were performed in loose sand to develop the experimental setup and methodology. During these initial experiments, it was observed that for a plain anchor with an open-ended shaft, a sand "plug" formed inside the shaft. This plug had a total length of about 15 cm, which was 13% of the total embedded shaft length. Thus, it was decided to conduct most of the experiments with plugged conditions – meaning the metal plate was attached to the bottom of the shaft to force a plugged condition. Also, it was found that the driver itself plus the balance bars put enough crowd force on the anchor for installation in loose sand. Hence, the crowd force was reduced from about 900 N to 680 N. When too much crowd force was applied to the driver, the anchor over-penetrated meaning that in one revolution the anchor embedded more than the pitch of the anchor. Perko (2009) suggests that to minimize disturbance, the anchor should be installed at a penetration rate that is at least 80% of the blade pitch for each revolutions of the anchor. The experimental setup

did not allow for the anchors to be installed at a constant displacement and for this reason installation was performed at constant crowd force.

4.1.2 Loose Sand Anchor Tests

The anchor tests are designated using a three-letter abbreviation, including the first letter L = loose or D = dense, second letter P = plain, R = rough, S = smooth, J = jetted, third letter O = open-ended or C = closed ended, followed by the test number. For example, DSO2 would be dense, smooth, open-ended anchor test number two. The results of all anchor tests are presented in Appendices A and B and a summary of these results is discussed below.

The plain, unmodified anchor test (LPC1) will be used as the baseline for comparison. As shown in Figure 21, advancement into the sand was higher than 80% of the anchor pitch throughout the last 90 cm of installation. The unit weight of the sand is within a range of 2% of the average for each layer. The anchor was installed in two runs with a short break in between due to a minor problem with the data acquisition at about 55 cm depth. The total installation depth was 115 cm and the average torque over the last 38 cm (three times the blade diameter) was 28 Nm, thus it has likely not been influenced by the break. The maximum pullout load was 1800 N [detailed plots in the appendix] at about 4.1 cm displacement [see Figure 24], which results in a torque factor of $64 m^{-1}$ for LPC1. The torque factor is defined as the pullout load [N] over the installation torque [Nm] as mentioned in the introduction. Therefore, the torque factor K_t has the unit m^{-1}.

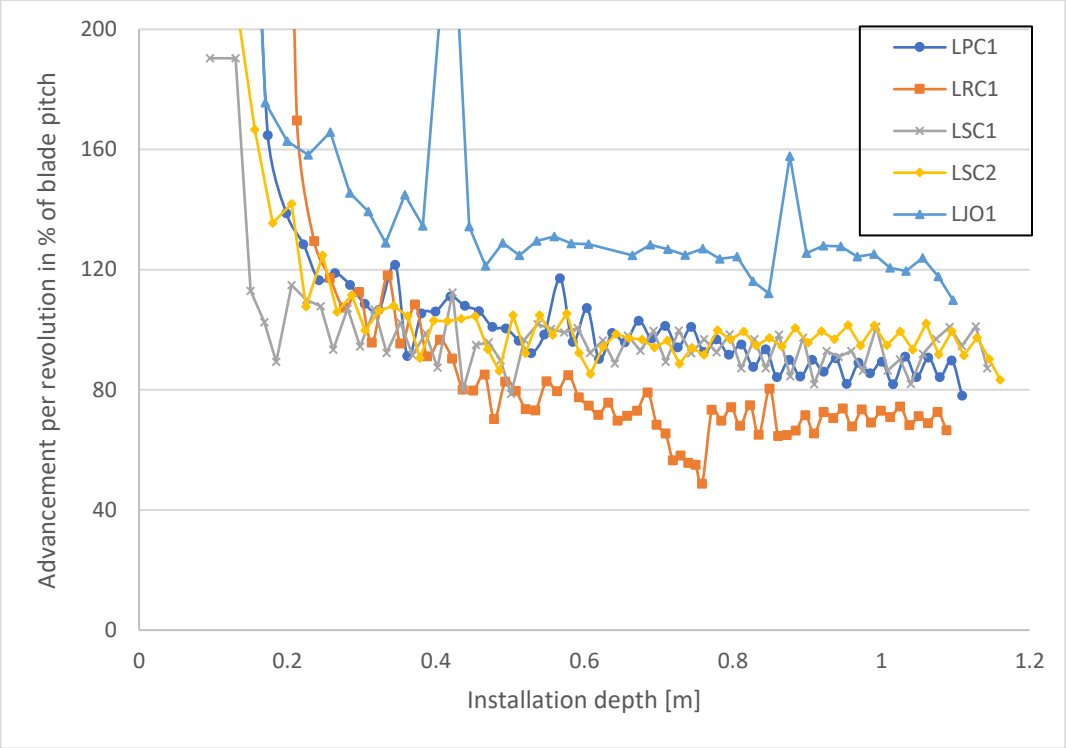

Figure 21 – Advancement per revolution during installation for loose sand tests

The rough anchor (LRC1) was installed without any problems or breaks. Results show slightly denser sand pluviation for the lower sand layers. The two upper layers show slightly looser density compared to the loose sand average. Like the plain anchor, the rough anchor was installed to a depth of 115 cm. Average installation torque over the last 38 cm was 32 Nm – an increase of 17% [see Figure 22]. Installation rate was somewhat lower with an average of 65% to 100% of the anchor pitch [see Figure 21]. Also, the pullout capacity with 2000 N at about 3 cm displacement is about 10% higher than for anchor LPC1. After the test, it was observed that the sheet of sandpaper was still attached to the blade. However, the torque factor appears to be slightly lower compared to the baseline anchor.

Table 5– Input and output values for anchor tests in loose sand

Anchor Type	Average sand relative density (%)	Installation depth (cm)	Total revolutions	Installation torque (Nm)	Ultimate Pullout load (N)	Torque factor (m^{-1})
LPC1	27	115	60	28	1800	64
LRC1	29	115	61	32	2000	62
LSC1	27	115	62.5	23	1450	63
LSC2	28	116	56	19.5	1450	75
LJO1	27	115	38	19	1250	66

For the smooth anchor (LSC1) the sand unit weight is close to the overall average for loose sand [see Figure 23]. Installation was performed without problems to a depth of 115 cm. Also, the installation rate was stable around 95% of the anchor pitch throughout almost the entire installation process. For the last three blade diameters, the average installation torque was 23 Nm [see Figure 22] – 17% lower than the plain anchor. Also, the pullout capacity was 20% lower with 1450 N [see Figure 24]. This results in a torque factor of 62 m^{-1} close to the rough anchors' value.

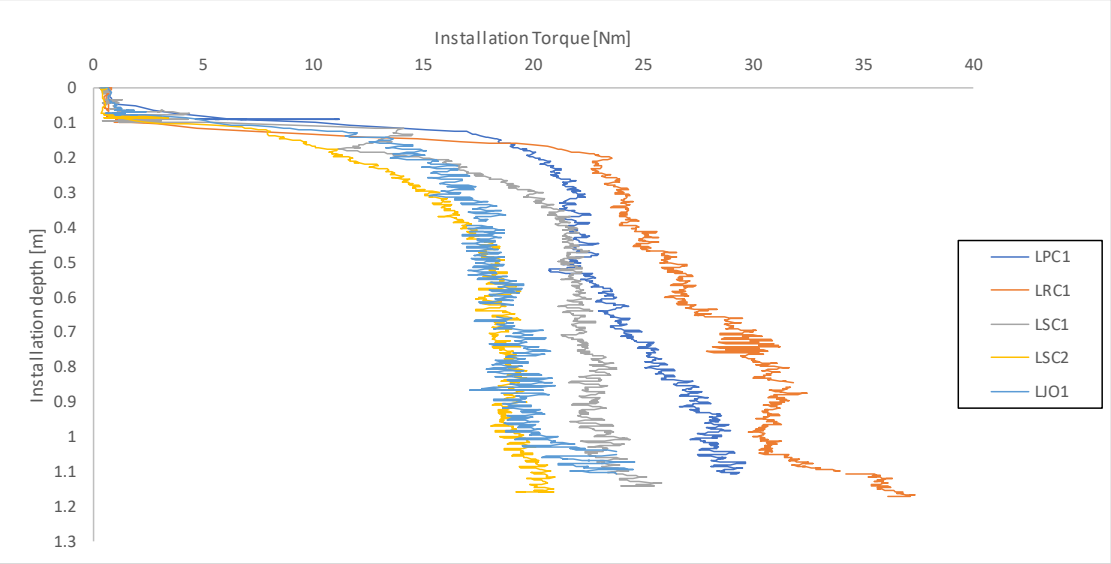

Figure 22 – Installation torque over depth for anchors in loose sand

Since the values for torque and pullout were much lower, the test was repeated to confirm the previous results. For LSC2, the second Teflon anchor, installation torque was even lower than for anchor LSC1. Yet, the pullout capacity remained more or less constant, resulting in a torque factor of 75 m^{-1}. Both smooth anchors had the pullout peak at about 4.5cm displacement. Also, the sand sample was clearly close to the average sand sample for loose sand. It should be noted, that installation depth for LSC2 was 116 cm. Since the two smooth surface anchors are consistent in pullout capacity but not in installation torque, it is questionable where the differences for two technically identical experiments.

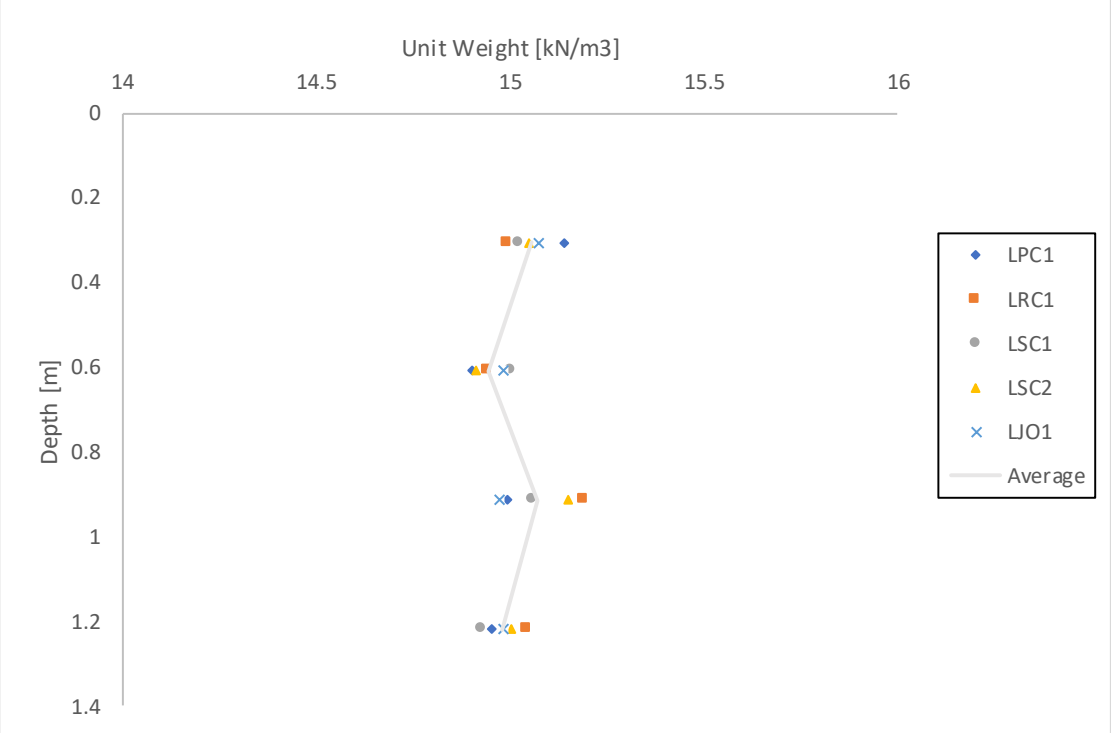

Figure 23 – Sand properties for loose sand experiments

The jetted anchor (LJO1), was installed in average sand conditions to a depth of 115 cm. For the jetted tests, the installation speed was reduced to7.75 rpm. The reason for the slower installation rate is the jetting (vacuuming) technique. Two tubes

are led down the pile shaft of which one vacuums sand out and one provides airflow from outside of the pile. As it turns out, these tubes were not able to transport the sand volume quick enough to maintain the installation speed of 12 rpm. The fastest possible rate was determined at 7.75 rpm, at which the vacuumed sand corresponds the theoretically displaced sand volume. However, it took only 38 revolutions to install anchor LJO1 with this technique– 40% less than anchor LPC1. Therefore, the advancement rate of the pile was frequently higher than 120% of the blade pitch [see Figure 21].

Installation was conducted in four runs. The three breaks are due to the vacuuming of the soil. About every 9 revolutions of installation, the vacuum hose had to be unwrapped from the anchor to ensure steady sand disposal. For each break, the vacuum cleaner was emptied, and the sand was weighed for each increment. The amount of sand vacuumed remained rather constant throughout the installation process and totaled to 1.915kg. 1.915kg is the equivalent amount of 87.5 cm height of inner shaft volume of sand vacuumed out. Also, installation torque and pullout load were the lowest of all anchor in loose sand 19 Nm and 1250 N respectively [see Figures 22 and 24]. A decrease of more than 30 % for each value. The peak pullout load was reached at 7.2 cm of displacement. The torque factor though, is almost the same as for the plain anchor. It should also be noted that the foam plug, to which the tubes were attached inside the pile, did not moved during installation and pullout.

During the pullout of all anchors in loose sand, surface deflections were not visible by eye during the peak load.

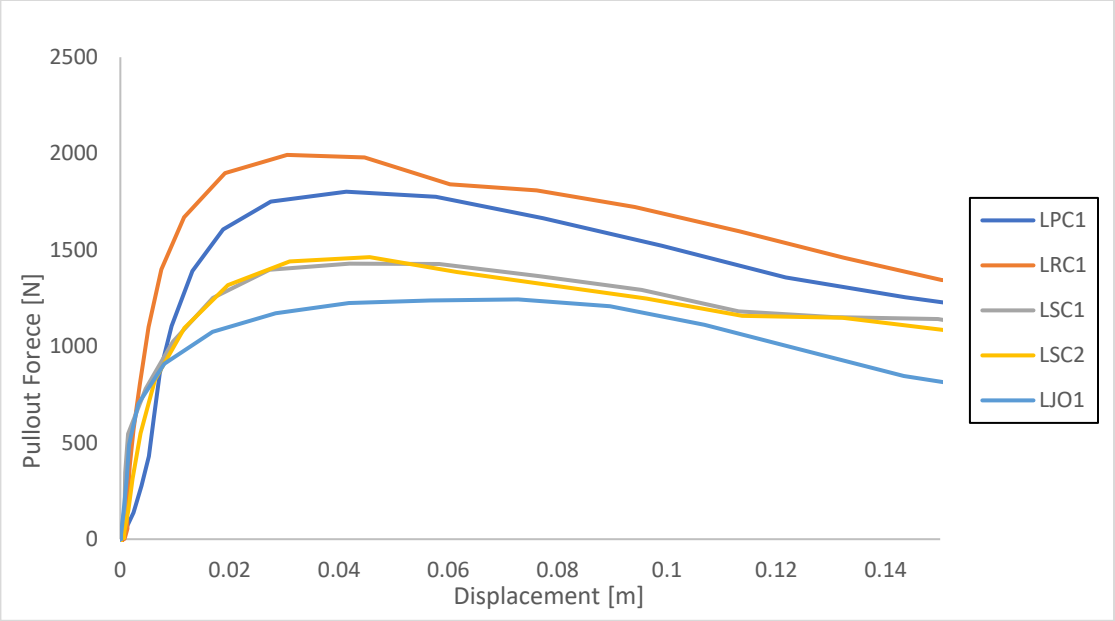

Figure 24 – Pullout load over displacement for anchors in loose sand

4.1.3 Dense Sand Anchor Tests

Similar to the tests in loose sand, the plain anchors (DCP 1 and DPC2) in dense sand will be used as a baseline for comparison. As shown in Figure 25 and Table 6 the unit weights were very consistent in all tests with an average of approximately 16.5 kN/m^3.

Table 6 - Input and output values for anchor tests in dense sand

Anchor Type	Average sand relative density (%)	Installation depth (cm)	Total revolutions	Installation torque (Nm)	Pullout load (N)	Torque factor (m^{-1})
DPC1	*65*	*115*	*87*	*204*	*8700*	*43*
DPC2	65	115	67	208	7500	36
DRC1	*65*	*115*	*86.5*	*210*	*8550*	*41*
DSC1	*65*	*115*	*65.5*	*182*	*9100*	*50*
DJO1	66	115	48	84	5800	69

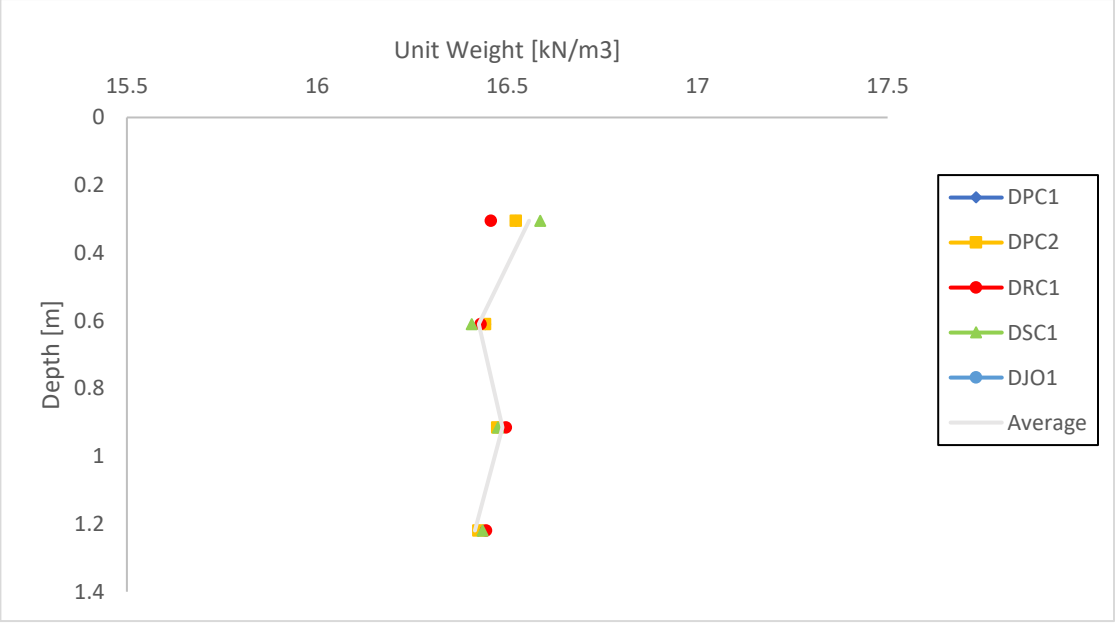

Figure 25 - Sand properties for dense sand experiments

After testing DPC1 using a crowd of 680 N, it was observed that 87 revolutions were necessary to install the anchor. As shown in Figure 26, this corresponds to less than 50% of the anchors pitch for a large part of installation. The installation rate started off high with an advancement over 300% of the pitch but then fell below 80% after only eight revolutions. Therefore, DCP2 was tested using a higher crowd force of 2550 N. The increase in crowd force allowed that anchor to penetrate at about 60% of the pitch [see Figure 26]. The average installation torque at the end of installation was 208 Nm [see Figure 27].

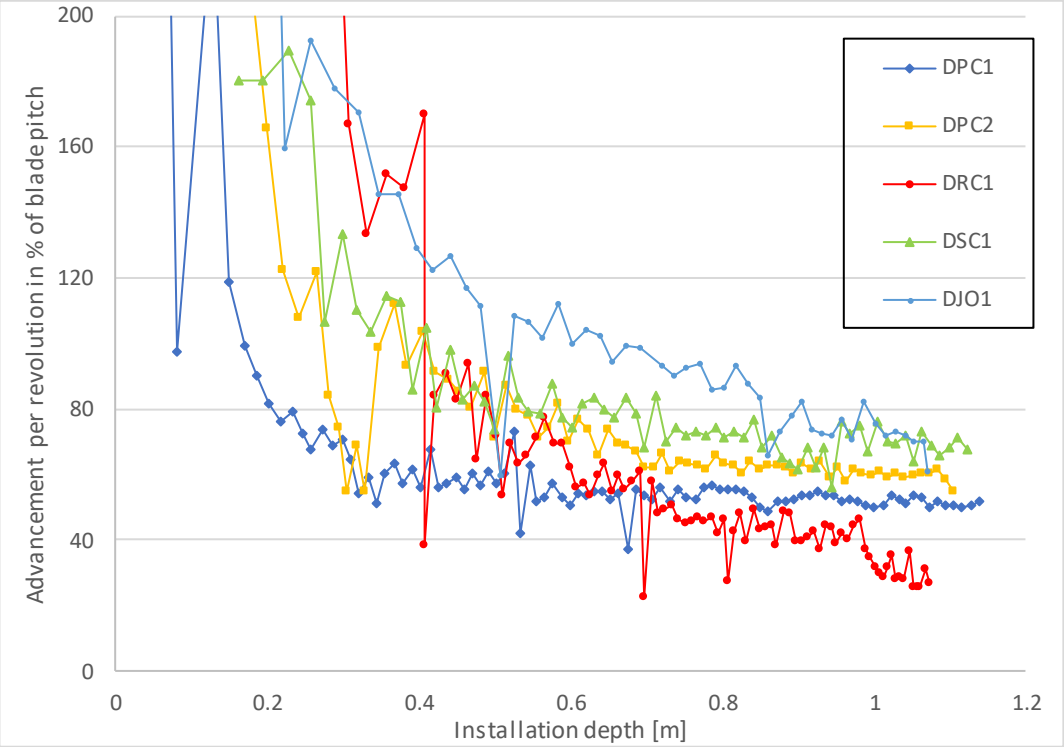

Figure 26 - Advancement per revolution during installation for dense sand tests

A pullout load of 7500 N was reached 3 cm displacement and thus a torque factor of 36 m^{-1} was calculated [see Figure 30].

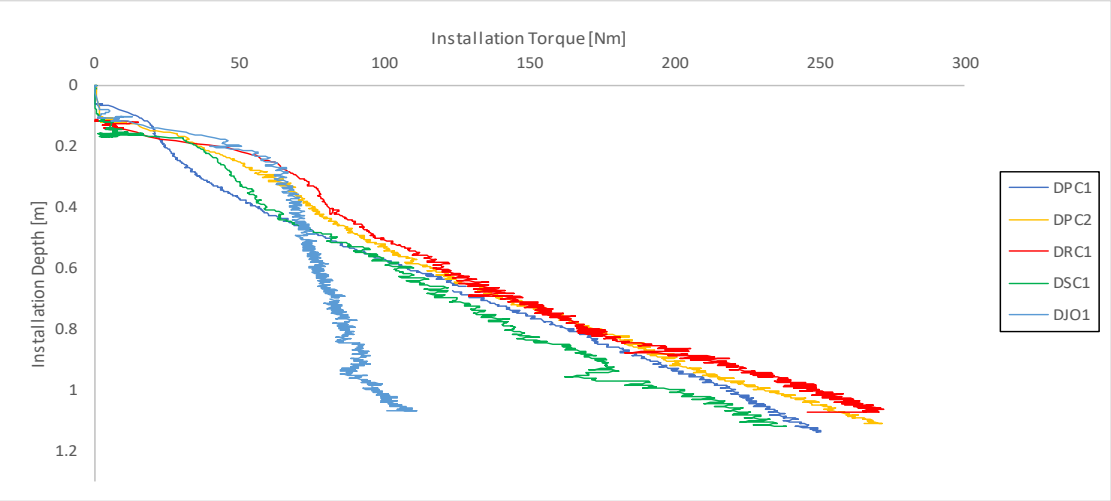

Figure 27 – Installation torque over depth for anchors in dense sand

Installation of the rough anchor (DRC1) was performed using the same crowd force as DCP2 (2550 N). However, as shown in Figure 25 the anchor underpenetrated. Installation torque and pullout load increased to 210 Nm and 8550 N respectively. The pullout load peak was reached at 2.5 cm displacement. The torque factor has also increased to 40 m^{-1}. However, it should be noted again that the anchor advancement into the sand was very unsteady. Also, after the pullout it was visible the about half of the sand paper from the bottom of the plate was removed [see Figure 28].

Figure 28 – Damaged sand paper on anchor DRC1 after installation and pullout

The fourth installed anchor in dense sand was prepared and coated with a sheet of Teflon. Since the Teflon is thicker than the sandpaper, the edge was sharpened to avoid the Teflon from peeling off [see Figure 17]. Installation occurred, as usual, with a rate of 12 rpm and was performed without any problems or breaks. Installation depth was 115cm and it took 65.5 revolutions to get the anchor down. This equals on average an advancement of 1.66cm per revolution or 93% of the anchor pitch [see Figure 26]. Nevertheless, after about half of the installation depth the advancement rate dropped below 80% of the blades' pitch. Installation torque for the last 38 cm was 182 Nm – about 10% lower than for anchor DPC2 [see Figure 27]. On the other hand, pullout load has not changed much and thus the torque factor increased by 38% to a total of 50 m^{-1}. The pullout peak was reached after 2.8 cm displacement of the pile. After that, the pullout has shown that the Teflon coating of the top plate was ripped off

and stayed on the plate with the smooth side faced down [see Figure 29]. It was not possible to determine at which depth the Teflon sheet came off, thus this experiment will likely be repeated.

Figure 29 – Damaged Teflon sheet on anchor DSC1 after pullout

A jetted version of the anchor, DJO1, was also installed in dense sand. A rate of 7.75 rpm was repeatedly chosen since the sand volume to vacuum out of the shaft does not change significantly with the increased sand density. Installation depth was, again, 115 cm, but only 48 revolutions were necessary to fully set the pile. The advancement rate is between 120% and 70% of the blade pitch for the most part of the installation [see Figure 26]. Anchor DJO1 has shown a 60% lower installation torque than anchor DPC1 – 84 Nm [see Figure 27]. Also, pullout load has decreased to 5800 N at 4.5 cm displacement, a reduction of 23% [see Figure 30]. Consequently, the torque factor has increased to 69 m^{-1}. Just as LJO1, during installation and pullout of DJO1, the foam plug did not move in the pile shaft. The vacuumed mass of sand

totaled 2556.8 g, which equals a shaft length of 106 cm of removed sand at a density of 16.5 kN/m^3.

During the pullout of all anchors in dense sand, surface deflections were not visible by eye while the peak load was reached.

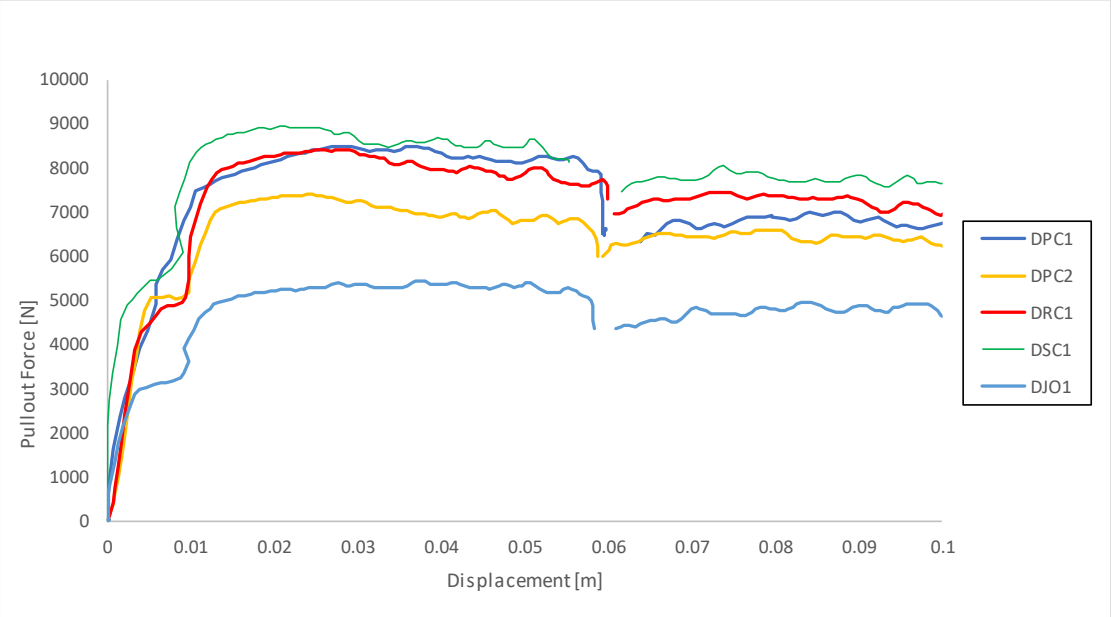

Figure 30 - Pullout load over displacement for anchors in dense sand

4.2 Discussion of Results

4.2.1 Anchor Penetration

For all tests in loose and dense sand, the penetration rate was recorded. As mentioned before, these experiments were limited to constant crowd force and could unfortunately not use a constant penetration rate. Therefore, the advancement into the soil is inconstant and not always in the range of >80% of the anchors' pitch [see Figures 21 and 26]. This suggests that soil has been disturbed by either augering the sample for under penetration or plunging the sample for overpenetration. Generally, one can say, that penetration rate in loose sand was within that range for anchors LPC1, LSC1 and LSC2 over the last 38 cm. On the contrary anchor LJO1 over penetrated the soil – the advancement was higher than 120% of the blade pitch throughout most of the installation process. This suggests that the jetting equipment eased the installation of the anchor. Also, only 48 total revolutions were needed to install the anchor to a depth of 115 cm. However, anchor LRC1 did not remain within the suggested advancement rate and has thus likely disturbed the soil during installation.

The installation of the anchors in dense sand was more problematic. None of the anchors remained above the range of 80 % the anchors' pitch and thus it is likely that all anchors have disturbed the soil sample during installation by "augering" [see Figure 26].

4.2.2 Installation Torque

Regarding the installation torque, it can generally be stated that a smoother surface and thus a lower interface friction angle decreases installation torque. This can clearly be seen when comparing anchors LSC1 and LSC2 to LPC1. The opposite effect occurs for a roughened surface, anchor LRC1 has a higher installation torque than LPC1 [see Figures 21 and 26]. Also, LJO1 had a decreased installation torque, which is likely caused by the reduced normal force on the upper anchor plate due to decreasing resistance under the anchor tip. The same effect could be reproduced in dense sand experiments, although differences were not as significant.

4.2.3 Pullout Capacity

Pullout capacities in loose sand ranged between 1250 N and 2000 N. The reason for the differences can be traced back to the installation process and the anchor plate surface. So, compared to LPC1, LRC1 had a slightly higher capacity [see Figure 31]. It is assumed that for the deep failure mode sand slips along the upper blade surface and that the increased roughness increases the resistance for that process. Also, LRC1 underpenetrated during installation, likely causing soil disturbance. Due to the under penetration the soil might have been augered and thus densified. Since these anchors were installed in loose sand, disturbance could lead to densification and thus the anchor capacity is increased.

For the smooth surface anchors the effect is assumed to be similar but reversed. As the installation is eased due to decreased interface friction between sand and Teflon, the pullout capacity is decreased since sand slips along the upper blade

surface. LSC1 and LSC2 have just like LPC1 likely not disturbed the soil during installation and thus are well comparable [see Figure 31].

Anchor LJO1 has the lowest pullout capacity of all anchors in loose sand. This might be reasoned by the disturbances caused by overpenetration during installation; the opposite of what happened for LRC1. Also, the soil under the anchor tip was vacuumed out which might possibly have decreased lateral earth pressure on the entire anchor.

The dense sand tests yielded a wider variability of results. The pullout loads ranged from 5800 N to 9100 N. Since none of the anchors have been installed at the recommended rate, and the surfaces of anchors DRC1 and DSC1 were destroyed during installation, it is well possible that the results presented are not meaningful. However, the pullout load of DRC1 has increased compared to DPC1, like in the loose sand tests. The reason is assumed to be an increased surface roughness again. Also, during installation the anchor possibly augered the soil, possibly causing disturbances. Yet, it is hard to say if the sample was densified or loosened in this case [see Figure 31].

Anchor DSC1 has also been installed likely causing soil disturbance. However, the pullout load is the highest of all anchors installed in dense sand. It is hard to explain this result, since the installation torque has decreased, like in the loose sand. Therefore, it was assumed, that the pullout load would be decreased as well. A possible explanation might be the soil disturbance during installation and the removed Teflon sheet. Due to these problems this test result is not meaningful.

The jetted anchor DJO1 had the lowest pullout load [see Figure 32], much like in the loose sand tests. It is assumed that the reasons for this observation are also the same: reduced lateral stresses and possibly disturbances during installation.

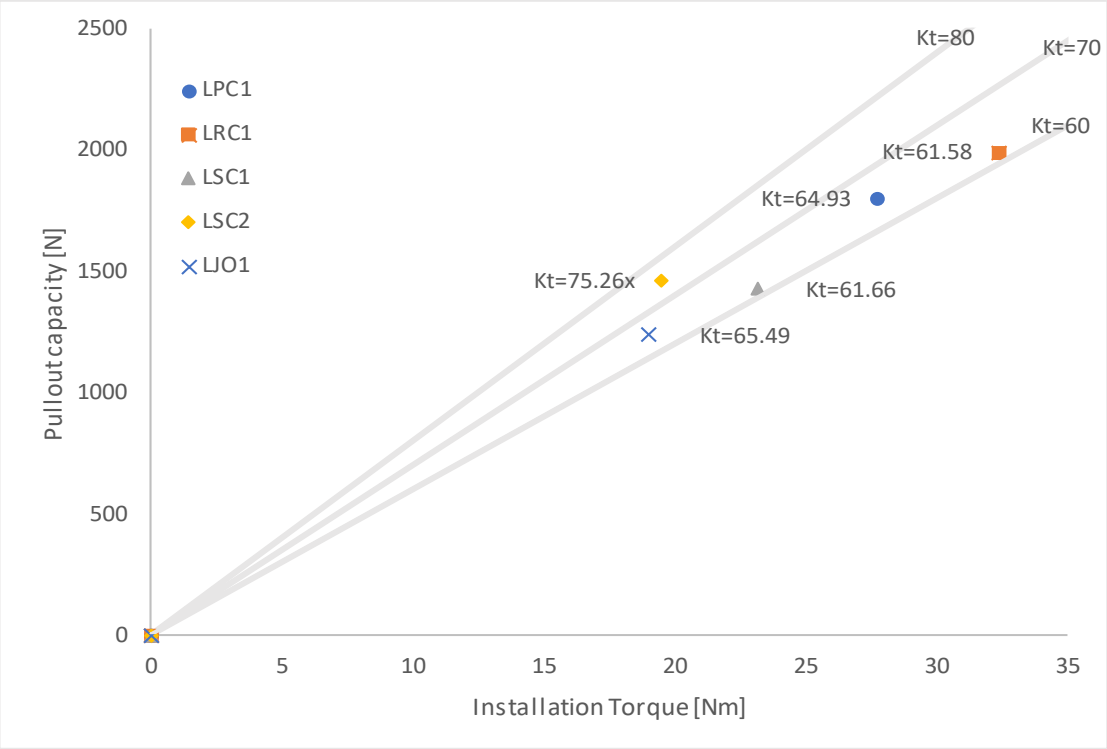

Figure 31 – Pullout capacity vs. Installation Torque for loose sand tests

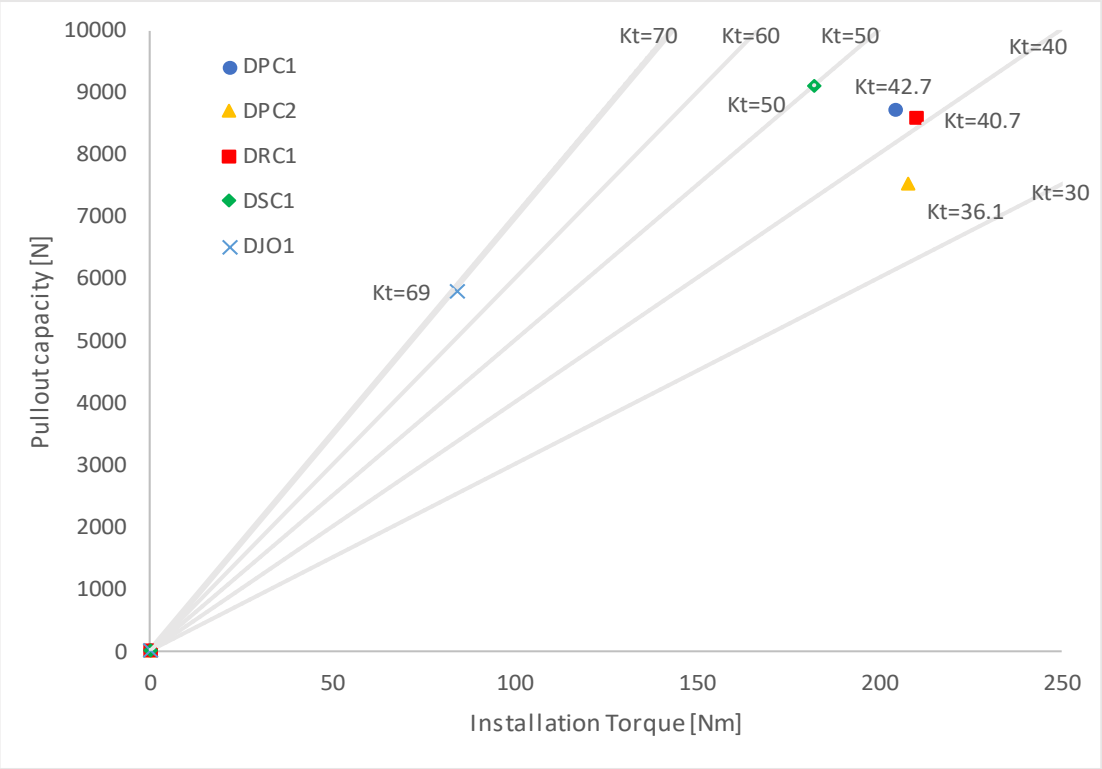

Figure 32 – Pullout capacity vs. Installation torque for dense sand tests

4.2.5 Geotechnical Efficiency

As stated in the objectives the goal was to find ways to improve the efficiency of a helical pile. An efficient pile is one that requires the least amount of torque to install (i.e. largest torque factor) but that maximizes the pullout capacity. The following definition for efficiency, therefore, is proposed which captures both aspects:

$$\eta = Qu \; x \; Kt = \frac{Q_u{}^2}{T} \qquad (8)$$

where Q_u = uplift capacity, T = installation torque and K_t = torque factor. The efficiencies were calculated for all tests and summarized in Tables 7 and 8. The largest number in each of the tables indicates the most efficient anchor.

Surprisingly, for the loose sand tests, the anchor with the rough blade surface has the highest value. This can be explained by the only slightly increased installation

torque but a much higher pullout load. The higher pullout load could be due to the significant augering that occurred that may have increase the density and strength of the soil above the anchor plate. Since the weight of all anchor tested is considered equal, this anchor also has the best capacity to weight ratio. On the contrary anchors LSC1 and LSC2 and especially LJO1 have a much lower efficiency, due to the low ultimate capacity [see Table 7].

For the dense sand tests, the anchor with the smooth blade surface had the highest efficiency, which has an increased capacity and a lower installation torque than the plain anchor. Still, the Teflon sheet of the anchor got ripped off during installation and thus its results are questionable.

Table 7 – Anchor Efficiency for loose sand tests

	LPC1	LRC1	LSC1	LSC2	LJO1
η	117,038	122,743	88,132	110,107	81,459

Table 8 – Anchor efficiency for dense sand tests

	DPC2	DPC1	DRC1	DSC1	DJO1
η	271,014	371,480	348,933	455,092	399,321

CHAPTER 5 - SUMMARY AND CONCLUSIONS

The primary objective of this thesis was to find ways to improve helical pile efficiency. A series of small-scale physical model experiments were conducted on anchors with different modifications to find ways that increase the torque factor and/or maximize the capacity. To fully compare efficiency, a concept was developed that includes the torque factor as well as the pullout capacity. The following findings can be summarized for anchor tests in loose and dense sand:

- Tests were performed under constant crowd and thus penetration rate varied with installation depth, and thus many anchors have under penetrated and some anchors have over penetrated during installation. This has likely caused soil disturbance, which makes it more difficult to compare results. Yet, some results suggest that under penetration (i.e. augering) in loose sand might actually densify the soil and increase the pullout capacity and efficiency.

- Regarding the installation torque it is reliable to say that smoother surfaces result in decreased installation torque. This was found for loose sand tests and could be reproduced in dense sand tests.

- Generally, it looks like pullout capacity behaves similar to installation torque; higher friction causes higher pullout loads and vice versa. This could be observed in loose sand tests and in most dense sand tests. The only exception is anchor DSC1. Although, for this anchor it is uncertain how the ripped off Teflon sheet changed the installation and pullout behavior.

- For the torque factor it is difficult to declare which modifications decrease or increase its values. Usually lower installation forces came along with lower pullout capacities and yet values vary a lot. It can be stated though, that improving the torque factor alone does not necessarily increase the overall anchor efficiency and benefits.

- When considering the geotechnical efficiency, the rough anchor had the highest efficiency in the loose sand. This could be due to densification of the soil during installation, which increased the pullout capacity. The smooth anchor appears to have the highest efficiency in dense sand due to the reduction in frictional forces during installation.

5.2 LIMITATIONS

Clearly one limitation of the conducted research is the inconstant anchor installation rate. For helical anchor installation in the field, a constant advancement of at least 80% of the anchor pitch is maintained. Therefore, crowd force is adjusted as needed and thus not a constant.

Besides that, anchor pullout is not performed at the same rate for loose and dense sample tests. Pullout curves for dense sand tests suggest, that a faster pullout rate results in higher loads as a slower pullout rate (see pullout of anchors DPC2 and DJO1 in the appendix).

Compared to conventional helical piles, the piles used in the experiments are not only smaller, but also the shaft diameter is fairly large compared to the helix diameter (Hubbellcdn.com 2018).

Moreover, this work mostly considers the capacity to installation torque ratio, but merely the capacity to weight ratio. To address overall efficiency of an anchor both ratios a possibly many more factors are to consider.

5.1 Suggestions for Future Research

To improve further testing it is suggested that the equipment be modified to install the anchors at constant rate rather than constant crowd. Also, it is recommended to use strong adhesives or coatings for anchor surface modifications, since the forces during installation caused damage to the treatments, particularly in the dense sand.

With regard to efficiency one should not only consider the torque factor, but also the pullout capacity and the pullout load to weight (or volume) ratio. Additionally, efficiency might include many more aspects, such as production and transportation costs, volume to capacity ratio, ecological footprint, benefits and losses of anchors in groups etc. This could only be achieved from a more thorough cost-benefit analysis.

APPENDICES

Appendix A: Calibration Data

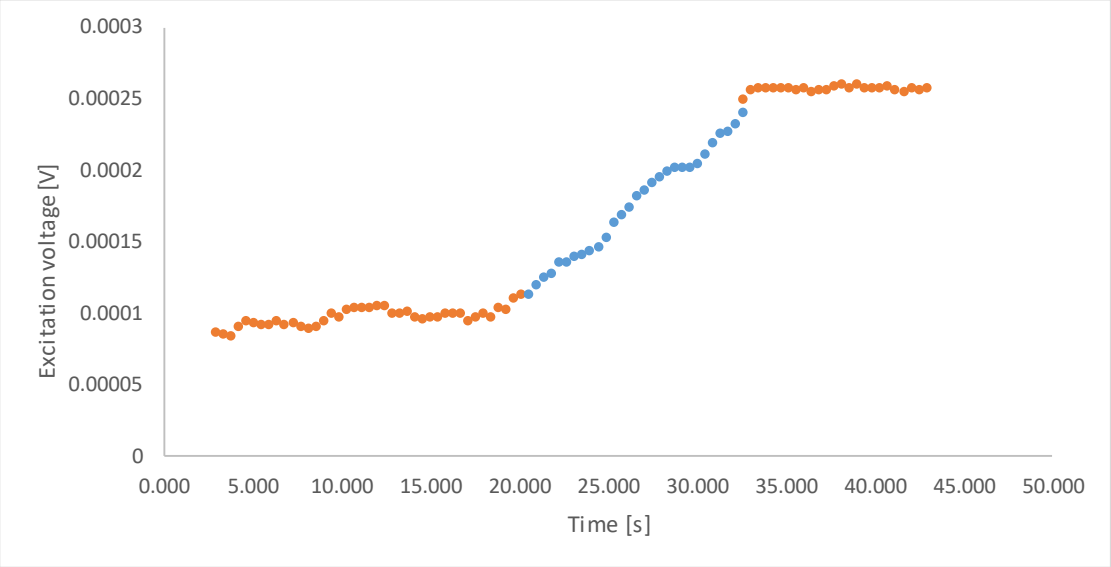

Figure 33 – Calibration of 20,000 lbs. load cell manufactured by Transducer Techniques

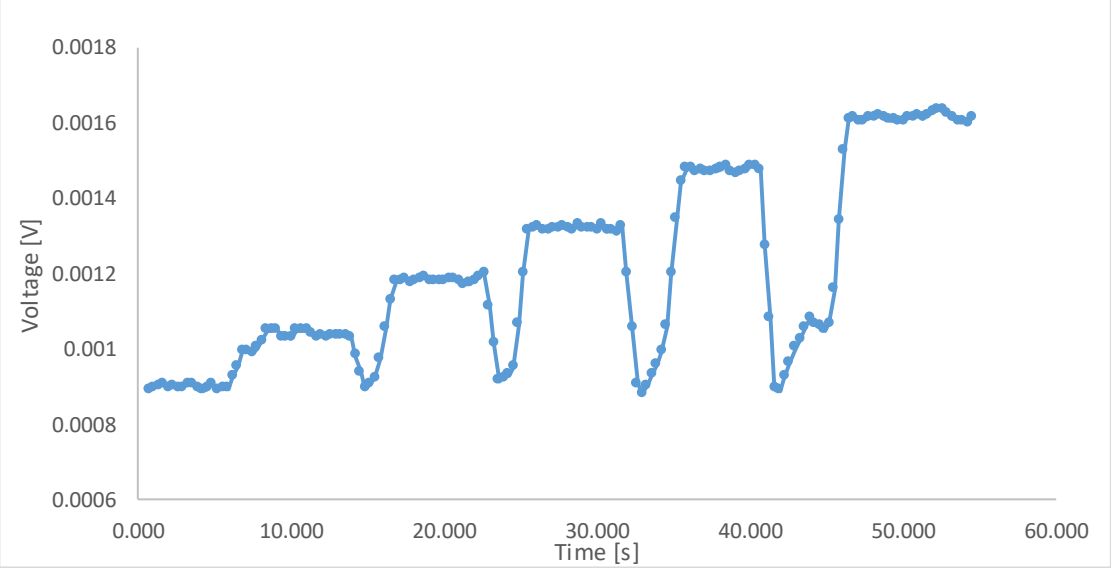

Figure 34 – Calibration of 5,000 lb.-in torque transducer manufactured by Transducer Techniques

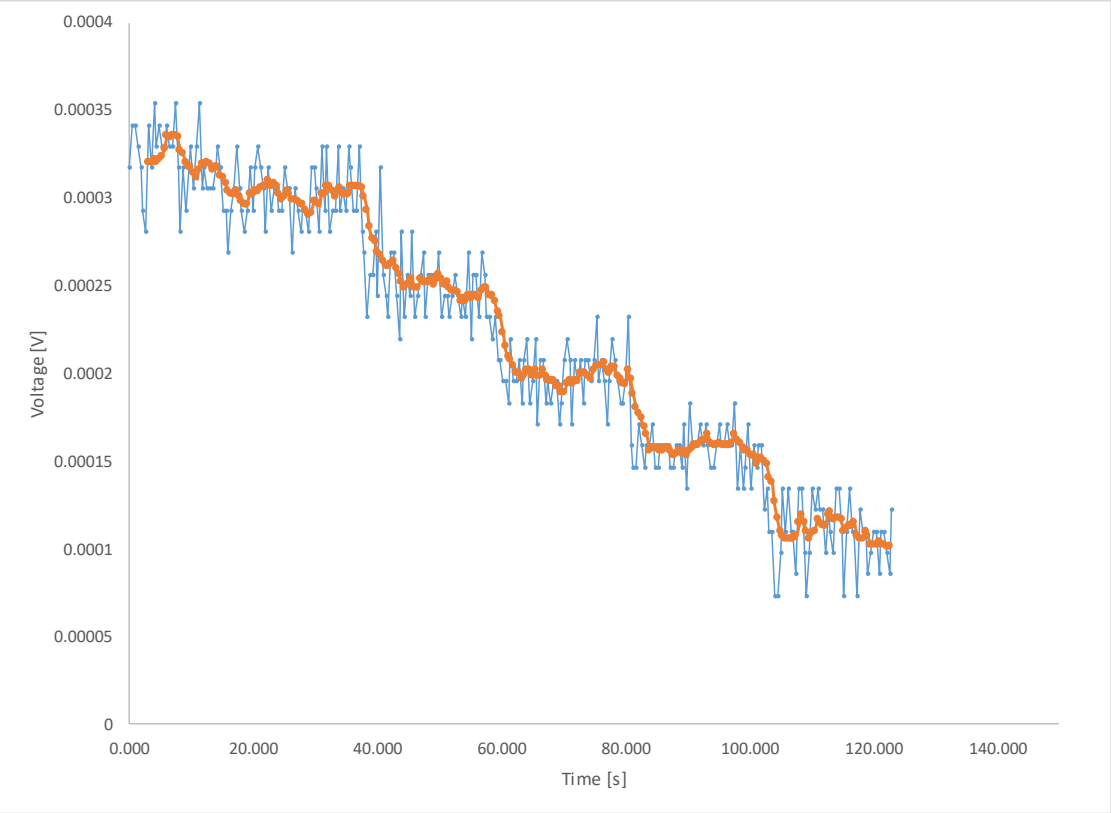

Figure 35 – Calibration of 10,000 lbs. through hole load cell manufactured by Omega

Appendix B: Loose sand Tests

For each anchor test, the plots of unit weight over depth, relative density over depth, installation torque over depth, average advancement per revolution during installation and pullout forces over depth are provided in that order.

Plain anchor [LPC1]

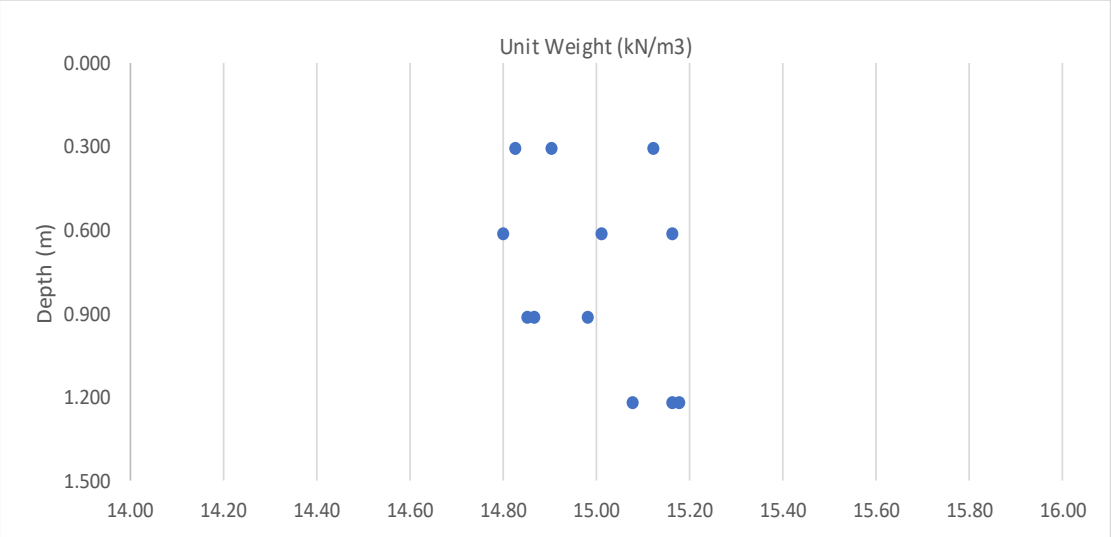

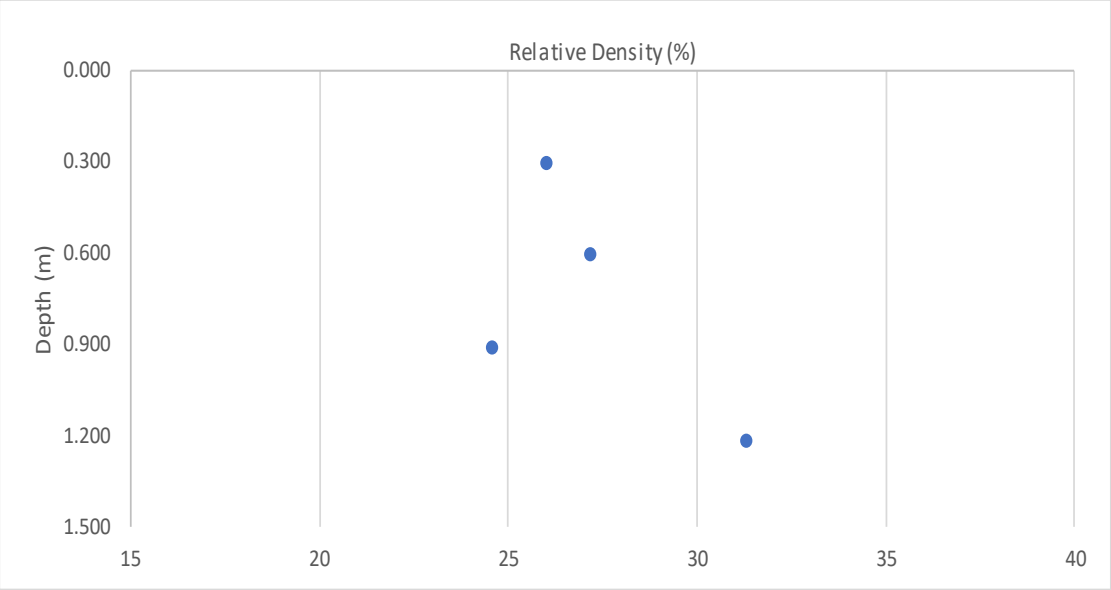

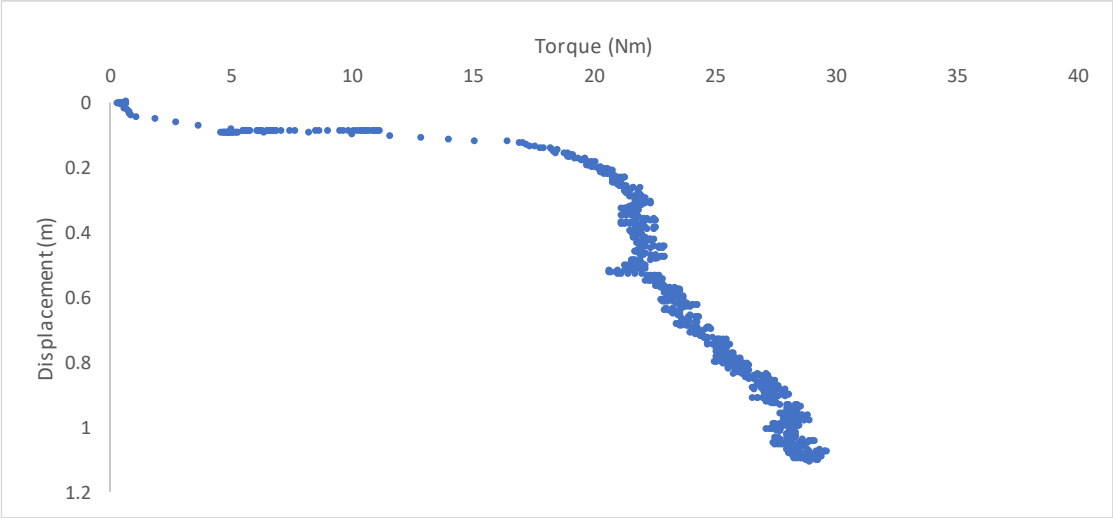
Torque (Nm)
0
5
10
15
20
25
30
35
40
Displacement (m)
0
0.2
0.4
0.6
0.8
1
1.2

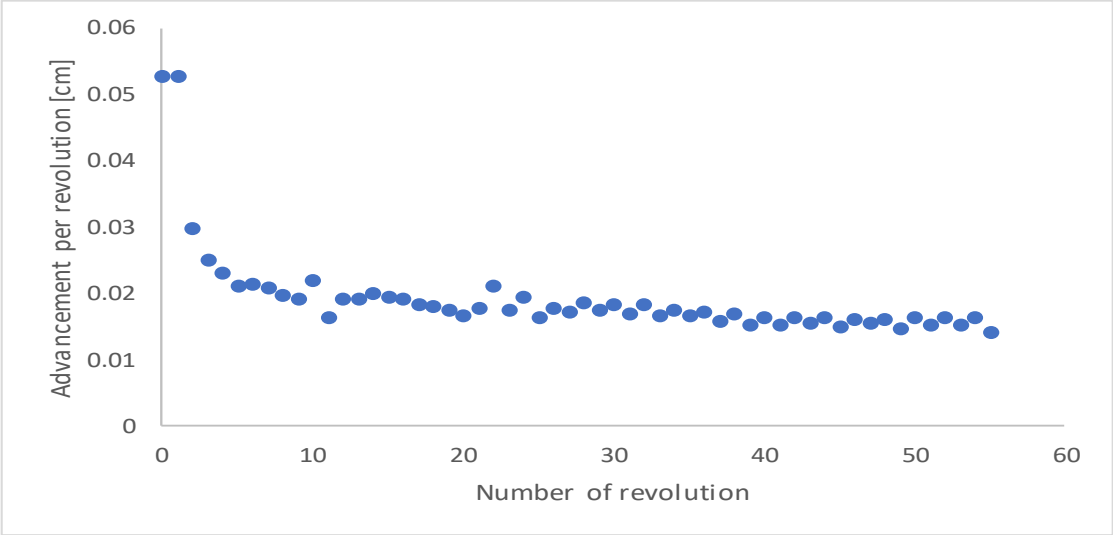
Advancement per revolution [cm]
0.06
0.05
0.04
0.03
0.02
0.01
0
0
10
20
30
40
50
60
Number of revolution

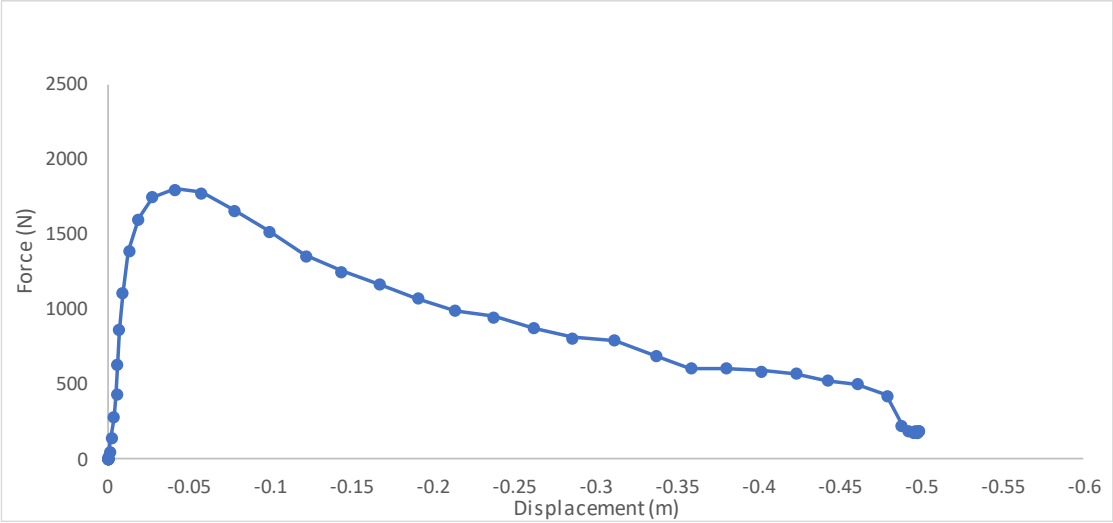
Force (N)
2500
2000
1500
1000
500
0
0
-0.05
-0.1
-0.15
-0.2
-0.25
-0.3
-0.35
-0.4
-0.45
-0.5
-0.55
-0.6
Displacement (m)

Rough anchor [LRC1]

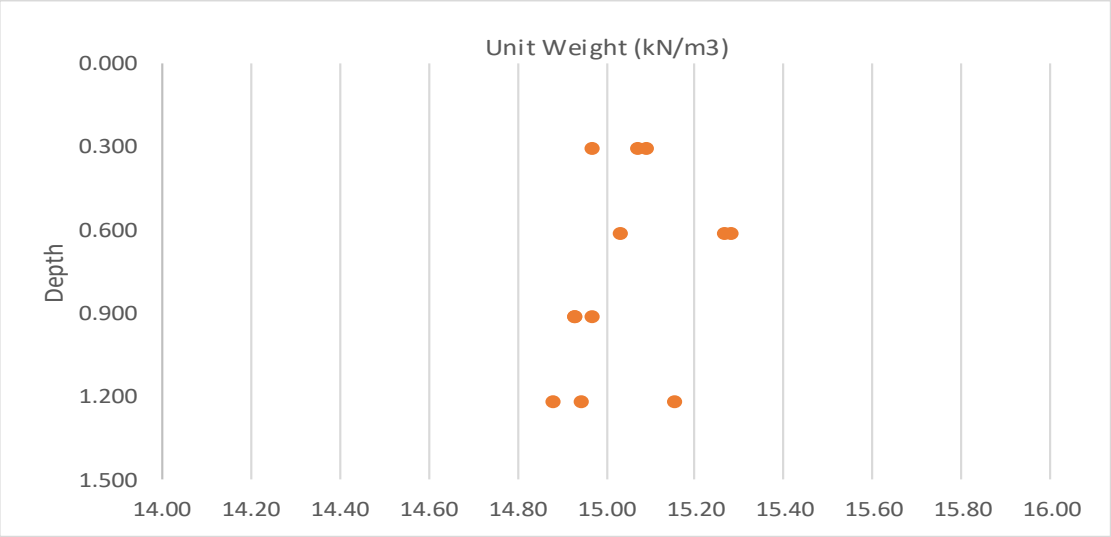

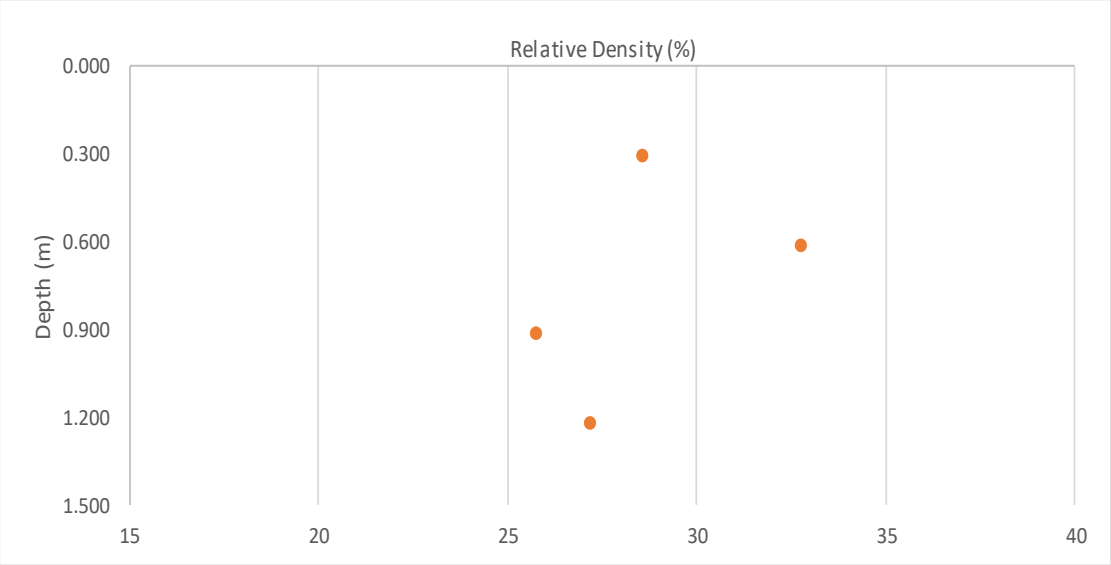

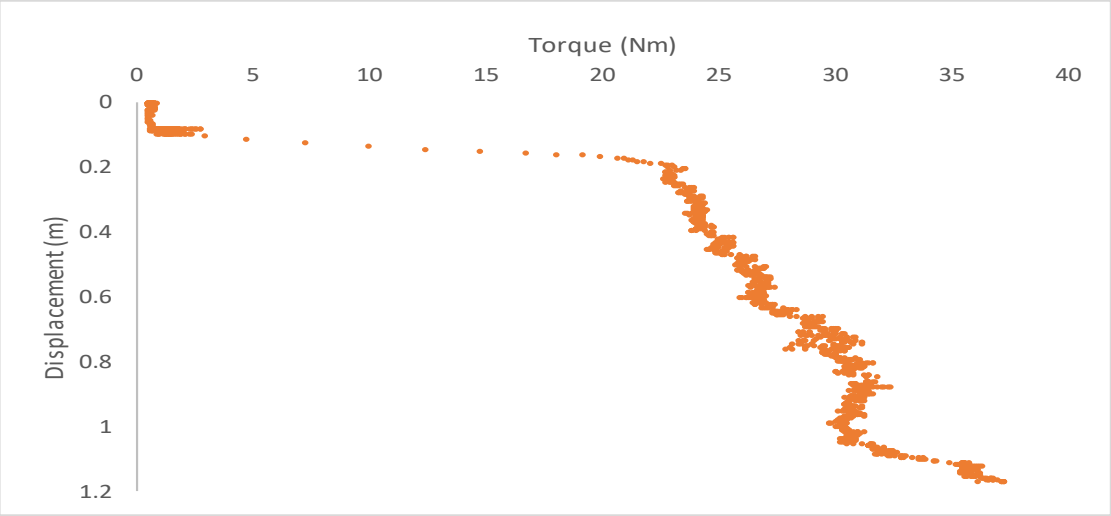
Torque (Nm)
0
5
10
15
20
25
30
35
40
Displacement (m)
0
0.2
0.4
0.6
0.8
1
1.2

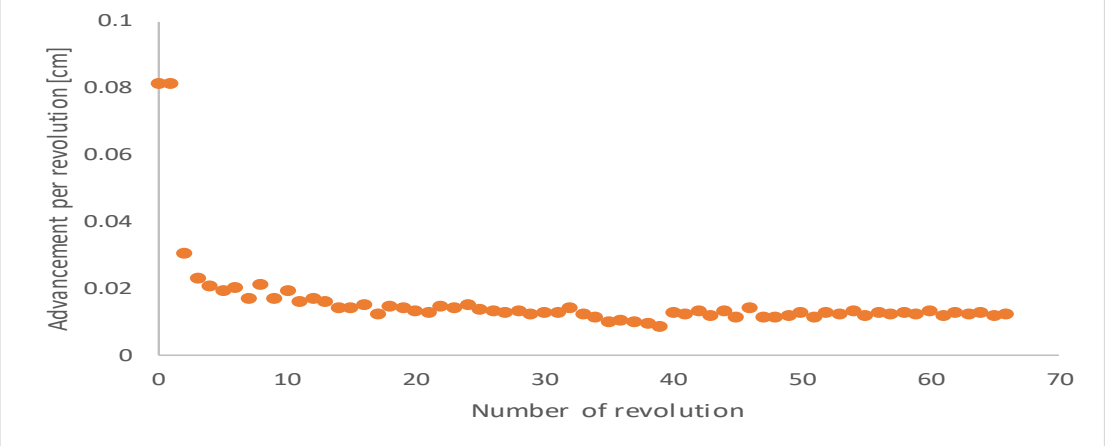
Advancement per revolution [cm]
0.1
0.08
0.06
0.04
0.02
0
0
10
20
30
40
50
60
70
Number of revolution

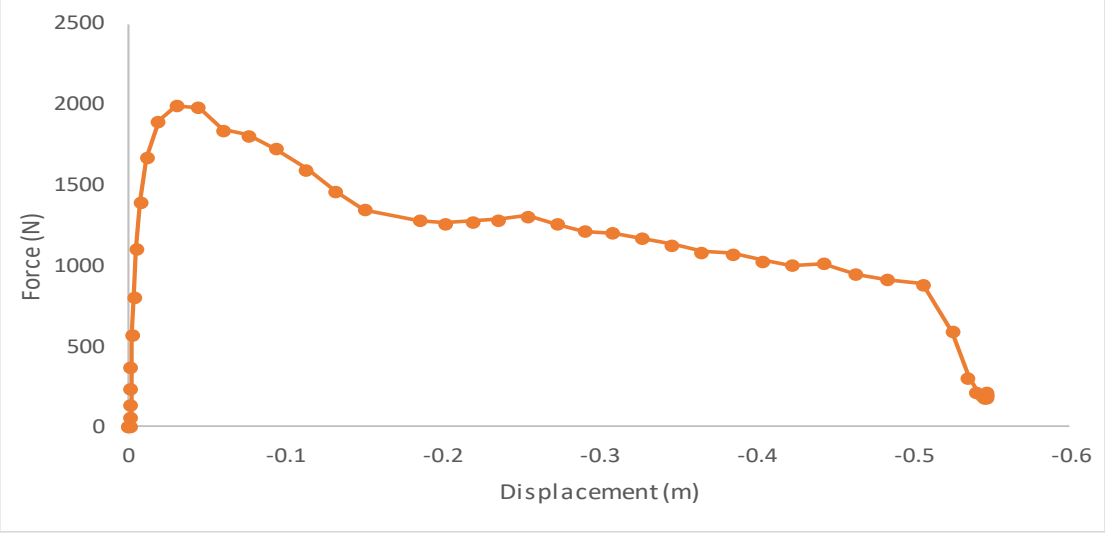
Force (N)
2500
2000
1500
1000
500
0
0
-0.1
-0.2
-0.3
-0.4
-0.5
-0.6
Displacement (m)

Smooth anchor 1 [LSC1]

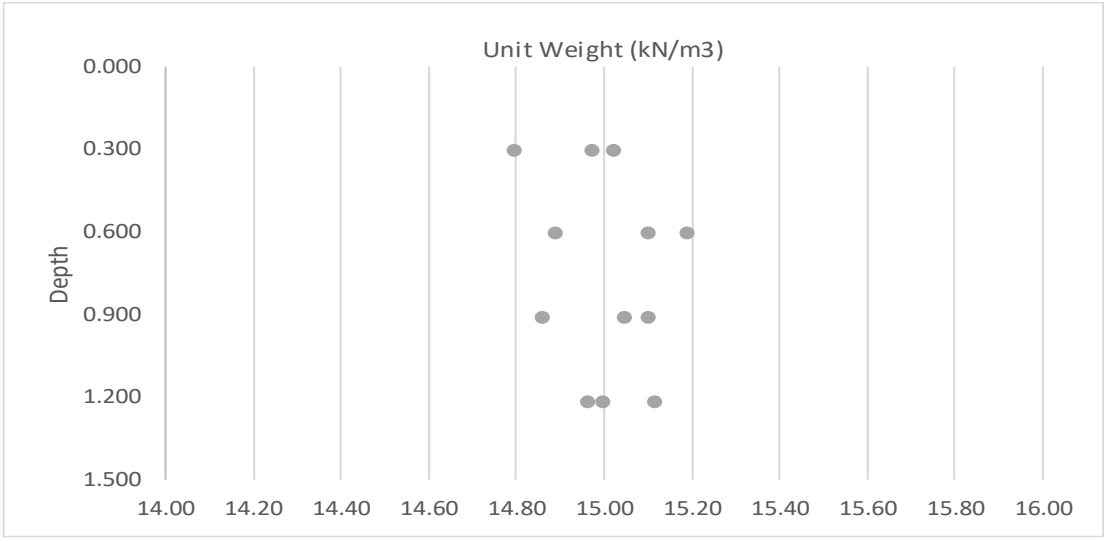

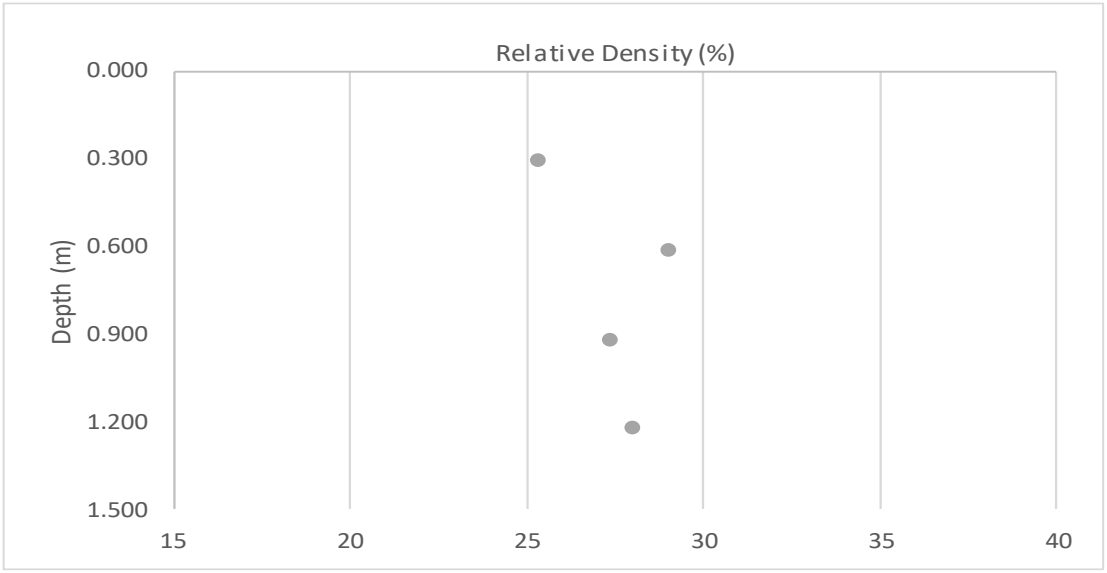

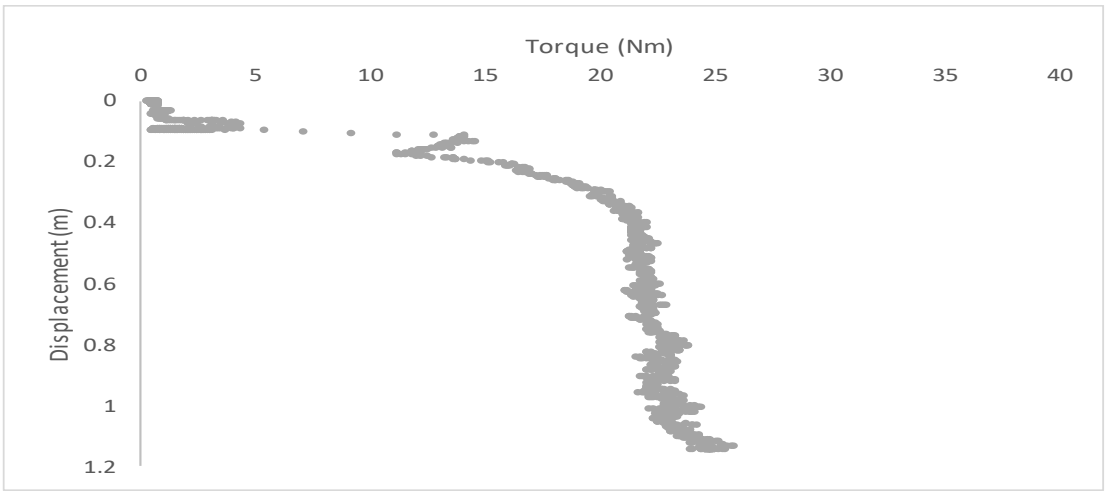
Torque (Nm)
0
5
10
15
20
25
30
35
40
Displacement (m)
0
0.2
0.4
0.6
0.8
1
1.2

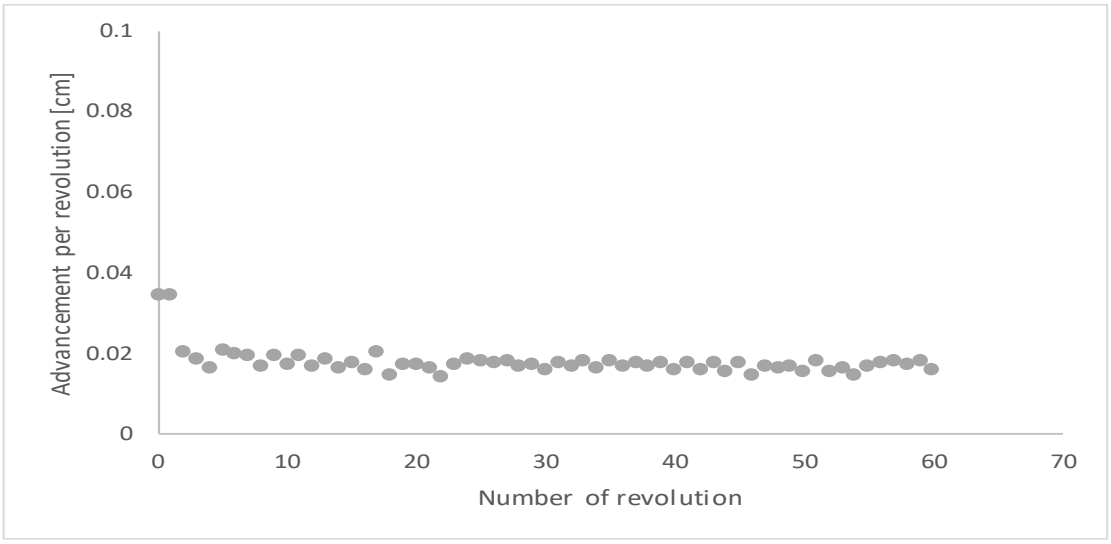
Advancement per revolution [cm]
0.1
0.08
0.06
0.04
0.02
0
0
10
20
30
40
50
60
70
Number of revolution

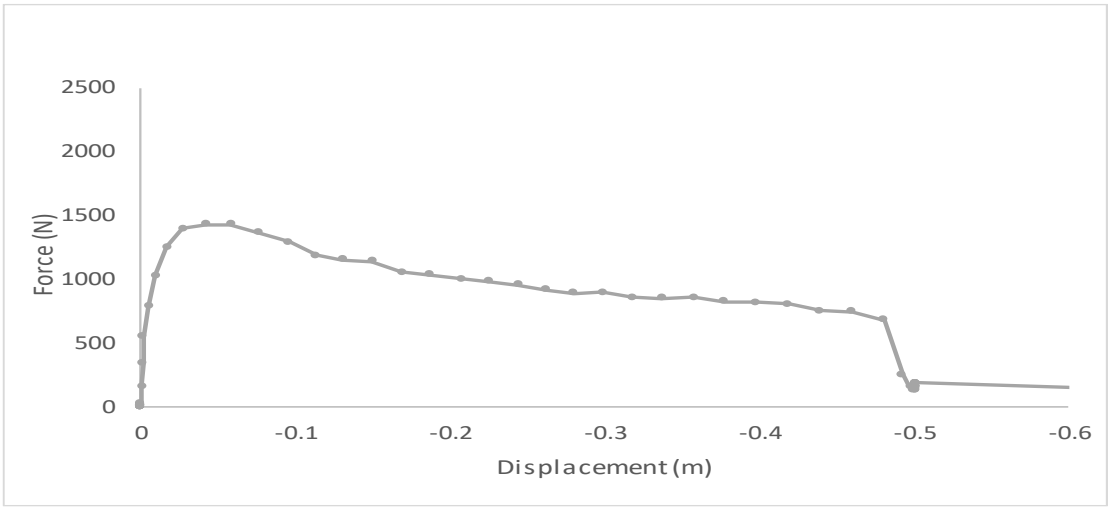
Force (N)
2500
2000
1500
1000
500
0
0
-0.1
-0.2
-0.3
-0.4
-0.5
-0.6
Displacement (m)

Smooth anchor 2 [LSC2]

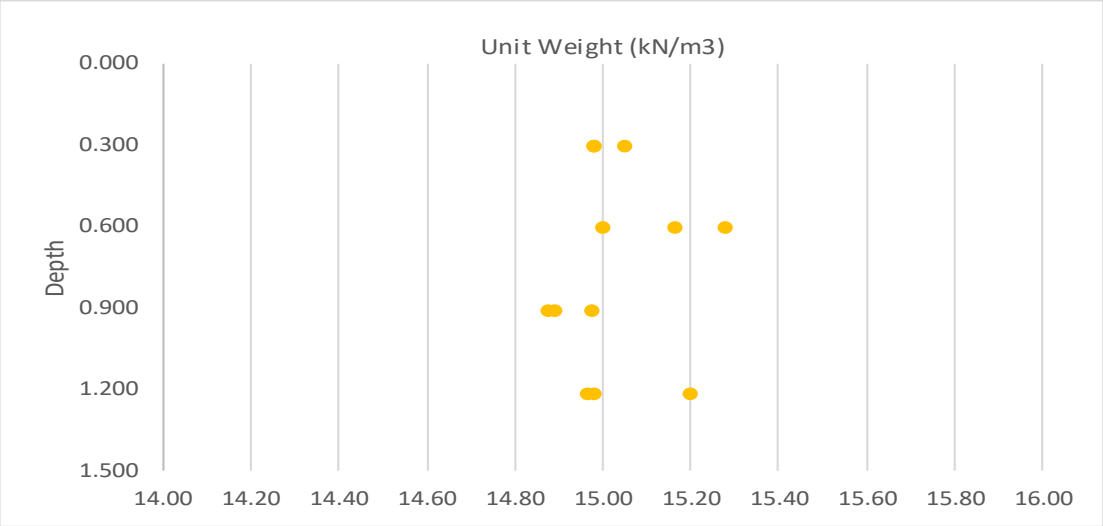

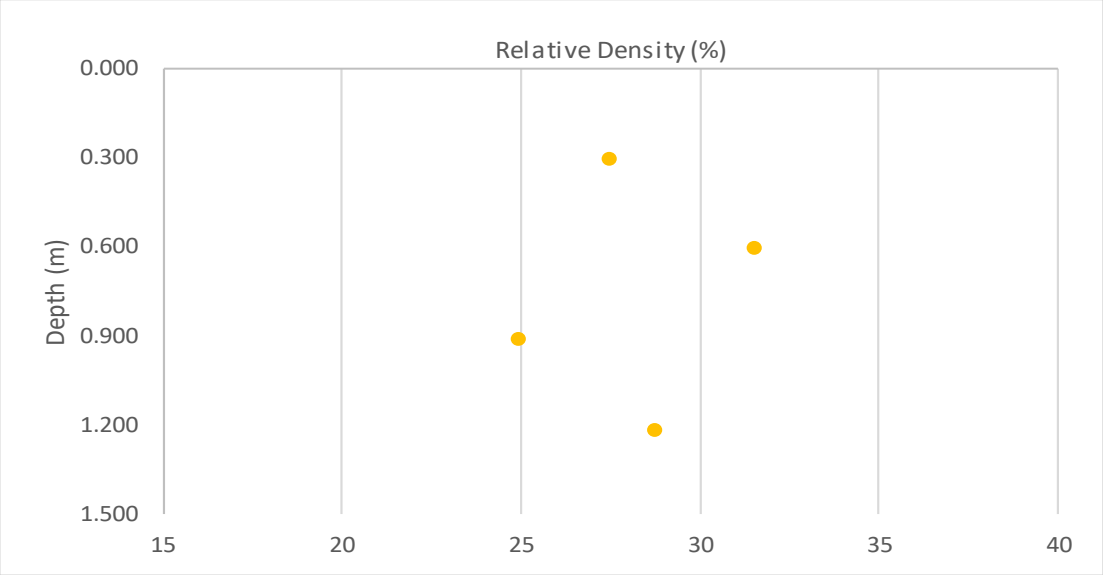

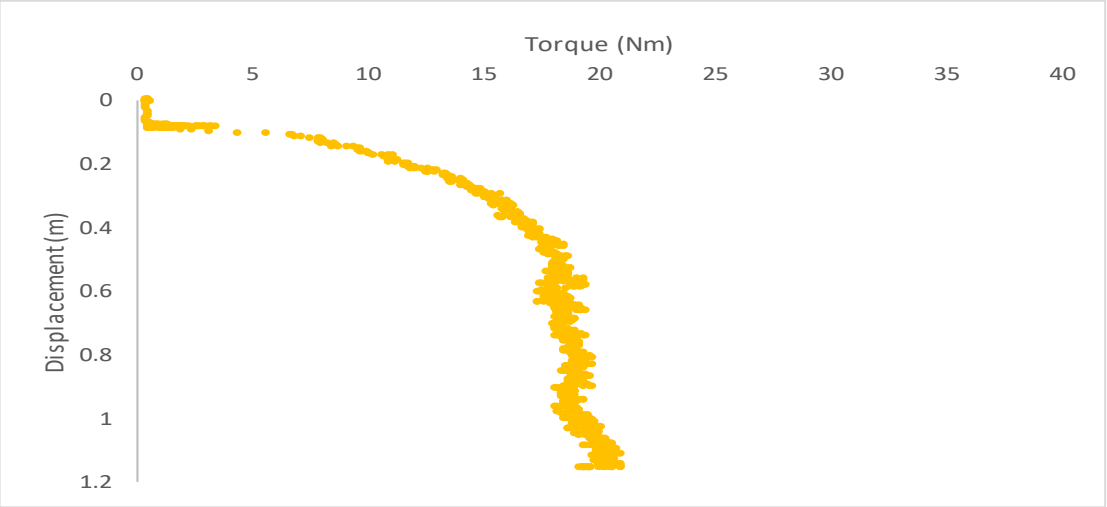
Torque (Nm)
0
5
10
15
20
25
30
35
40
Displacement (m)
0
0.2
0.4
0.6
0.8
1
1.2

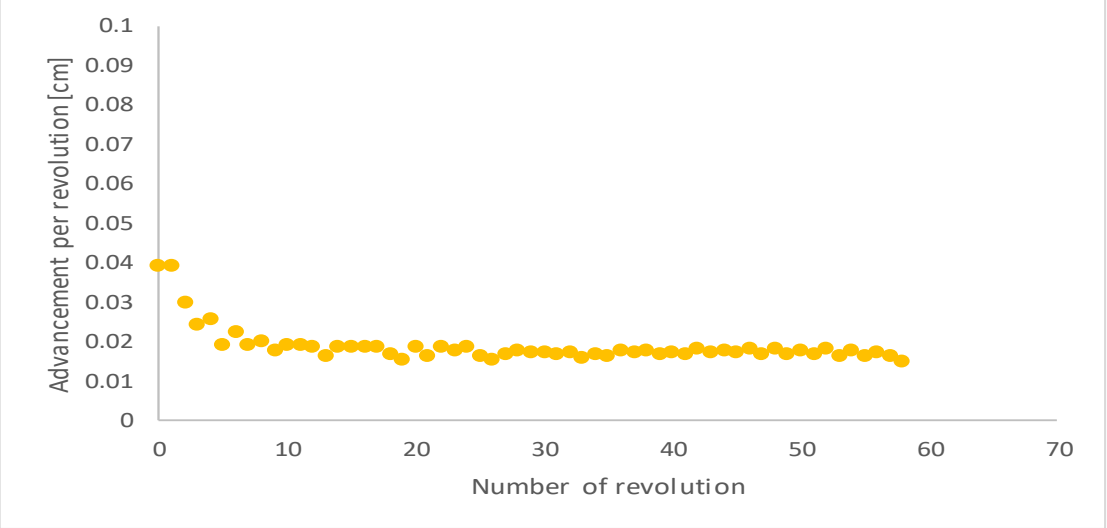
Advancement per revolution [cm]
0.1
0.09
0.08
0.07
0.06
0.05
0.04
0.03
0.02
0.01
0
0
10
20
30
40
50
60
70
Number of revolution

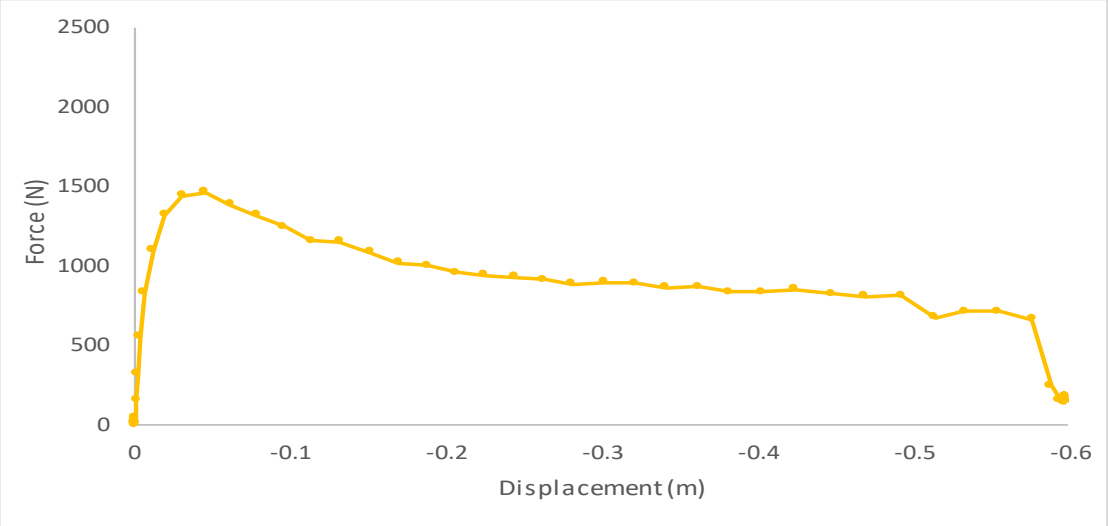
Force (N)
2500
2000
1500
1000
500
0
0
-0.1
-0.2
-0.3
-0.4
-0.5
-0.6
Displacement (m)

Jetted anchor [LJO1]

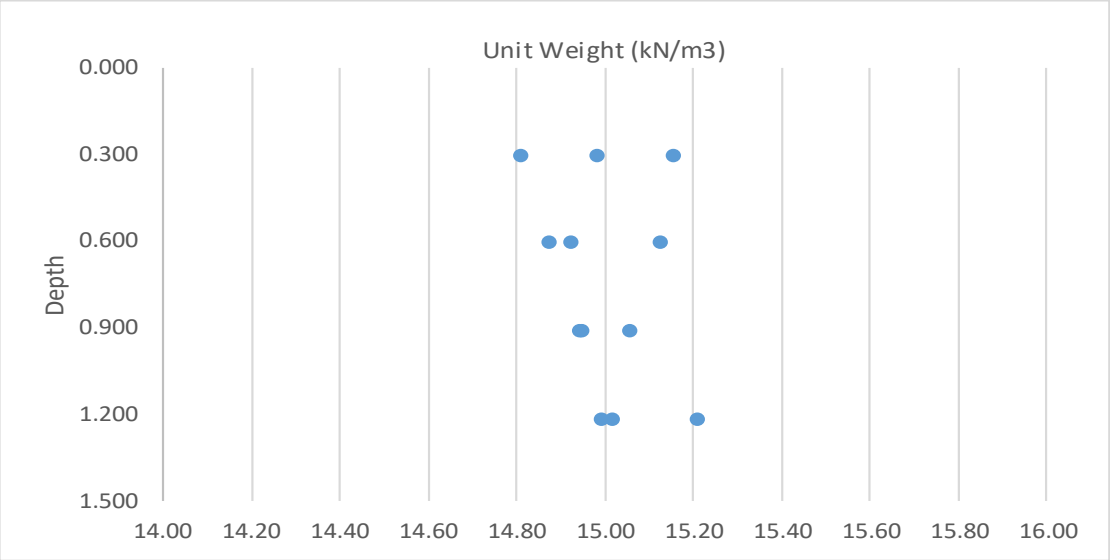

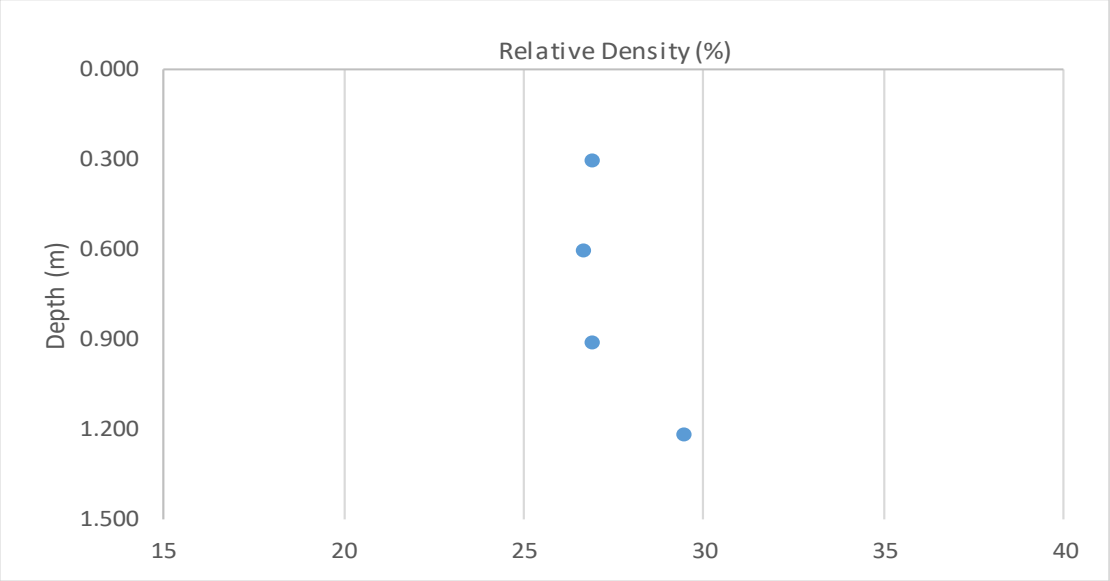

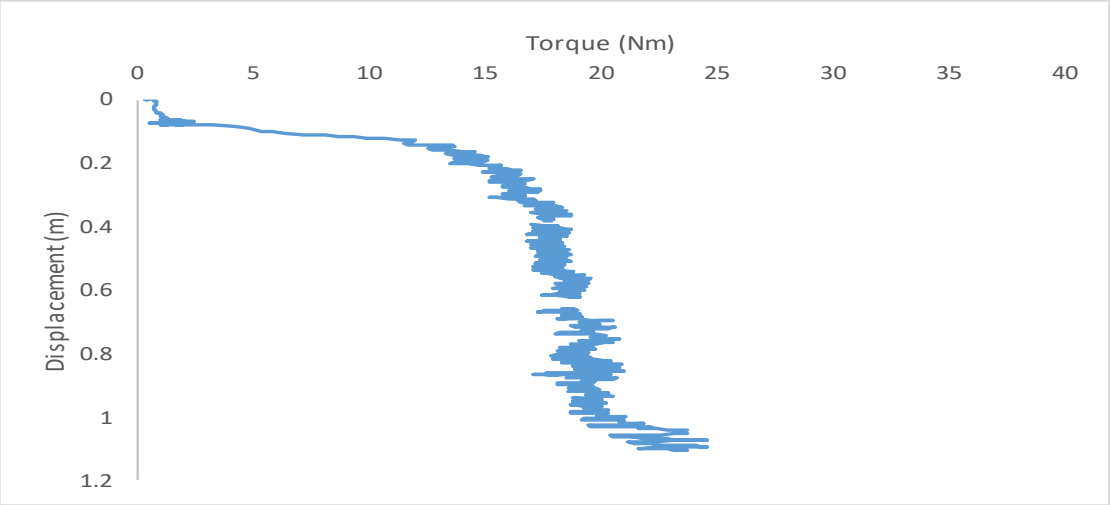
Torque (Nm)
0
5
10
15
20
25
30
35
40
Displacement (m)
0
0.2
0.4
0.6
0.8
1
1.2

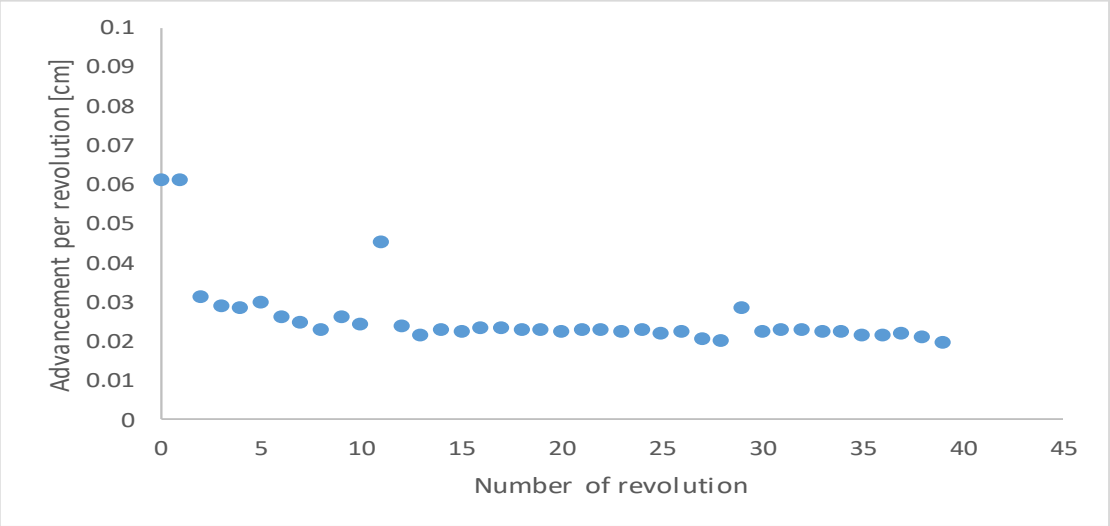
Advancement per revolution [cm]
0.1
0.09
0.08
0.07
0.06
0.05
0.04
0.03
0.02
0.01
0
0
5
10
15
20
25
30
35
40
45
Number of revolution

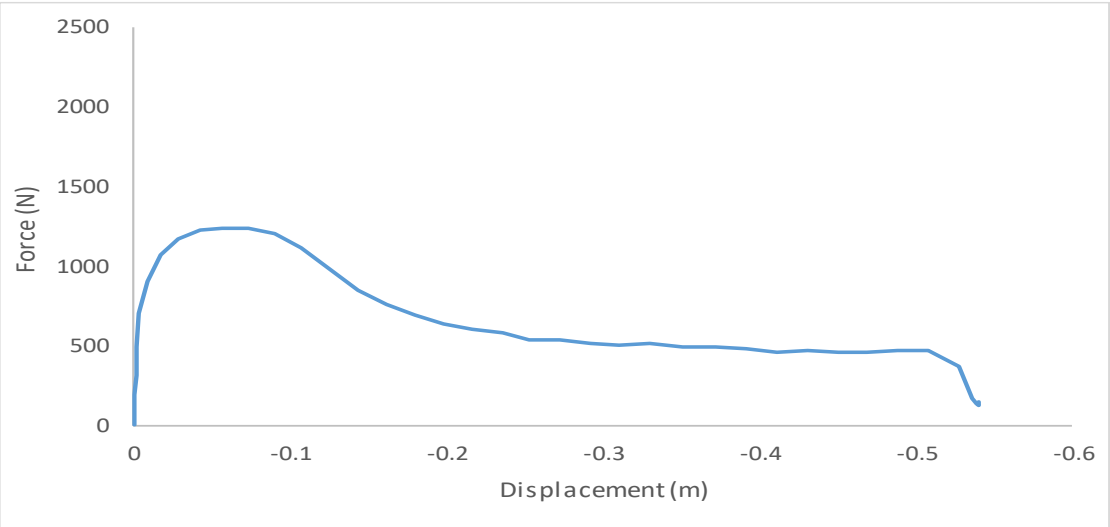
Force (N)
2500
2000
1500
1000
500
0
0
-0.1
-0.2
-0.3
-0.4
-0.5
-0.6
Displacement (m)

Appendix C: Dense sand Tests

For each anchor test, the plots of unit weight over depth, relative density over depth, installation torque over depth, average advancement per revolution during installation and pullout forces over depth are provided in that order.

Plain anchor 1 [DPC1]

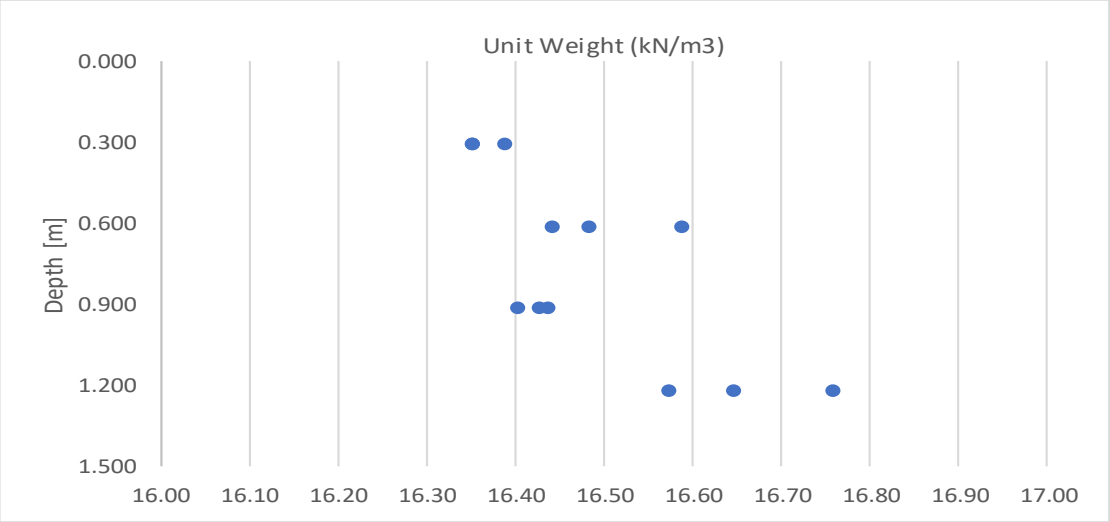

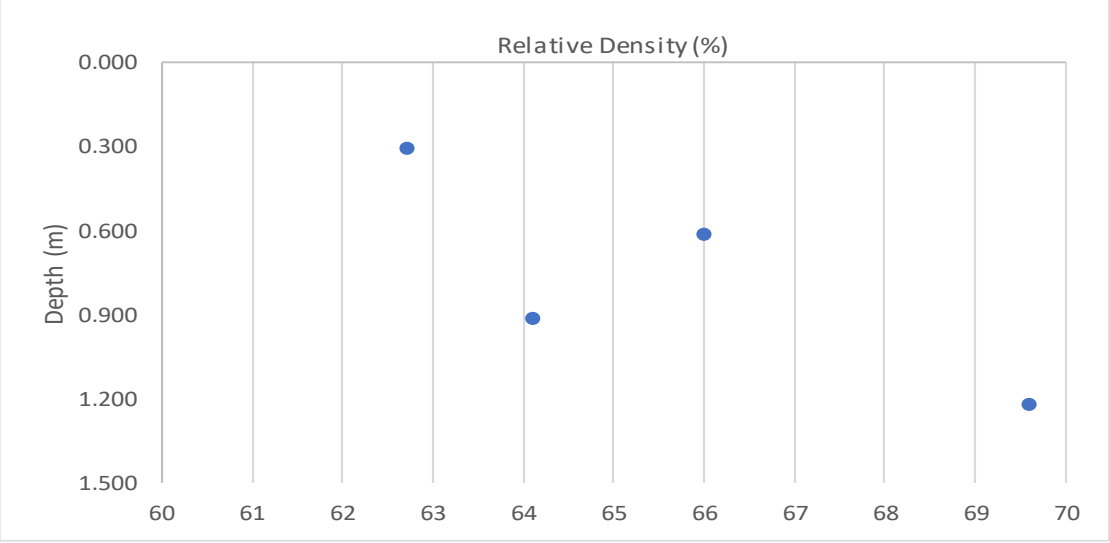

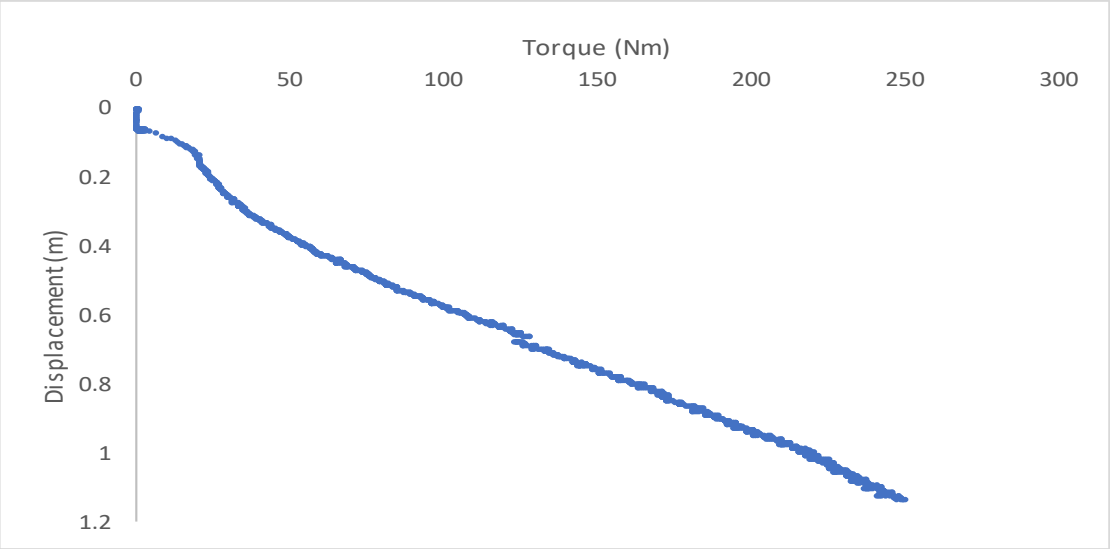
Torque (Nm)
0
50
100
150
200
250
300
Displacement (m)
0
0.2
0.4
0.6
0.8
1
1.2

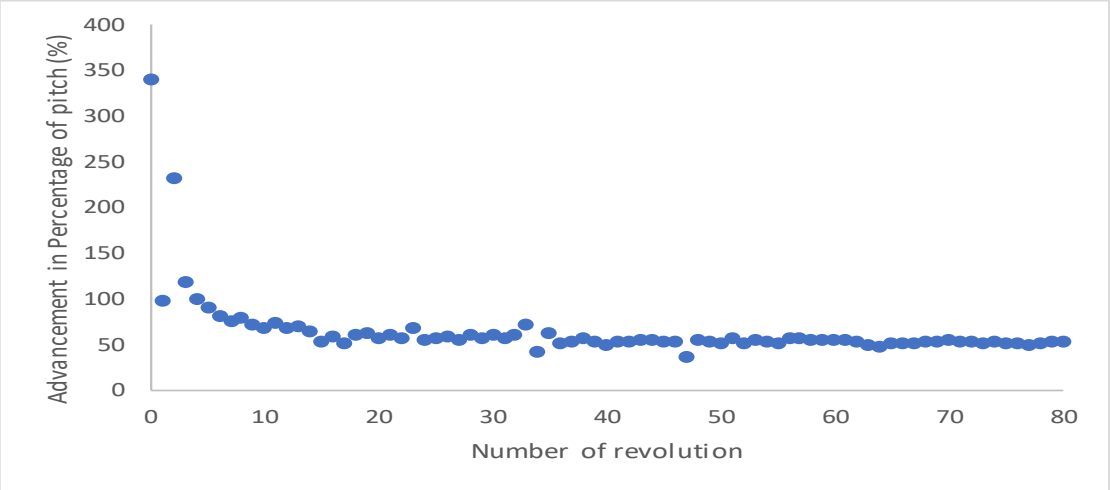
Advancement in Percentage of pitch (%)
400
350
300
250
200
150
100
50
0
0
10
20
30
40
50
60
70
80
Number of revolution

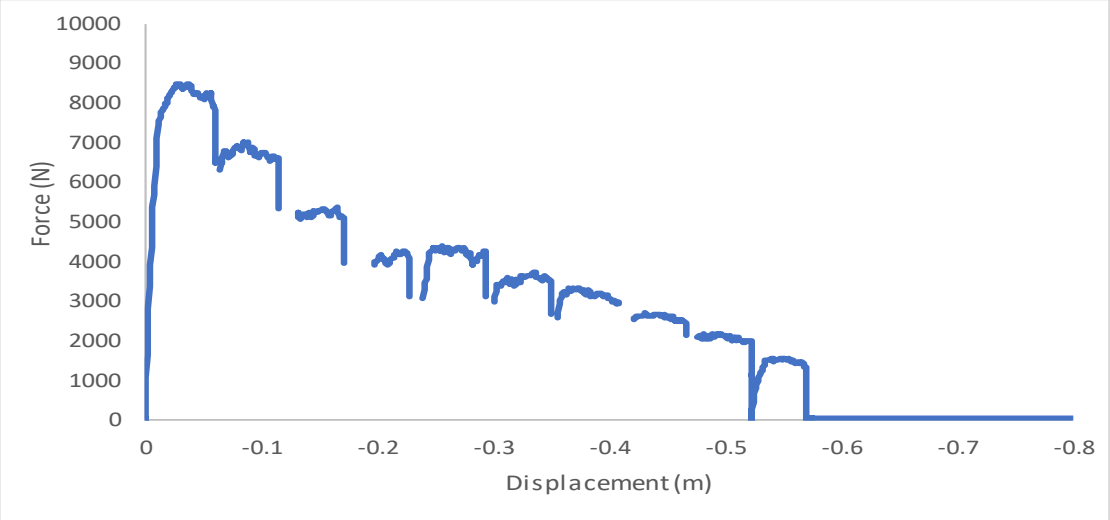
Force (N)
10000
9000
8000
7000
6000
5000
4000
3000
2000
1000
0
0
-0.1
-0.2
-0.3
-0.4
-0.5
-0.6
-0.7
-0.8
Displacement (m)

Plain anchor 2 [DPC2]

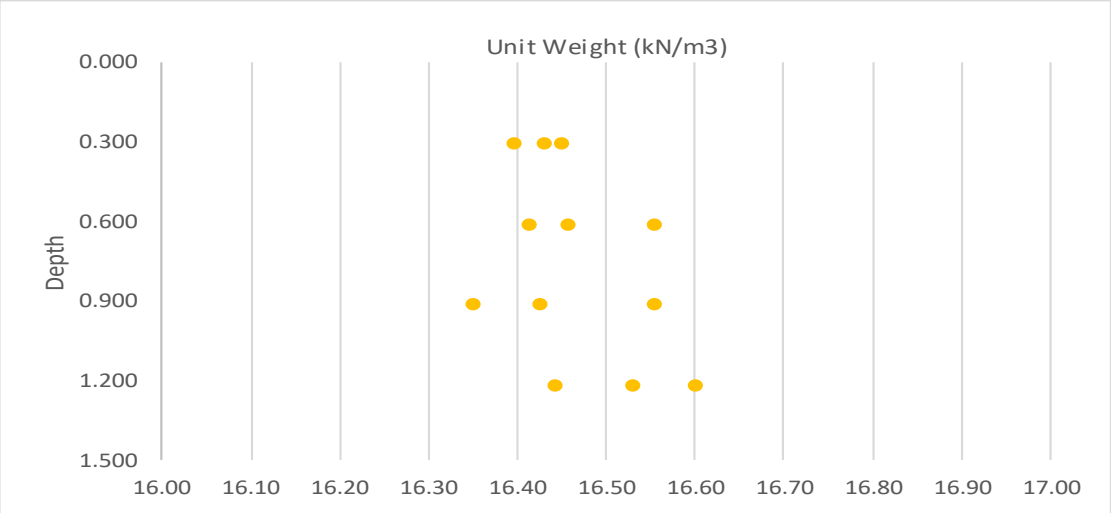

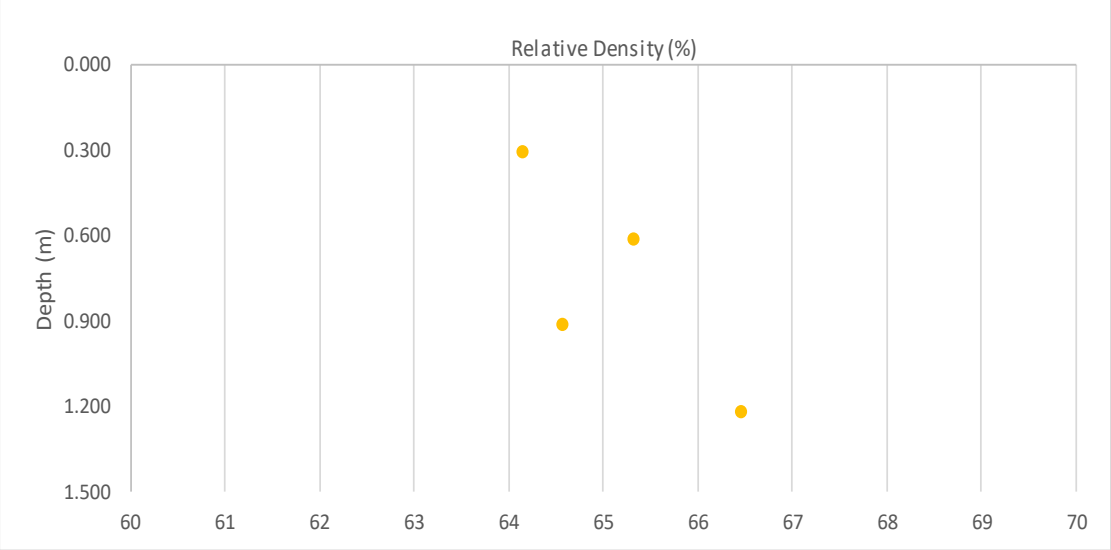

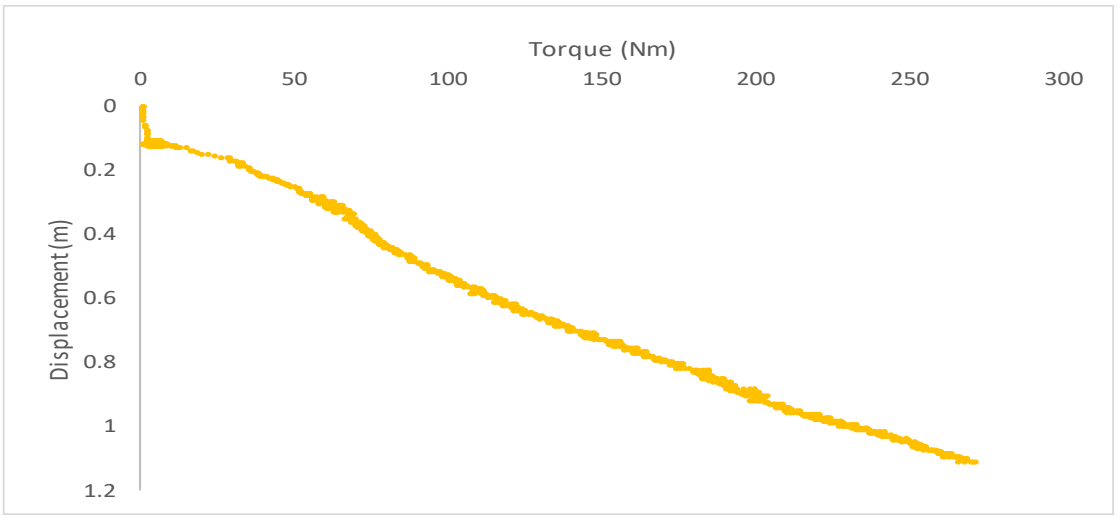
Torque (Nm)
0
50
100
150
200
250
300
Displacement (m)
0
0.2
0.4
0.6
0.8
1
1.2

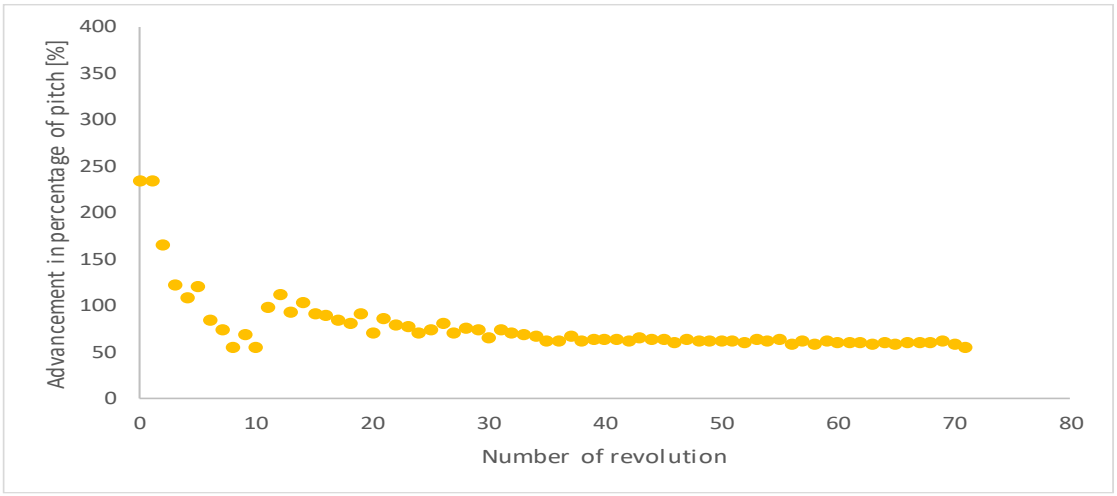
Advancement in percentage of pitch [%]
400
350
300
250
200
150
100
50
0
0
10
20
30
40
50
60
70
80
Number of revolution

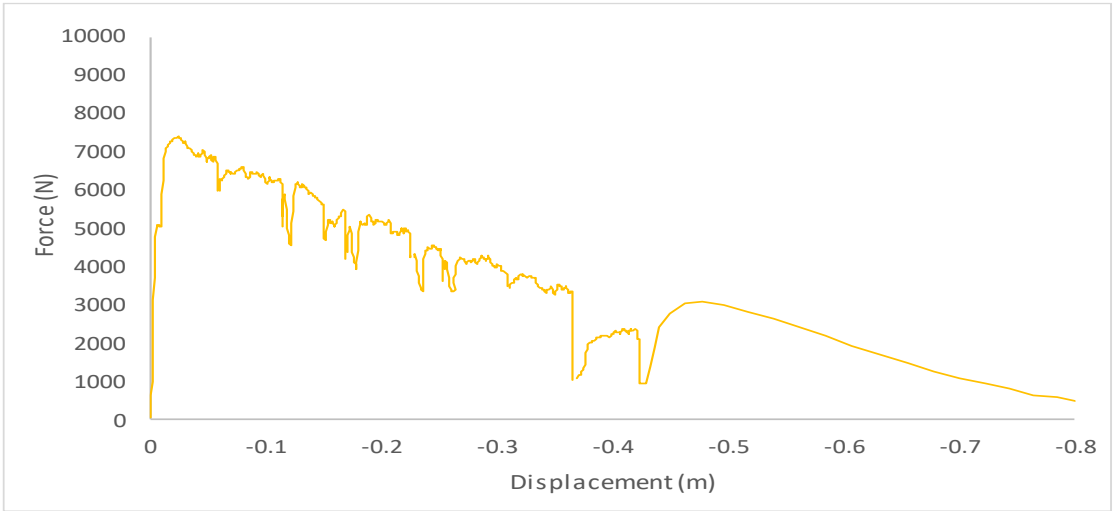
Force (N)
10000
9000
8000
7000
6000
5000
4000
3000
2000
1000
0
0
-0.1
-0.2
-0.3
-0.4
-0.5
-0.6
-0.7
-0.8
Displacement (m)

Rough anchor [DRC1]

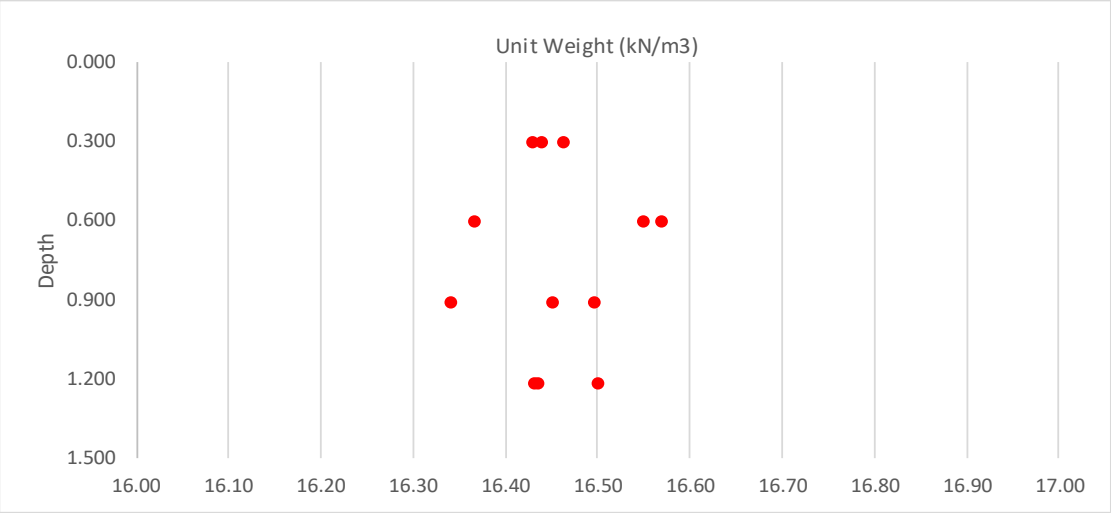

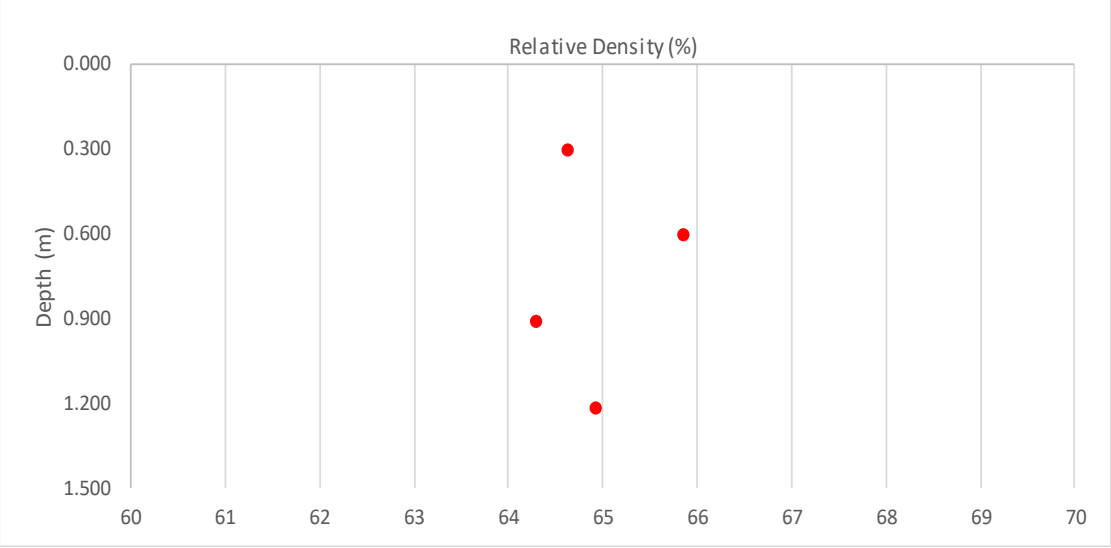

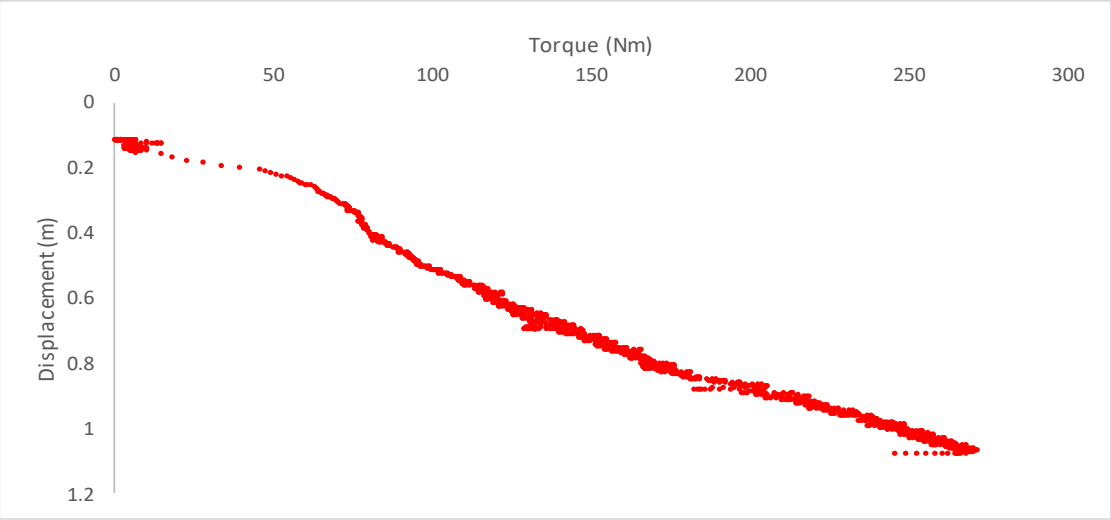
Torque (Nm)
0
50
100
150
200
250
300
Displacement (m)
0
0.2
0.4
0.6
0.8
1
1.2

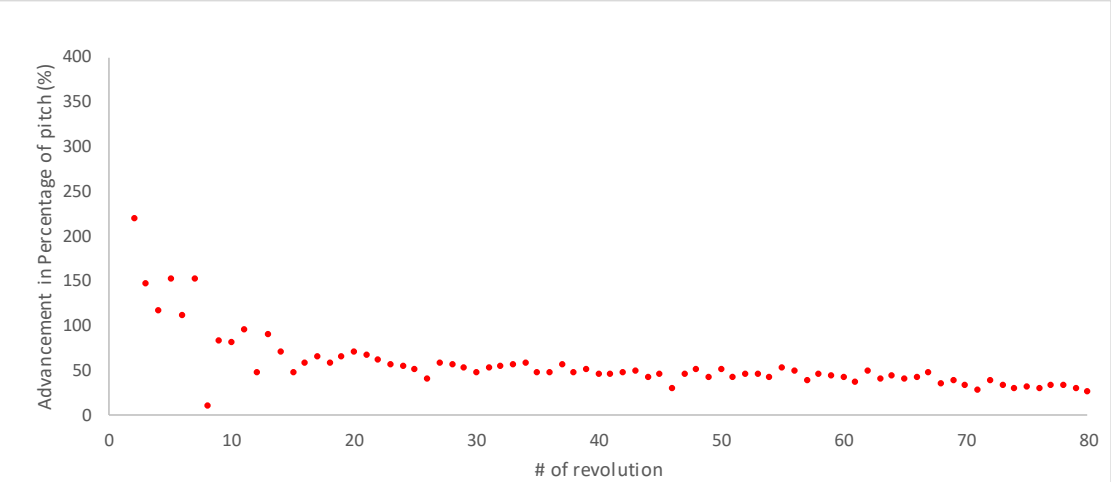
Advancement in Percentage of pitch (%)
400
350
300
250
200
150
100
50
0
0
10
20
30
40
50
60
70
80
# of revolution

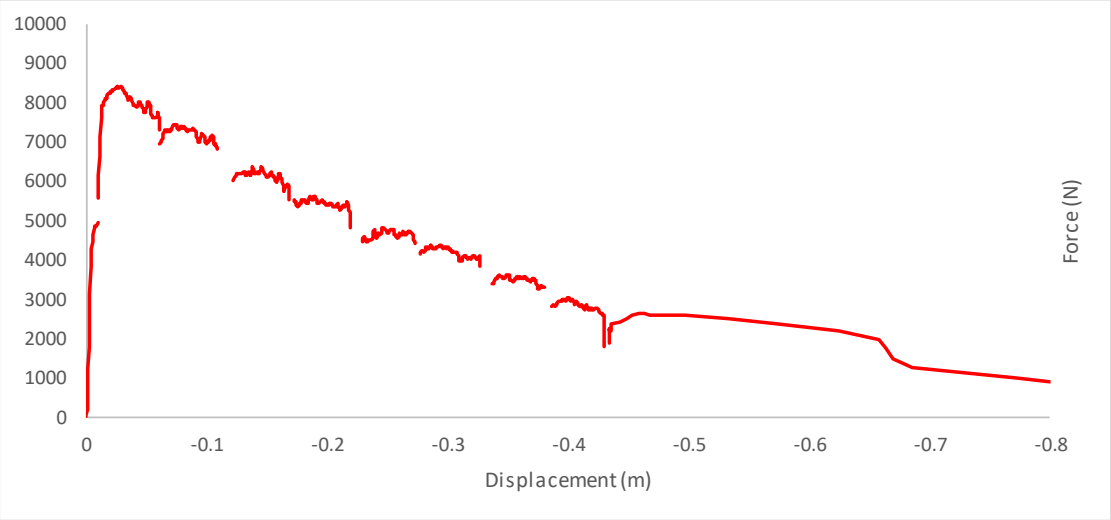
10000
9000
8000
7000
6000
5000
4000
3000
2000
1000
0
Force (N)
0
-0.1
-0.2
-0.3
-0.4
-0.5
-0.6
-0.7
-0.8
Displacement (m)

Smooth anchor [DSC1]

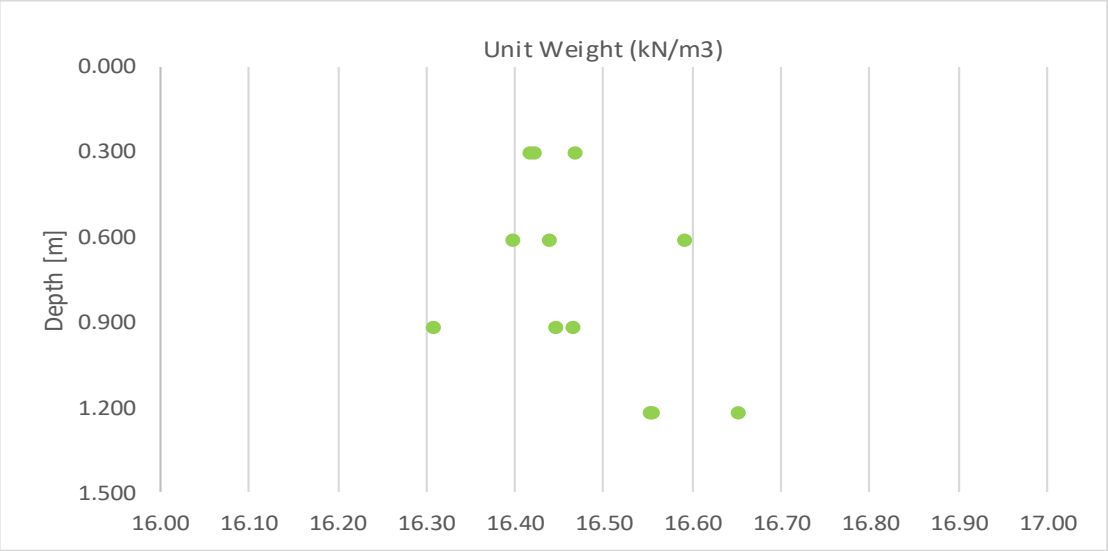

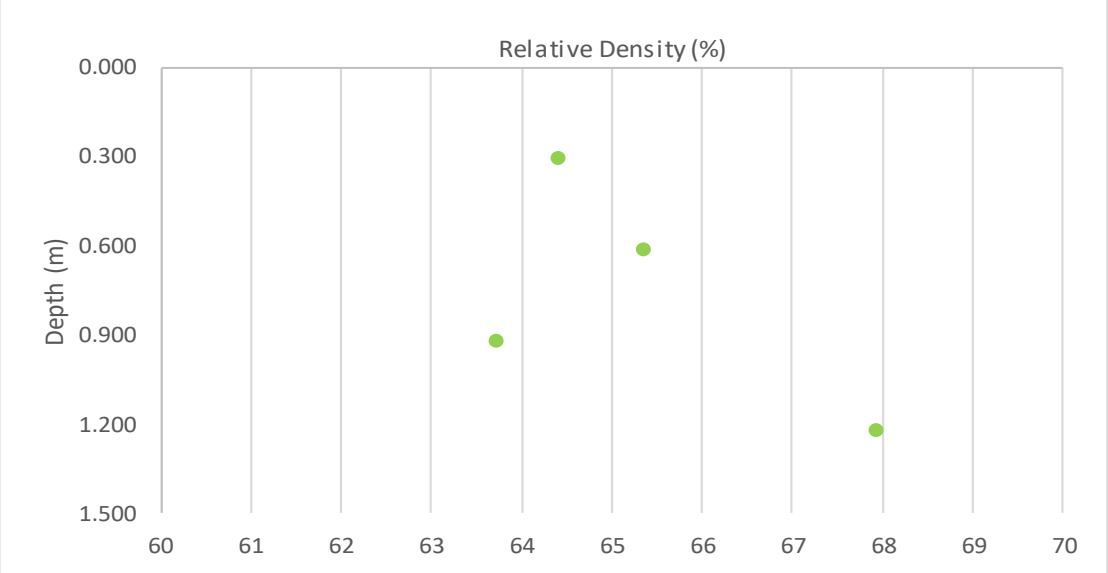

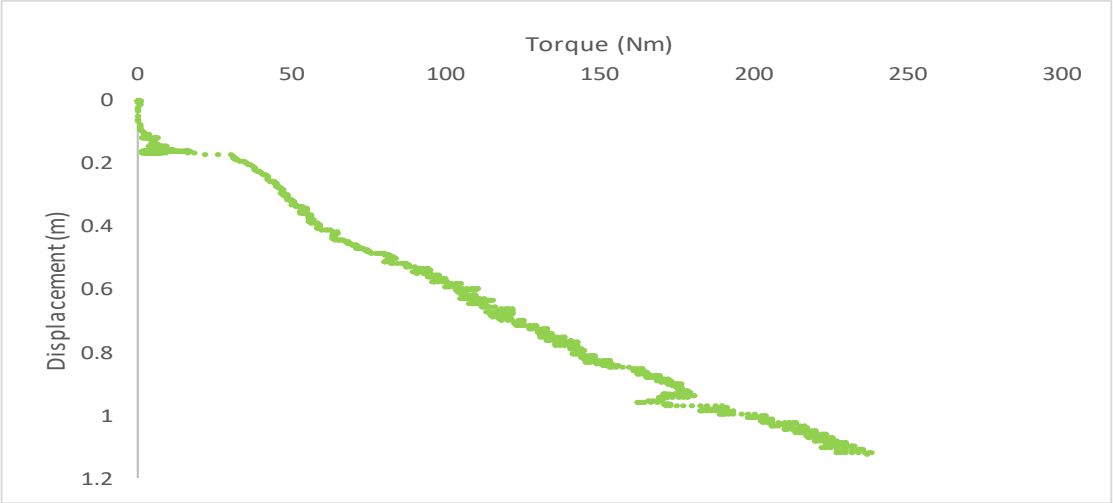
Torque (Nm)
0
50
100
150
200
250
300
Displacement (m)
0
0.2
0.4
0.6
0.8
1
1.2

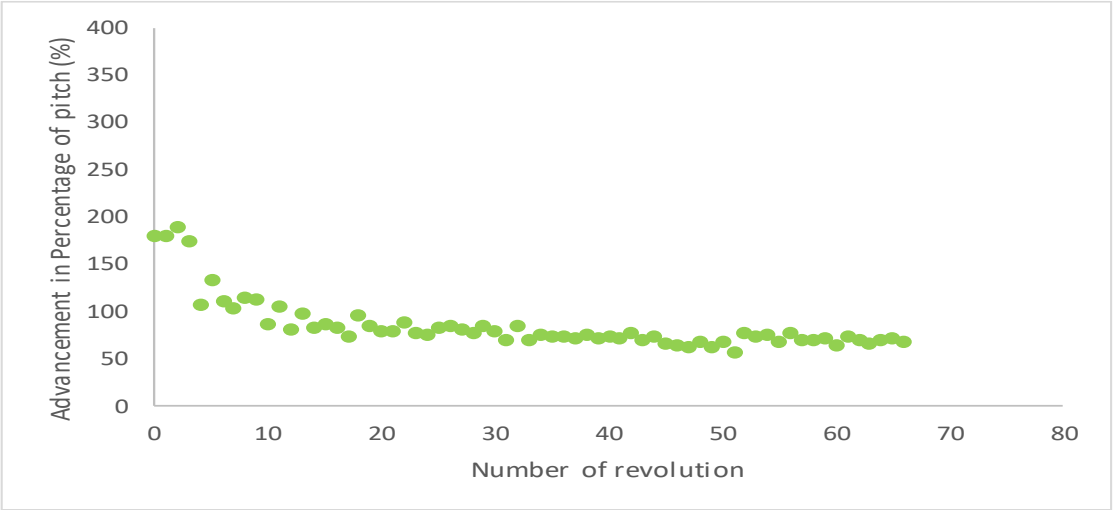
Advancement in Percentage of pitch (%)
400
350
300
250
200
150
100
50
0
0
10
20
30
40
50
60
70
80
Number of revolution

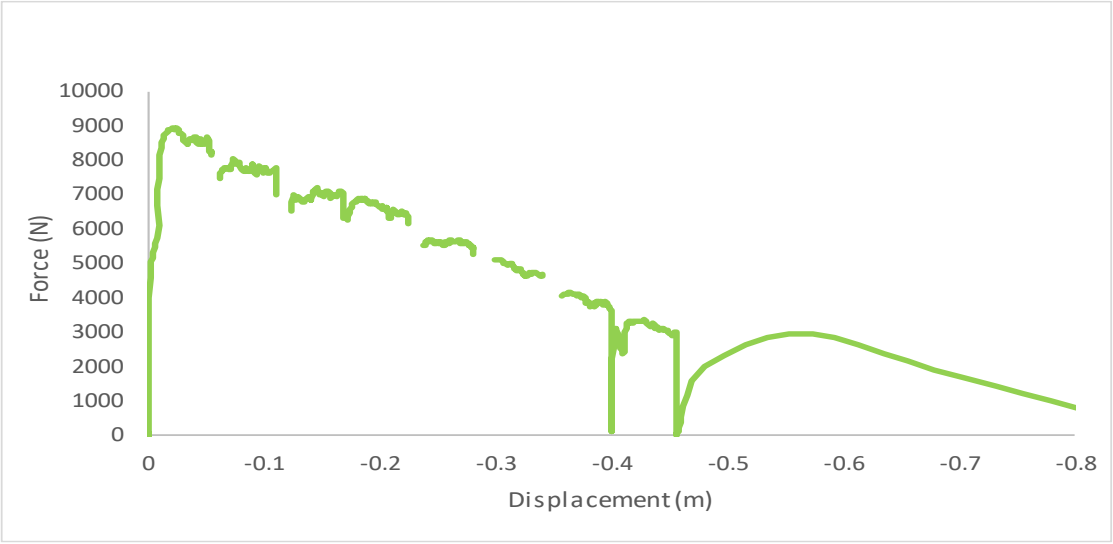
Force (N)
10000
9000
8000
7000
6000
5000
4000
3000
2000
1000
0
0
-0.1
-0.2
-0.3
-0.4
-0.5
-0.6
-0.7
-0.8
Displacement (m)

Jetted anchor [DJO1]

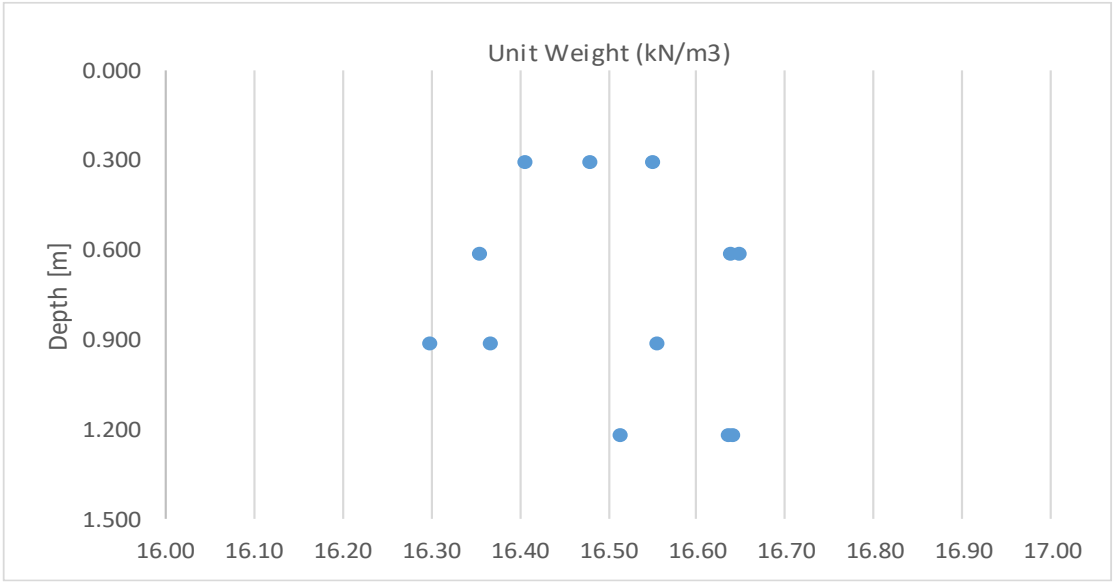

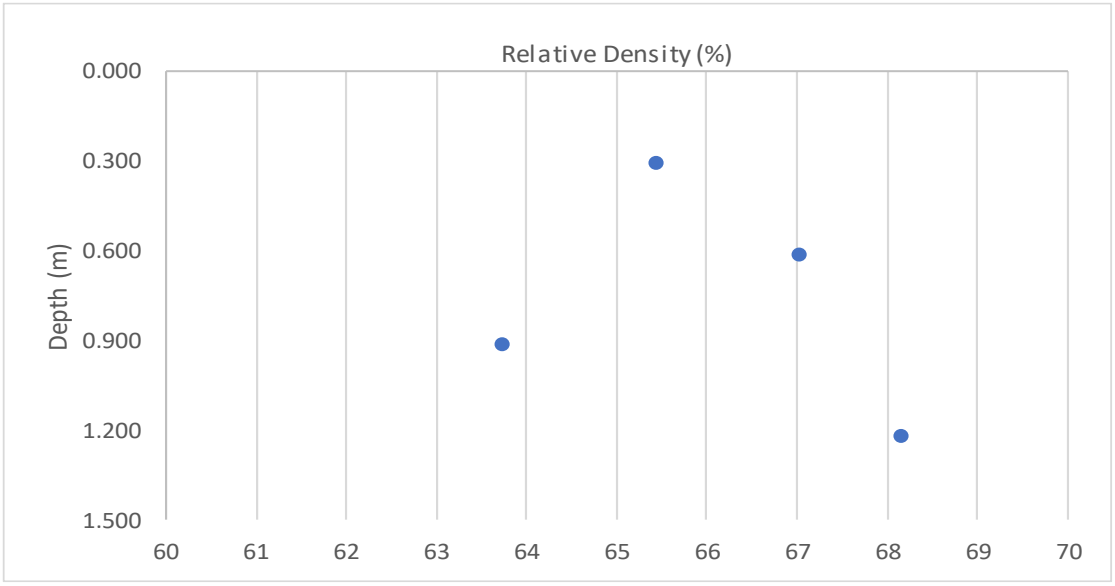

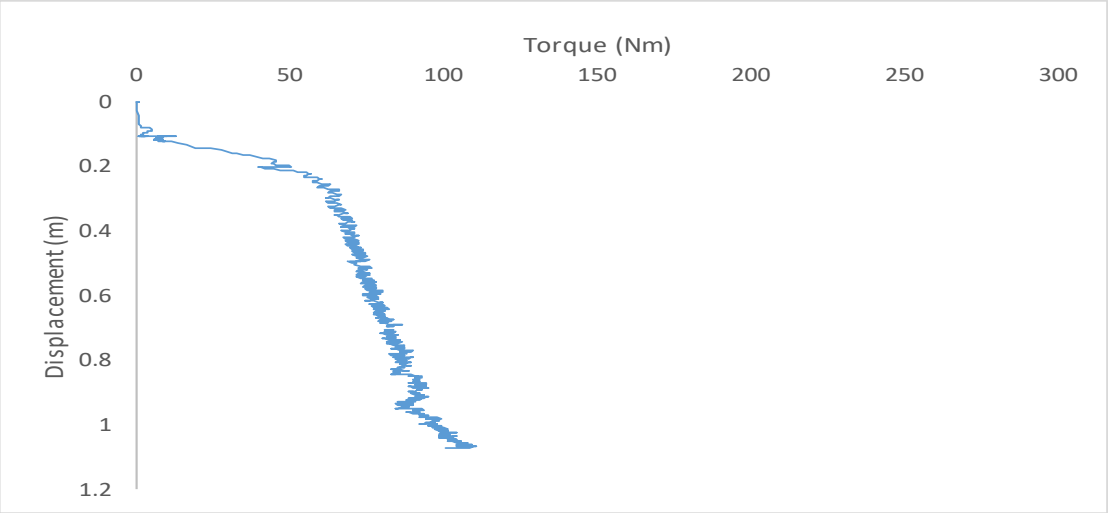
Torque (Nm)
0
50
100
150
200
250
300
Displacement (m)
0
0.2
0.4
0.6
0.8
1
1.2

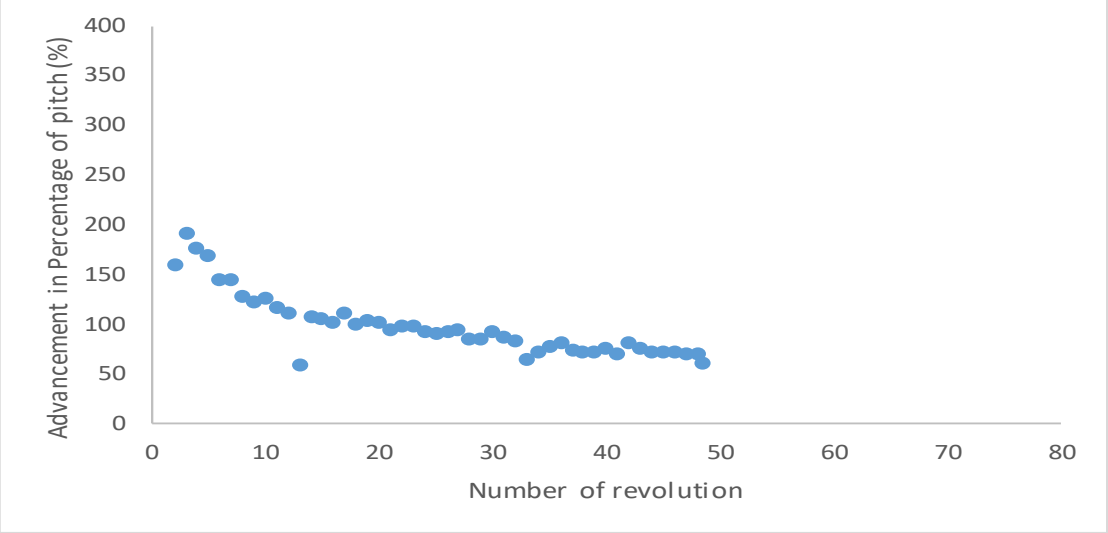
Advancement in Percentage of pitch (%)
400
350
300
250
200
150
100
50
0
0
10
20
30
40
50
60
70
80
Number of revolution

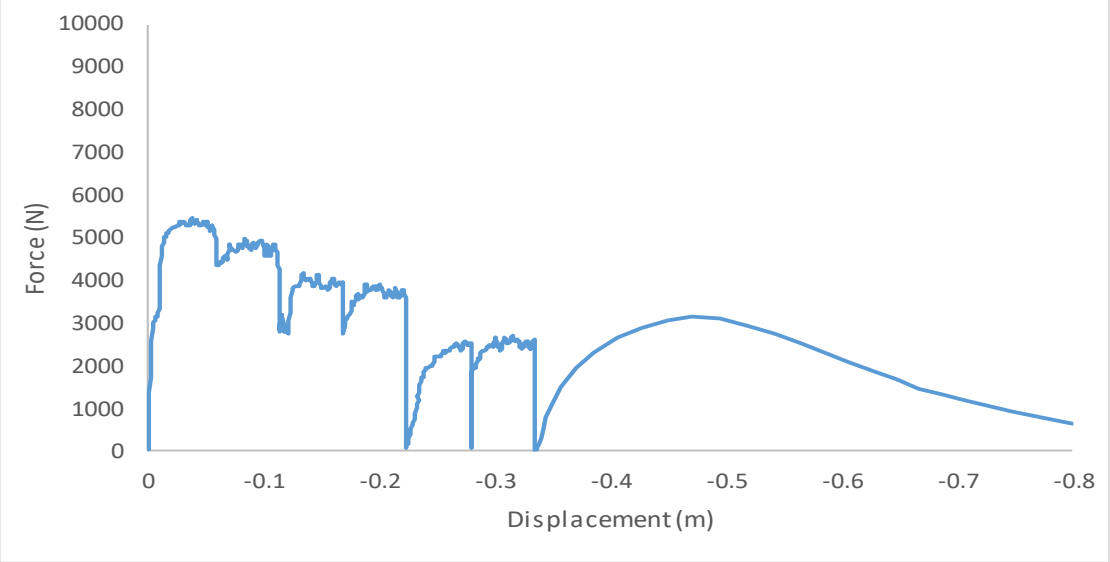
Force (N)
10000
9000
8000
7000
6000
5000
4000
3000
2000
1000
0
0
-0.1
-0.2
-0.3
-0.4
-0.5
-0.6
-0.7
-0.8
Displacement (m)

Jetted anchor [DJO2]

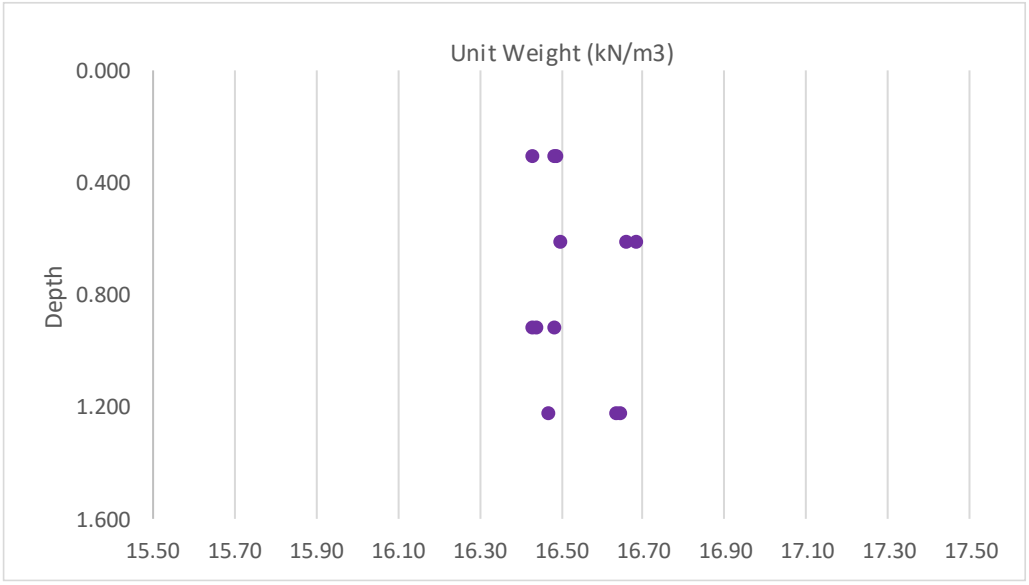

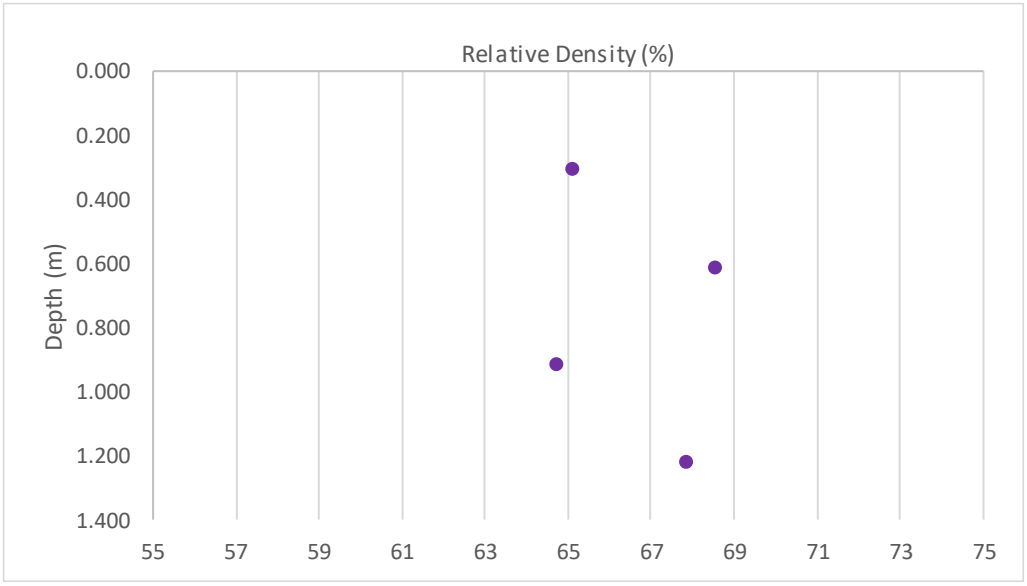

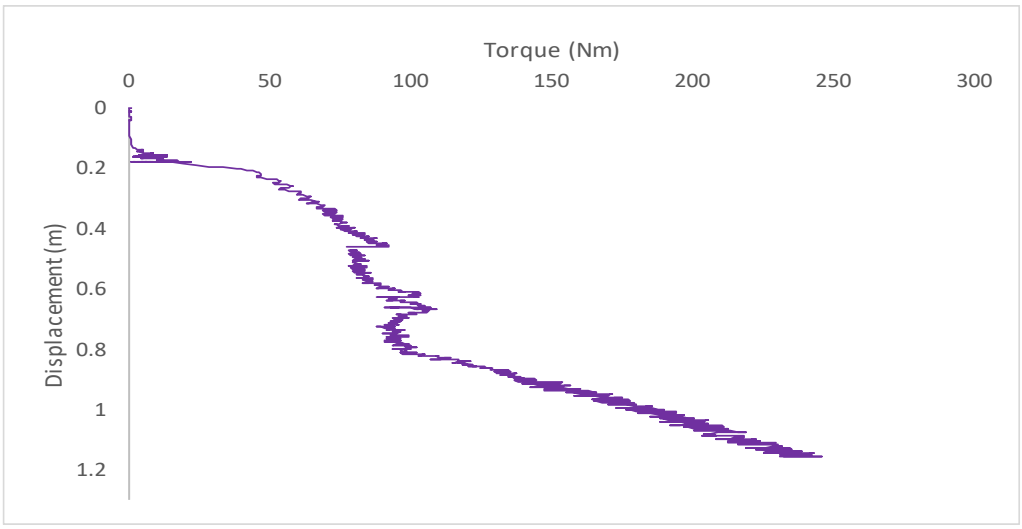
Torque (Nm)
0
50
100
150
200
250
300
Displacement (m)
0
0.2
0.4
0.6
0.8
1
1.2

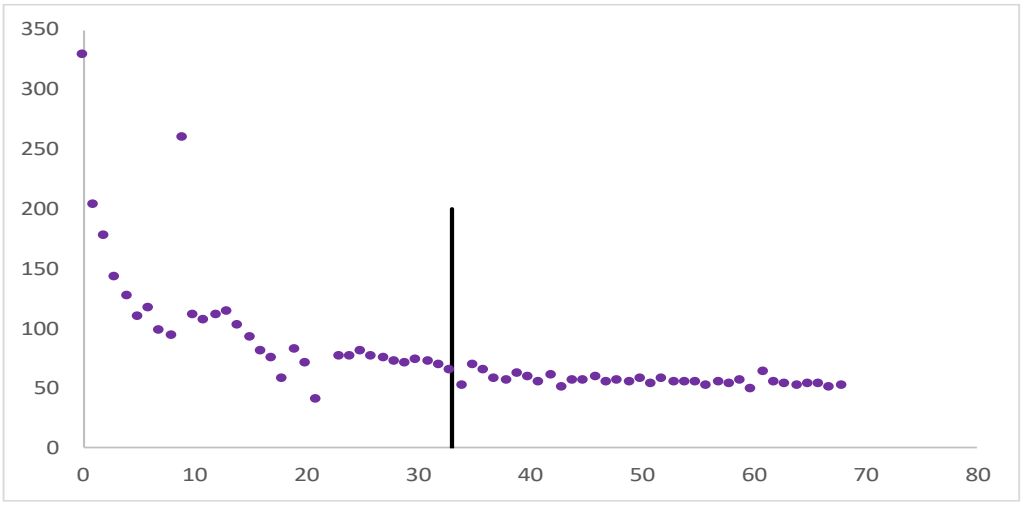
350
300
250
200
150
100
50
0
0
10
20
30
40
50
60
70
80

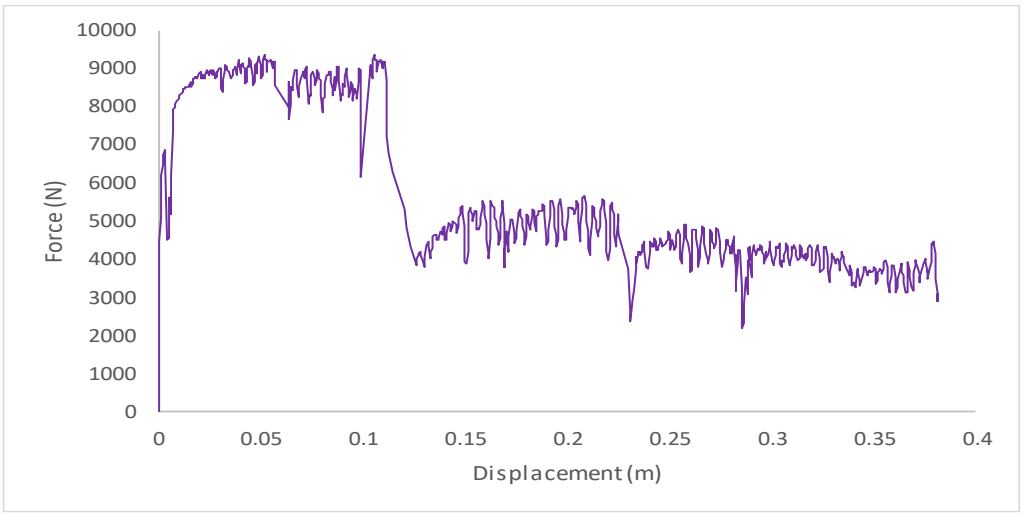
Force (N)
10000
9000
8000
7000
6000
5000
4000
3000
2000
1000
0
0
0.05
0.1
0.15
0.2
0.25
0.3
0.35
0.4
Displacement (m)

BIBLIOGRAPHY

Bradshaw et al (2016): Scaling Considerations for 1-g Model Horizontal Plate Anchor Tests in Sand. Published in Geotechnical Testing Journal Vol. 39.

Byrne, B. W., Houlsby G. T. (2015): Helical piles: an innovative foundation design option for offshore wind turbines. Published by The Royal Society.

Clemence, S.P., Crouch, L.K., and Stephenson, R. W. (1994): Prediction of Uplift Capacity for Helical Anchors in Sand. Published in Second Geotechnical Engineering Conference, Cairo, Egypt, Vol. I, pp. 332-343.

Davidson et al. (2018): Centrifuge modelling of screw piles for offshore wind energy foundations. Published in: Physical modelling in geotechnics: proceedings of the 9th International Conference on Physical Modelling in Geotechnics (ICPMG 2018).

De Hollanda, Cristina and Aoki, Nelson (2010): Relationship between installation torque and uplift capacity of deep helical piles in sand. Published in Canadian geotechnical journal Vol. 47.

Ghaly, Ashraf M. (1995): Drivability and Pullout Resistance of Helical Units in Saturated Sands. Published in „Soils and Foundations Vol. 35, No. 2 61-66“, June 1995, Japanese Society of Soil Mechanics and Foundation Engineering.

Ghaly, Ashraf and Hanna, Adel (1991): Experimental and theoretical studies on installation torque of screw anchors. Published in Department of Civil Engineering, Concordia University Canada.

Ghaly et al. (1991): Uplift Behavior of Screw Anchors in Sand. I: Dry Sand. Published in Journal of Geotechnical Engineering Vol. 117, Issue 5 (May 1991)

Hoyt, R.M. and Clemence, S.P. (1989): Uplift Capacity of Helical Anchors in Soil. Published in 12th International Conference on Soil Mechanics and Foundation Engineering, Brazil.

Perko, Howard A. (2001): Energy Method for Predicting Installation Torque of Helical Foundations and Anchors. Published in New technological and Design Developments in Deep Foundations, ASCE Press, Reston, VA.

Perko, H. A. (2009): Helical piles: a practical guide to design and installation. J. Wiley, Hoboken, NJ.

Meyerhof, G.G. and Adams, J.I. (1986): The ultimate uplift capacity of foundations. Published in Canadian Geotech. Journal Vol. 5.

Mitch, M.P. and Clemence, S.P. (1985): The uplift capacity of helix anchors in sand. Proc. Uplift Behavior of Anchor Foundations in Soil, S.P. Clemence, Ed., ASCE.

Terzaghi, K., Peck, R., & Mesri, G. (1996): Soil mechanics in engineering practice. (Third ed.). New York: Wiley.

Wang, Liu, Tai, Zang, & Zhang. (2017): Frost jacking characteristics of screw piles in seasonally frozen regions based on thermo-mechanical simulations. Published in Computers and Geotechnics, 91, 27-38.

Pictures taken form:

https://www.boem.gov/Offshore-Wind-Energy/

https://hubbellcdn.com/catalogfull/04-Anchors.pdf

https://www.omega.com/pptst/LC8151.html

https://www.omega.com/pptst/OMB-DAQ55.html

http://www.te.com/usa-en/product-SP2-50.html

https://www.transducertechniques.com/swo-load-cell.aspx

https://www.transducertechniques.com/trs-torque-sensor.aspx